

EFFECTS OF MATERIALS ON THE DESIGN OF MECHANICAL HOUSING FOR SPACECRAFT ELECTRONIC PACKAGES

A DISSERTATION

*Submitted in partial fulfilment of the
requirements for the award of the degree
of*

MASTER OF TECHNOLOGY

in

MECHANICAL ENGINEERING

(With Specialization in Production and Industrial Systems Engineering)

By

SUMIT KUMAR



**DEPARTMENT OF MECHANICAL AND INDUSTRIAL ENGINEERING
INDIAN INSTITUTE OF TECHNOLOGY ROORKEE
ROORKEE-247667 (INDIA)
APRIL, 2019**

CANDIDATE’S DECLARATION

I hereby declare that the work carried out in this thesis titled “**EFFECTS OF THE MATERIALS ON THE DESIGN OF MECHANICAL HOUSING FOR SPACECRAFT ELECTRONICS PACKAGES**” presented on behalf of partial fulfilment of the requirement for the award of the degree of **Master of Technology** with specialization in **Production and Industrial System Engineering** submitted to the department of **Mechanical & Industrial Engineering, Indian Institute of Technology Roorkee, India**, under the supervision of **Dr. Kaushik Pal**, Associate Professor, MIED, IIT Roorkee and **Mr. Jiwan Kumar**, Associate Director, Capacity Building Programme Office, ISRO HQ Bangalore, India.

I have not submitted the matter embodied in this report for the award of any other degree or diploma.

Date: 16th April 2019

Place: Roorkee

(**Sumit Kumar**)

CERTIFICATION

This is to certify that the above statement made by the candidate is correct to the best of my knowledge and belief.

Mr. Jiwan Kumar

Associate Director

Capacity Building Programme Office

ISRO HQ, Bangalore-560017, India

Dr. Kaushik Pal

Associate Professor

MIED, IIT Roorkee

UK-247667, India

Acknowledgement

I wish to express my deep sense of gratitude and sincere thanks to my guide **Dr. Kaushik Pal**, Associate Professor, Mechanical and Industrial Engineering department, IIT Roorkee, for being helpful and a great source of inspiration. I would like to thank him for providing me with an opportunity to work on this excellent and innovative field of research. I would like to thank my co-guide **Mr. Jivan Kumar Pandit**, Associate Director, Capacity Building Programme Office, ISRO HQ Bangalore for his valuable suggestions and constant support that gave me confidence to complete my work. I wish to thank both of them for their constant guidance and suggestions without which I would not have successfully completed this thesis.

I would also like to thank **Dr. Dinesh Kumar**, HOD MIED, IIT Roorkee for his constant support during my studies. I also would like to thank all the teaching and non-teaching staff members of the department who have contributed directly or indirectly in successful completion of my thesis work.

Date: 16th APRIL, 2019

Place: Roorkee

SUMIT KUMAR

M.Tech 2nd year,

PISE

Enrol. No. 16540010

Abstract

The design of the mechanical housings involves trade-off between the electrical, mechanical, and environmental requirements of the mission for the electronic subsystem of spacecraft. The function of mechanical housings for electronics is to ensure its integrity and functionality during launch and on-orbit space environment in a spacecraft mission. These comprises of severe vibrations at the time of launch, considerable variations in temperature throughout the mission, and radiation degradation while in orbit.

This study deals with design and analysis of the mechanical housings assembly for an electronic package used in a spacecraft. It mainly focuses on the static and dynamic behavior of electronic packages and behavior of printed circuit boards (PCBs) under harsh vibration environment with various boundary conditions imposed on them.

The finite element model, of the mechanical housings assembly for the electronic package has been generated using UG-NX software by choosing different materials like Aluminum alloy AL6061, Magnesium alloy AZ31B and Beryllium-Aluminum alloy AM162, to predict the behavior of the assembly subjected to static and dynamic loading. Modelling and simulation of the entire packages have been done by choosing Aluminum alloy (Al6061), Magnesium alloy (AZ31B) and Beryllium-Aluminum alloy (AM162) by UG-NX software. Using this software, stress and displacement is evaluated at the critical locations by quasi-static analysis under 25g and 20g conditions and fundamental frequency is evaluated by normal mode simulation. Random mode simulation has been done to find out the transmissibility and G_{rms} value on the package at the time of launch phase.

From the simulation, it was observed that maximum displacement value of the critical locations of the package is least for Beryllium-Aluminum alloy (AM162) and also transmissibility and G_{rms} value on the package is least for Beryllium-Aluminum alloy (AM162)

Keywords: Electronic packages (EP), power spectral density (PSD), Quasi-static simulation, Random simulation, fundamental frequency, transmissibility.

Contents

CANDIDATE'S DECLARATION	i
CERTIFICATION	i
Acknowledgement	ii
Abstract	iii
List of figures	vi
List of tables	ix
Chapter 1	1
INTRODUCTION	1
1.1 Overview	1
1.2 Design of the Electronic Package	4
1.3 Types of Electronics Packages	6
Chapter 2	7
LITERATURE SURVEY	7
2.1 Objectives of the present work	14
Chapter 3	15
METHODOLOGY AND ANALYSIS PROCEDURE	15
3.1 Problem Definition	15
3.2 Project Methodology	15
3.2.1 Selection of material	15
3.2.2 Need for Modal Analysis:	21
3.2.3 Selection of boundary conditions	21
3.2.4 Effect of rib thickness	31
3.2.5 Effect of material composition	33
Chapter 4	34
CONCEPTUAL MODELLING OF THE PACKAGE	34
4.1 Design considerations for PCB	34
4.1.1 Transmissibility of PCB	35
4.1.2 Analysis of PCB by analytical method	42
4.1.3 Modeling of PCB	43

4.2 Design Considerations for Tray	44
4.3 Three dimensional modeling of electronic package.....	45
Chapter 5.....	47
FINITE ELEMENT MODELING	47
5.1 Overview	47
5.2 Steps in FEM.....	47
5.3 Selection of Type of Element.....	49
5.3.1 Geometry Size and Shape.....	49
5.3.2 Based On the Type of Analysis	51
5.4 Basic Requirements of Electronic Package.....	51
5.5 FE Model of the PCB.....	52
5.6 FE Model of the Package Assembly	53
5.6.1 Screws and Studs modeled as Bars	55
5.6.2 Tray modeled as 3D elements and PCB Modeled as 2D Shell elements	56
5.7 General Mesh Generations.....	58
5.8 Mesh refinement and verification	59
Chapter 6.....	60
ANALYSIS AND RESULTS	60
6.1 Overview	60
6.2 Significance of Linear Static and Modal Analysis in Fe Software	60
6.2.1 Linear Static Analysis.....	60
6.2.2 Factor of safety	78
6.3 Modal Analysis	80
6.3.1 Fundamental frequency of vertical mounting package for different materials	83
6.3.2 Fundamental frequency of horizontal mounting package for different materials	85
6.4 Random Analysis	87
6.4.1 Basic Failure modes in Random Vibration	88
6.4.2 Random vibration input curve	89
6.4.3 Random analysis for vertical mounting electronic package.....	92
6.4.4 Random analysis for horizontal mounting electronic package.....	102
Chapter 7.....	114
CONCLUSION.....	114
7.1 Scope for future work.....	116
REFERENCES	117

List of Figures

FIG 1.1: INTERDEPENDENCE OF ELECTRONIC PACKAGES ON VARIOUS DISCIPLINES	2
FIG 1.2: TYPICAL POWER ELECTRONIC PACKAGE	5
FIG 1.3: EXPLODED VIEW OF ELECTRONIC PACKAGE	5
FIG 1.4: HORIZONTAL MOUNTING PACKAGE	6
FIG 1.5: VERTICAL MOUNTING PACKAGE	6
FIG 2.1: CORRELATION OF DISPLACEMENT OF PCB WITH SPRING MASS SYSTEM.....	8
FIG 2.2: DYNAMIC MODEL OF VIBRATION-ISOLATED ELECTRONIC BOX CONTAINING PCB.....	9
FIG 2.3: HEAVY ELECTRONIC COMPONENT MOUNTED ON A PCB	10
FIG 2.4: ANALYTICAL MODEL TO OBSERVE NATURAL FREQUENCIES	11
FIG 3.1: FE MODEL OF PCB (A) SOLID MESH DEPICTION (B) WIREFRAME MESH DEPICTION	22
FIG 3.2: 1ST MODE BEHAVIOR OF PCB FOR 4 BOUNDARY CONDITIONS.....	22
FIG 3.3: 2ND MODE BEHAVIOR OF PCB FOR 4 BOUNDARY CONDITIONS	23
FIG 3.4: FE MODEL OF PCB FOR 8 BOUNDARY CONDITIONS.....	23
FIG 3.5: 1ST MODE BEHAVIOR OF PCB FOR 8 BOUNDARY CONDITIONS.....	24
FIG 3.6: 2ND MODE BEHAVIOR OF PCB FOR 8 BOUNDARY CONDITIONS	24
FIG 3.7: FE MODEL OF PCB FOR 9 BOUNDARY CONDITIONS	25
FIG 3.8: 1ST MODE BEHAVIOR OF PCB FOR 9 BOUNDARY CONDITIONS.....	25
FIG 3.9: 2ND MODE BEHAVIOR OF PCB FOR 9 BOUNDARY CONDITIONS	26
FIG 3.10: FE MODEL OF TRAY FOR 4 BOUNDARY CONDITIONS	27
FIG 3.11: 1ST MODE BEHAVIOR OF TRAY FOR 4 BOUNDARY CONDITIONS.....	27
FIG 3.12: FE MODEL OF TRAY FOR 6 BOUNDARY CONDITIONS	28
FIG 3.13: 1ST MODE BEHAVIOR OF TRAY FOR 6 BOUNDARY CONDITIONS.....	28
FIG 3.14: FE MODEL OF TRAY ASSEMBLED WITH PCB WITH SCREW CONNECTIONS.....	30
FIG 3.15: 1ST MODAL BEHAVIOR OF TRAY ASSEMBLED WITH PCB WITH SCREW CONNECTIONS.....	30
FIG 3.16: FE MODEL OF TRAY ASSEMBLED WITH PCB WITH SCREW CONNECTIONS IN WIREFRAME VIEW	31
FIG 3.17: 1ST MODE BEHAVIOR OF TRAY ASSEMBLED WITH PCB WITH SCREW CONNECTIONS	32
FIG 4.1: AN ASSEMBLED TRAY WITH PCB AND ELECTRONIC COMPONENTS MOUNTED.....	34
FIG 4.2: FE MODEL OF PCB AND APPROXIMATION OF PCB AS MATHEMATICAL MODEL	37
FIG 4.3: FRONT VIEW OF THE PACKAGE.....	43
FIG 4.4: ISOMETRIC VIEW OF THE PACKAGE	43
FIG 4.5: DEPICTION OF PCB AND TRAY	44
FIG 4.6: REPRESENTATION OF TRAY WITH ELECTRONIC COMPONENTS	45
FIG 4.7: ISOMETRIC VIEW OF INTEGRATED VERTICAL STACKED MODULE	46
FIG 4.8: ISOMETRIC VIEW OF INTEGRATED HORIZONTAL STACKED MODULE	46
FIG 5.1: FE MODEL OF PCB.....	53
FIG 5.2: FE MODEL OF HORIZONTAL MOUNTING PACKAGE	54
FIG 5.3: FE MODEL OF VERTICAL MOUNTING PACKAGE.....	54

FIG 5.4: ELEMENTS USED IN FE MODELING	56
FIG 5.5: FE MODELING OF TRAY	57
FIG 5.6: FE MODELING OF TRAY WITH PCB	57
FIG 6.1: MAXIMUM DISPLACEMENT OF VERTICAL MOUNTING ELECTRONIC PACKAGE UNDER 25G LOADING FOR AL6061	62
FIG 6.2: MAXIMUM DISPLACEMENT OF VERTICAL MOUNTING ELECTRONIC PACKAGE UNDER 20G LOADING FOR AL6061	62
FIG 6.3: MAXIMUM STRESS OF VERTICAL MOUNTING EP UNDER 25G LOADING FOR AL6061	63
FIG 6.4: MAXIMUM STRESS OF VERTICAL MOUNTING EP UNDER 20G LOADING FOR AL6061	63
FIG 6.5: MAXIMUM DISPLACEMENT OF VERTICAL MOUNTING ELECTRONIC PACKAGE UNDER 25G LOADING FOR AZ31B	64
FIG 6.6: MAXIMUM DISPLACEMENT OF VERTICAL MOUNTING ELECTRONIC PACKAGE UNDER 20G LOADING FOR AZ31B	65
FIG 6.7: MAXIMUM STRESS OF VERTICAL MOUNTING EP UNDER 25G LOADING FOR AZ31B.....	65
FIG 6.8: MAXIMUM STRESS OF VERTICAL MOUNTING EP UNDER 20G LOADING FOR AZ31B.....	66
FIG 6.9: MAXIMUM DISPLACEMENT OF VERTICAL MOUNTING EP UNDER 25G LOADING (AM162)	67
FIG 6.10: MAXIMUM DISPLACEMENT OF VERTICAL MOUNTING PACKAGE UNDER 20G LOADING FOR AM162.....	67
FIG 6.11: MAXIMUM STRESS OF VERTICAL MOUNTING EP UNDER 25G LOADING FOR AM162	68
FIG 6.12: MAXIMUM STRESS OF VERTICAL MOUNTING EP UNDER 20G LOADING FOR AM162	68
FIG 6.13: MAXIMUM DISPLACEMENT OF HORIZONTAL MOUNTING EP UNDER 25G LOADING FOR AL6061	70
FIG 6.14: MAXIMUM DISPLACEMENT OF HORIZONTAL MOUNTING EP UNDER 20G LOADING FOR AL6061	71
FIG 6.15: MAXIMUM STRESS OF HORIZONTAL MOUNTING EP UNDER 25G LOADING FOR AL6061..	71
FIG 6.16: MAXIMUM STRESS OF HORIZONTAL MOUNTING EP UNDER 20G LOADING FOR AL6061..	72
FIG 6.17: MAXIMUM DISPLACEMENT OF HORIZONTAL MOUNTING EP UNDER 25G LOADING FOR AZ31B	73
FIG 6.18: MAXIMUM DISPLACEMENT OF HORIZONTAL MOUNTING EP UNDER 20G LOADING FOR AZ31B	73
FIG 6.19: MAXIMUM STRESS OF HORIZONTAL MOUNTING EP UNDER 25G LOADING FOR AZ31B ..	74
FIG 6.20: MAXIMUM STRESS OF HORIZONTAL MOUNTING EP UNDER 20G LOADING FOR AZ31B ..	74
FIG 6.21: MAXIMUM DISPLACEMENT OF HORIZONTAL MOUNTING PACKAGE UNDER 25G LOADING FOR AM162.....	75
FIG 6.22: MAXIMUM DISPLACEMENT OF HORIZONTAL MOUNTING PACKAGE UNDER 20G LOADING FOR AM162.....	76
FIG 6.23: MAXIMUM STRESS OF HORIZONTAL MOUNTING PACKAGE UNDER 25G LOADING FOR AM162.....	76
FIG 6.24: MAXIMUM STRESS OF HORIZONTAL MOUNTING PACKAGE UNDER 20G LOADING FOR AM162.....	77

FIG 6.25: FE MODEL OF VERTICAL MOUNTING EP SUBJECTED TO MODAL ANALYSIS.....	81
FIG 6.26: FE MODEL OF HORIZONTAL MOUNTING EP SUBJECTED TO MODAL ANALYSIS	82
FIG 6.27: FUNDAMENTAL FREQUENCY AND MODE SHAPE OF VERTICAL MOUNTING EP (AL6061) .	83
FIG 6.28: FUNDAMENTAL FREQUENCY AND MODE SHAPE OF VERTICAL MOUNTING EP (AZ31B) ..	84
FIG 6.29: FUNDAMENTAL FREQUENCY AND MODE SHAPE OF VERTICAL MOUNTING EP (AM162)..	84
FIG 6.30: FUNDAMENTAL FREQUENCY AND MODE SHAPE OF HORIZONTAL MOUNTING EP FOR AL6061	85
FIG 6.31: FUNDAMENTAL FREQUENCY AND MODE SHAPE OF HORIZONTAL MOUNTING EP FOR AZ31B	86
FIG 6.32: FUNDAMENTAL FREQUENCY AND MODE SHAPE OF HORIZONTAL MOUNTING EP FOR AM162.....	86
FIG 6.33: WHITE- NOISE CURVE WITH A CONSTANT INPUT POWER SPECTRAL DENSITY (PSD	90
FIG 6.34: INPUT CURVE OF POWER SPECTRAL DENSITY (PSD) USED FOR SPACECRAFT.....	91
FIG 6.35: TRANSMISSIBILITY OF VERTICAL EP AT NODE 140816 FOR AL6061 MATERIAL.....	94
FIG 6.36: PSD CURVE AT NODE 140816 OF VERTICAL MOUNTING EP FOR AL6061 MATERIAL.....	95
FIG 6.37: TRANSMISSIBILITY OF VERTICAL EP AT NODE 139052 FOR AZ31B MATERIAL	97
FIG 6.38: PSD CURVE AT NODE 139052 OF VERTICAL MOUNTING EP FOR AZ31B MATERIAL	98
FIG 6.39: TRANSMISSIBILITY OF VERTICAL EP AT NODE 140720 FOR AM162 MATERIAL	101
FIG 6.40: PSD CURVE AT NODE 140720 OF VERTICAL MOUNTING EP FOR AM162 MATERIAL.....	101
FIG 6.41: TRANSMISSIBILITY OF HORIZONTAL EP AT NODE 432328 FOR AL6061 MATERIAL.....	104
FIG 6.42: PSD CURVE AT NODE 432328 OF HORIZONTAL MOUNTING EP FOR AL6061 MATERIAL	105
FIG 6.43: TRANSMISSIBILITY OF HORIZONTAL EP AT NODE 398116 FOR AZ31B MATERIAL.....	107
FIG 6.44: PSD CURVE AT NODE 398116 OF HORIZONTAL MOUNTING EP FOR AZ31B MATERIAL.	108
FIG 6.45: TRANSMISSIBILITY OF HORIZONTAL EP AT NODE 437040 FOR AM162 MATERIAL	110
FIG 6.46: PSD CURVE AT NODE 437040 OF HORIZONTAL MOUNTING EP FOR AM162 MATERIAL	111

List of Tables

TABLE 3.1: PROPERTIES OF VARIOUS MATERIALS USED IN ELECTRONIC PACKAGES	19
TABLE 3.2: MODAL VALUES OF PCB FOR VARIOUS BOUNDARY CONDITIONS.....	26
TABLE 3.3: MODAL VALUES OF TRAY FOR VARIOUS BOUNDARY CONDITIONS.....	29
TABLE 3.4: MODAL VALUES OF TRAY FOR VARIOUS RIB THICKNESS	32
TABLE 3.5: MODAL VALUES OF TRAY FOR VARIOUS RIB THICKNESS WITH VARIOUS MATERIAL PROPERTIES.....	33
TABLE 5.1: FINITE ELEMENT DETAILS USED IN FE MODEL	55
TABLE 6.1: COMPARISON OF MAXIMUM STRESS AND DISPLACEMENT OF VERTICAL MOUNTING PACKAGE FOR AL6061, AZ31B AND AM162 MATERIALS	69
TABLE 6.2: COMPARISON OF MAXIMUM STRESS AND DISPLACEMENT OF HORIZONTAL MOUNTING PACKAGES FOR AL6061, AZ31B AND AM162 MATERIALS	78
TABLE 6.3: CALCULATIONS OF FOS FOR MAXIMUM STRESS OF BOTH TYPE OF MOUNTINGS FOR ALL THREE MATERIALS	79
TABLE 6.4: DETAILS OF ELEMENT USED IN FE MODEL	82
TABLE 6.5: COMPARISON OF FUNDAMENTAL FREQUENCY FOR DIFFERENT MATERIALS	87
TABLE 6.6: DIFFERENT MODES OF FREQUENCY AND MASS PARTICIPATION FOR AL6061 MATERIAL WITH Y- DIRECTION ENFORCED MOTION	93
TABLE 6.7: DIFFERENT MODES OF FREQUENCY AND MASS PARTICIPATION OF AZ31B MATERIAL WITH Y- DIRECTION ENFORCED MOTION	96
TABLE 6.8: DIFFERENT MODES OF FREQUENCY AND MASS PARTICIPATION OF AM162 MATERIAL WITH Y- DIRECTION ENFORCED MOTION	99
TABLE 6.9: COMPARISON FOR VERTICAL MOUNTING PACKAGE WITH DIFFERENT MATERIALS.....	102
TABLE 6.10: DIFFERENT MODES OF FREQUENCY AND MASS PARTICIPATION FOR AL6061 MATERIAL WITH Z- DIRECTION ENFORCED MOTION.....	103
TABLE 6.11: DIFFERENT MODES OF FREQUENCY AND MASS PARTICIPATION OF AZ31B MATERIAL WITH Z- DIRECTION ENFORCED MOTION.....	105
TABLE 6.12: DIFFERENT MODES OF FREQUENCY AND MASS PARTICIPATION OF AM162 MATERIAL WITH Z- DIRECTION ENFORCED MOTION.....	109
TABLE 6.13: COMPARISON FOR HORIZONTAL MOUNTING PACKAGE WITH DIFFERENT MATERIALS	112
TABLE 6.14: COMPARISON OF MASS DETAILS OF BOTH TYPE OF EP WITH DIFFERENT MATERIALS	112

Chapter 1

INTRODUCTION

1.1 Overview

In spacecraft technology, electronics play a significant role in communication, attitude and orbit control, power distribution, on-board housekeeping and other payload related functions. So, safeguarding electronics and to guarantee its reliability is of utmost importance. Generally aerospace industry aims at designing and producing systems which have a life of not less than 20 years. To achieve the level of expectations of the aerospace industry great emphasis is laid on the complicated and delicate structure of electronic systems. The spacecraft structures are subjected to various forms of vibration over wide frequency ranges and acceleration levels during launch and on-orbit course. These induced vibrations greatly affect the functionality of electronic packages, which holds electronic components and devices within a spacecraft. According to study, vibration factors account for about 27% in the environmental cause of airborne electronic equipment failure. So, the study of dynamic characteristics of electronic equipment becomes essential to ensure performance of electronics in intended manner.

The spacecraft has electronic packages to perform different functions like control, guidance, power supply and distribution, data handling, navigation, guidance, propulsion subsystem, telecommunication, guidance, landing system etc. Electronic system used in defence equipment such as, missiles, communication system and control devices in submarines, helicopters, submarines and ships operate in severe environment condition. A study has been observed most electronic components failures because of a high temperature, for example, thermal loading and thermal shocks. Components failure rate of spacecraft specifically the launch survival is the main mechanical issue and the failure of electronic hardware as per the mechanical perspective, over 50% are because of a thermal problem, 25% because of vibration issues, 20% are because of humidity and 5% are because of dust and different reasons.

The function of EP in spacecraft mission is to provide reliable support to the electronic circuit and their safety, signal sharing, heat dissipation, power distribution and manufacturability and serviceability etc. EP is a multidisciplinary area encompassing mechanical, electronics,

chemistry, physics, industrial engineering, mathematics etc. The electronic packaging form a part of the spacecraft mass budget and optimizing their mass with the use of advanced materials and innovative design could substantially contribute in the overall mass saving of the spacecraft.

The advancement of technology has paved the way for innovative designs, creation of new materials and more information about service requirements. Several studies are performed to analyze and isolate vibration in electronic systems. Hence, packaging of electronic components must consider the factors related to the mechanical failures, cooling/heating, radio frequency, and protection from an electrostatic discharge etc. In order to have a reliable on-orbit operational life (ranging between 5–20 years), these spacecraft electronic packaging must have stiff enclosures built up of materials having enhanced desirable mechanical properties. Hence, it is important to design and test the EP to ascertain that there should be no failures which may be critical to the spacecraft mission.

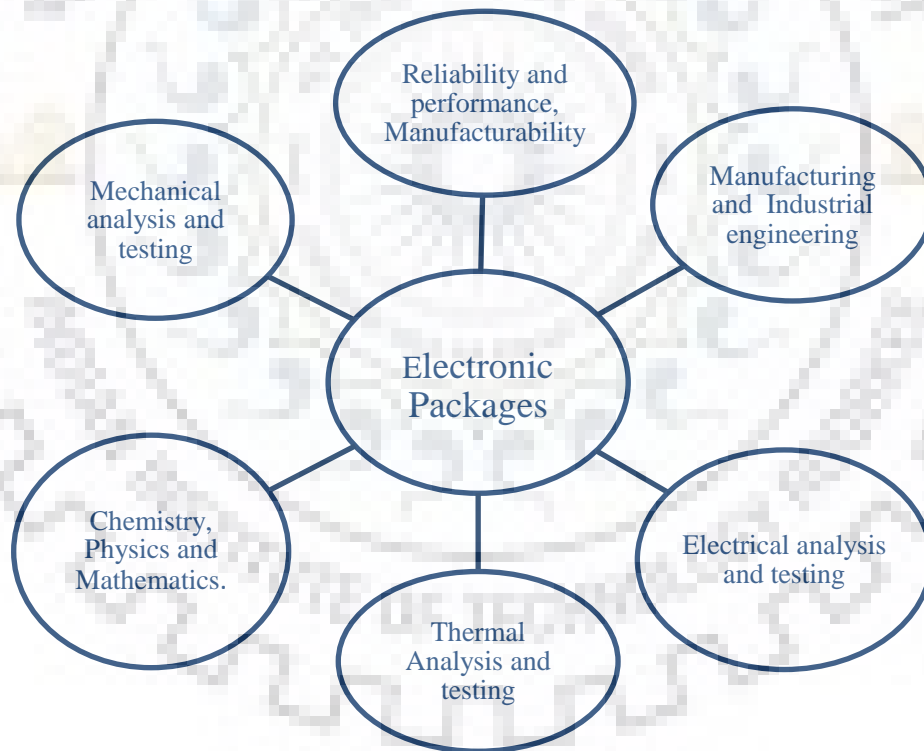


Fig 1.1: Interdependence of electronic packages on various disciplines

Printed Circuit Boards are the key part in electronic devices, which supports other vital electronic components such as resistors, diodes, capacitors etc. When the electronic components

get mounted on the electrical circuit and the components are soldered to the board, and then it is called Printed Circuit Board assembly.

Printed Circuit Boards are used in various fields,

- Avionic industries such as spacecraft, aerospace industries, and military systems to perform intended functions.
- Common products, including computers, mobiles, etc.
- High reliability systems, such as equipment's where continuous performance is essential of paramount importance.

The electronic components such as resistors, diodes, capacitors etc., are to be protected from harsh vibration environment, which can lead to high large displacements when large forces are applied on them and in turn can develop high dynamic stresses which lead to resonance and damage to the structure.

Mechanical housings for electronic packages are specifically designed to safeguard these electronic components against failure caused by unfavorable environmental conditions. The design of these electronic packages should be in such a way that it is capable of meeting the desired specifications for dynamic loading, strength, weight and should be able to perform with greater reliability. Several studies have been carried out on electronic packages to analyze and minimize the vibration response such that they work efficiently.

The scope of this work is to design the electronic package having a reliable lifespan of about 15-20 years with enhanced performance in spacecraft applications. The design of complex structures of electronic systems requires extra care in order to achieve high reliability in the field of spacecraft industries. The determination of dynamic response of spacecraft electronic packages play very important role in order to maximize their survival during the launch environment.

In this work an electronic package of a spacecraft has been considered, which is modeled using UG-NX (an FE software). The FE model is analyzed to study the static and dynamic responses considering various parameters with different boundary conditions and materials. The post processing is carried out using MSC-NASTRAN as a solver.

In design and analysis of mechanical housings for spacecraft electronic packages, different parameters has to be considered such as, selection of material, geometrical considerations types of loads and boundary conditions imposed on packages.

Fabrication of EP requires materials possessing the characteristics such as low density, high stiffness & strength, increased fatigue life, homogeneous, extended life, simplicity, ease of fabrication and should be economical.

The packaging assembly consists of PCB (over which electronic components are mounted) and then this PCB is assembled into a single mechanical module. PCBs are generally aligned / assembled into box/tray like structures which is called 'Electronic Package' and are retained in position by screws. PCBs are extremely delicate in nature, depending on the environmental condition, structure, material utilized and its application area. Few numbers of such mechanical modules comprise the electronic package assembly.

The optimal design of the packages and the study of various boundary conditions become necessity in order to avoid failure in electronic devices. This keeps them safe from failures during the harsh launch and space environment. In the analysis, different boundary conditions, different materials, varying the thickness of package has been considered. Iterations are carried out for different parameters to optimize the design.

1.2 Design of the Electronic Package

The EP structure is used to protect and support the PCB's and other electronic devices. It is important to determine the natural frequency of the PCB and package for their safety during dynamic loading. If the frequency of the package and PCB are same or closer to one another, it may prompt be coupling of their transmissibility and resonance of electronic system may occur, leading to failure of the packages. Hence to avoid this resonance EP is designed according to the octave standard. According to octave principle natural frequency of the PCB should be twice than the package. This is shown by Eq-1.1,

$$O_f = \frac{f_{PCB}}{f_{PACKAGE}} \geq 2 \quad (\text{Eq-1.1})$$

EP is usually consisting of one or more trays to mount PCB's. Fig 1.2 shows typical electronic package. Fig 1.3 shows exploded view of EP.

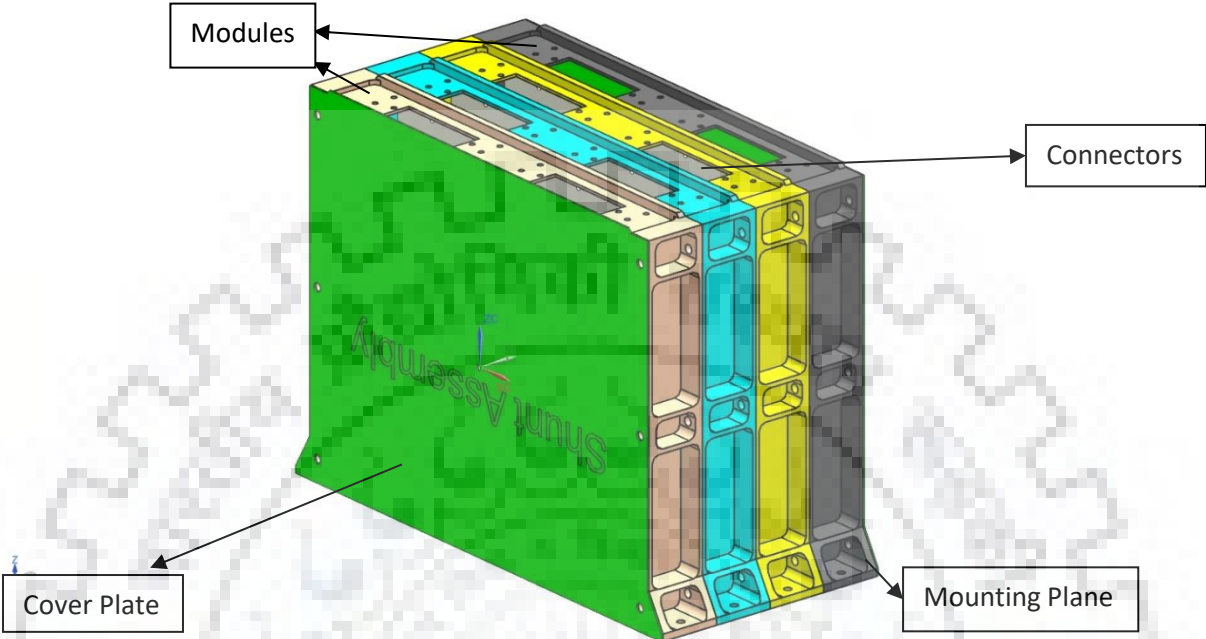


Fig 1.2: Typical power electronic package

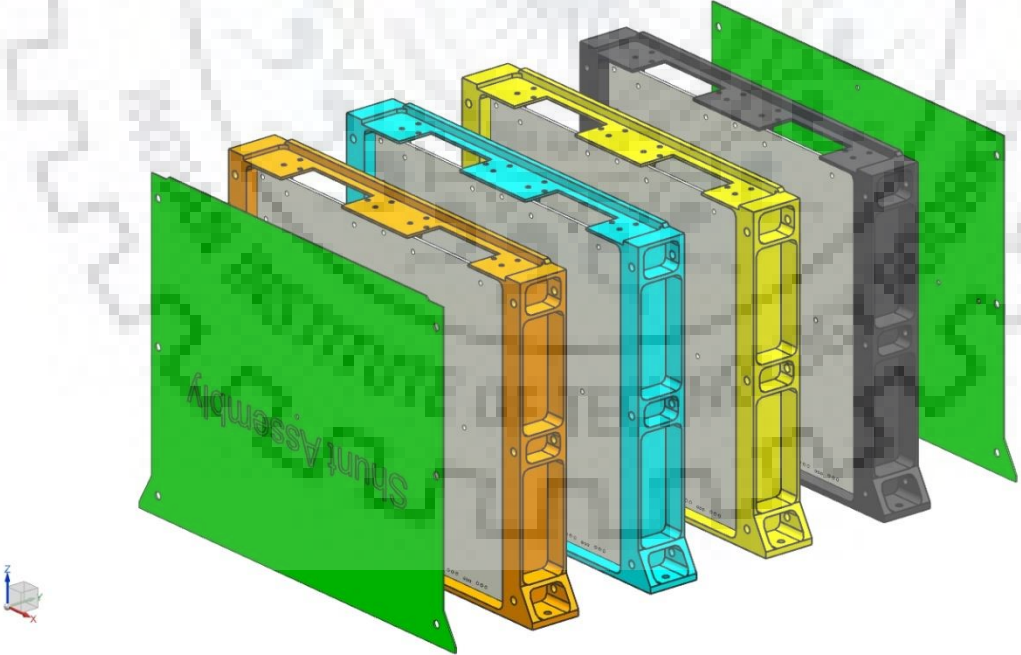


Fig 1.3: Exploded view of vertical stacked electronics packages

1.3 Types of Electronics Packages

Electronics packages are classified on the basis of their functionality. Some packages are used in the spacecraft for power generation so these packages are called power electronic packages. Like that some packages are used for data storage and data handling, these are called data handling packages, some packages function is to control the spacecraft motion in the orbit, these are called On Board Control packages.

On the basis of mounting orientation, all packages are divided into two categories:

1. Vertical Mounting Electronics Packages
2. Horizontal Mounting Electronics Packages

Electronics packages consist of PCBs and for giving enough support, mechanical housing is made with sufficient no. of mounting locations for PCBs. Complete packages are divided into modules or mechanical trays that are used to give enough support to PCBs.

Therefore, if the mounting location of packages on the spacecraft is such that the mounting plane of the package is parallel to the mounting plane of the PCB then this type of package is called horizontal mounting packages and if the mounting location of packages on the spacecraft is such that the mounting plane of the package is perpendicular to the mounting plane of the PCB then this type of package is called vertical mounting packages.

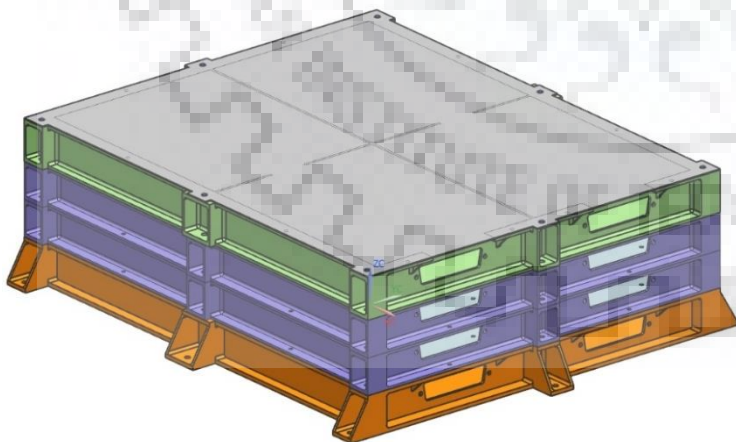


Fig 1.4: Horizontal mounting package

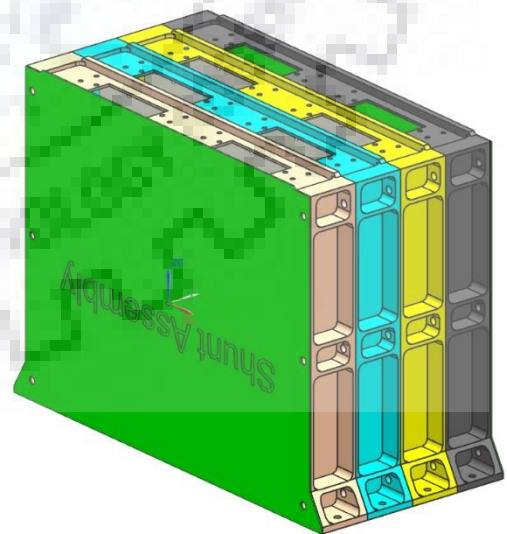


Fig 1.5: Vertical mounting package

Chapter 2

LITERATURE SURVEY

Studies on electromechanical structures under vibration impact are critical and lot of analysis is performed to isolate vibration in electronic equipment's. Normal issues brought on by mechanical vibration are cracks, contact and short circuits, which propagate failure of electronic parts. Many researchers have studied different objectives to understand the vibration behavior of electronic components. Extensive literature survey has been done and these studies are presented hereunder.

Steinberg [1] presented analytical and empirical methods for analyzing vibration of electronic assemblies.

Apparently Steinberg's model is the best known empirical model for the purpose of estimating the life of component subjected to vibration (Steinberg 1973, 1988, 2001). Steinberg first published his referenced book, *Vibration Analysis for Electronic Equipment*, in 1973. He revised this book twice, in 1988 and in 2001. His approach was purely based on testing and experience. His first model is as follows:

$$d = 0.003 X b \quad \dots\dots\dots (Eq-2.1)$$

Where, d is the maximum board displacement, and b is the dimension of the shorter side of a rectangular PCB.

The PCB is modeled to be a single degree of freedom system in which the maximum displacement should be below 0.003 X b which is given by Eqn 2.1. Later he designed a little more complex model with respect to the critical displacement accounted for the style, size, and component location on the PCB. However the model failed to work outside the range and configuration of the assembly specified in the derivation of the model.

Steinberg's critical PCB displacement value is determined empirically. Figure 2-1 shows that the calculated displacement of the PCB differs from the actual displacement as it is a fictitious value correlated assuming the PCB to be a simple spring mass system. Steinberg also assumed that the PCB was simply supported along all four edges. Steinberg assumed that the maximum damage

due to fatigue occurred at the center of the PCB, which is the point of maximum displacement and maximum curvature. A position factor is employed to measure the damage of components mounted at other discrete positions. Steinberg's empirical equation is simple and user friendly in estimating the fatigue life of a component subjected to random vibration. The latest model includes different package styles. For example, in Equation (2-2) the constant c for a standard dual inline package will be 1; but for the BGA the constant will be 2.25. This factor c adjusts the life for packages that are not as robust as the standard dual inline package.

$$Z_0 = \frac{0.00022B}{chr\sqrt{L}} \dots\dots\dots (Eq-2.2)$$

where, Z_0 - Maximum or critical PWB displacement (in), B - Length of PCB edge parallel to component (in), L - Length of electronic component (in), h - Height or thickness of PWB (in), r - Relative position factor for component on printed board, c - Constant for different types of electronic components.

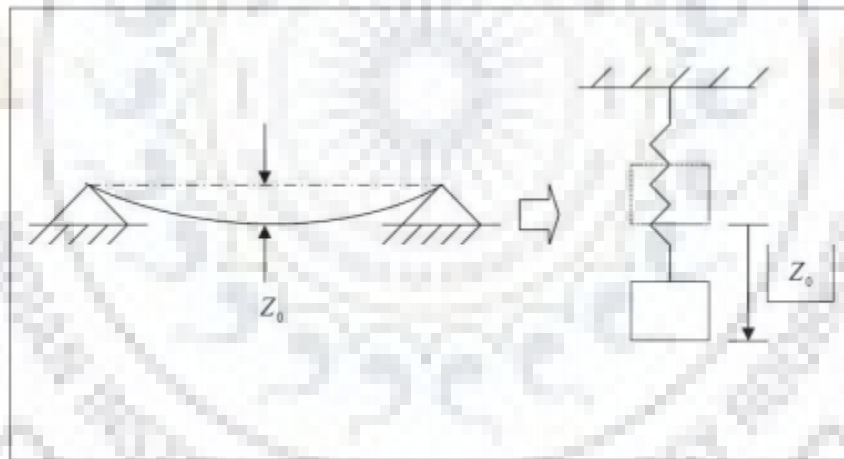


Fig 2.1: Correlation of displacement of PCB with spring mass system

As soon as the maximum or critical PCB displacement is calculated on the basis of board, package style and dimensions, the actual PCB displacement is calculated considering the specific vibration exposure. Steinberg frequently recommended estimation of actual PCB displacement with a fictitious displacement calculated assuming the PCB to be a simple single degree of freedom system which resulted in the calculation of displacement from the natural frequency as given in the Equation (2-3).

$$Z_o = \frac{0.2485 * G_{in} * Q}{f_n^2} \dots\dots\dots (Eq-2.3)$$

Where, Z_o is the displacement in meters, G_{in} is the input acceleration in units of G, f_n is the natural frequency in units of cycles/second or Hz, and Q is the transmissibility of the system (approximated as the square root of the natural frequency).

Veprík [2] studied the isolation of electronic assemblies from vibration and explained the vibration of such type of systems as follows:

“In spite the fact that electronic box is a complex, sometimes nonlinear, dynamic structure containing sensitive internal components, the design for vibration isolation normally relies on the traditional simplified linear model of flexural suspended body.”

Thus he used a double degree-of-freedom mass, spring and damper system to solve vibration isolation problems related to electronic box (Figure 2-2).

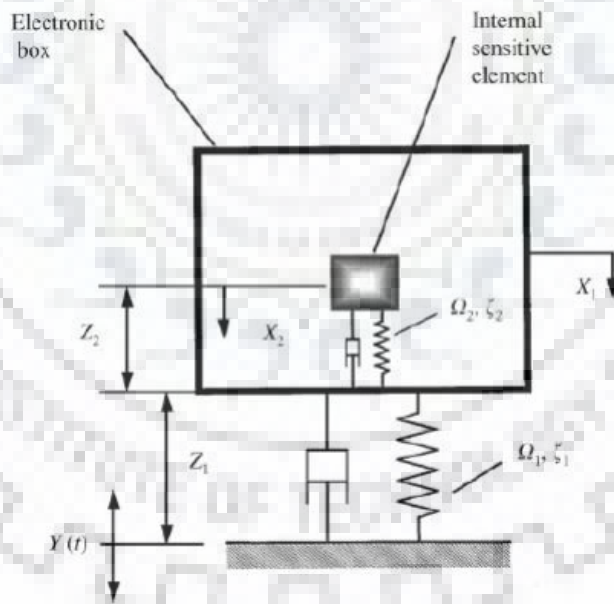


Fig 2.2: Dynamic model of vibration-isolated electronic box containing PCB

Veprík and Babitsky laid emphasis on the dynamic response of the printed circuit board so as to perform vibration isolation of electronic packages. This approach resulted in improved protection of the electronic packages from harmonic and random vibration as compared to traditional

approaches where isolation is based on compromising damping and stiffness properties of mounts.

Ho, Veprík and Babitsky also studied ruggedized design of printed circuit board. They designed a miniature wideband dynamic absorber and showed that it can suppress the dynamic response of the system theoretically and experimentally. The printed circuit board was modeled to be a multi degree of freedom system as higher modes were also important in this analysis.

Suhir [3] studied component vibrations in electronic equipments. He derived a formula for the natural frequency of a heavy electronic component mounted on a circuit board with a plated through hole.

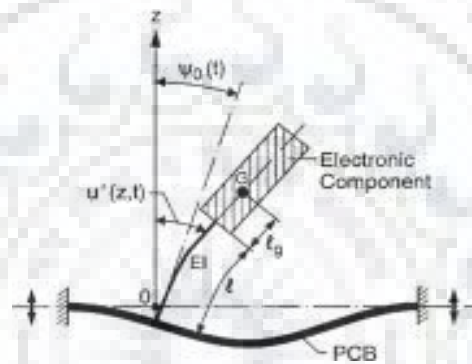


Fig 2.3: Heavy electronic component mounted on a PCB

Esser and Huston [4] worked on an active mass damping of printed circuit boards, assumed PCB to be a lumped mass. They did not consider the continuous vibration modes since they were only interested in the first mode of the PCB.

Jung et al. [5] studied the structural vibrations of an electronic component by using analytical modeling, finite element modeling and testing. In their analytical model they assumed PCB to be a 1 DOF structure. They solved the problem by applying Steinberg's formulations for natural frequency and maximum desired displacement.

Cifuentes [6] also carried out studies and research to identify factors affecting the dynamic behavior of PCB. He faced four issues (i) validity of estimates based on the first mode of vibration, (ii) geometric nonlinearities, (iii) component location on the board, and (iv) mass and stiffness values.

Perkins and Sitaraman [7] conducted an investigation of the effects on the vibration characteristics of an electronic system because of electronic component. They performed vibration experiments and developed an analytical model for observing the effect of solder joint stiffness and mass of the component on the natural frequencies and mode shapes of the system (Figure 2-4).

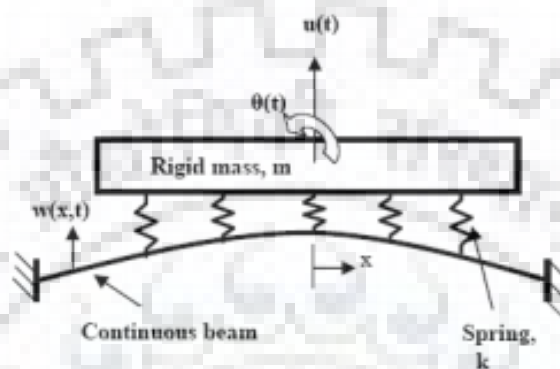


Fig 2.4: Analytical model to observe natural frequencies

They also predicted failure locations and behavior of the failed solder joints using the method of finite element analysis. Their results showed that the attached component on the printed circuit board leads to the fall of natural frequency because of the added mass; however localized stiffness is imparted to the PCB. They also observed the fact that solders in the vicinity of the clamped boundaries suffers the maximum bending and fails at the earliest.

Cifuentes and Kalbag [8] studied optimization of supported locations of a PCB which influences the values of natural frequency of PCB. They used finite element modeling in their solutions.

Liguore and Followell [9] studied the fatigue caused in solder joints because of the vibrations. They conducted investigation on the effect of location, size and type of component (leadless vs leaded). Results indicated that the smaller components mounted at regions where vibration responses were higher had longer fatigue lives in comparison to the larger components mounted on a lower amplitude area. Moreover the test results of three different sizes of components unveiled that the fatigue life is logarithmically inversely proportional to the diagonal length of the component. Furthermore the significant observation indicated the increase in durability of leaded components exposed to vibration loading than the leadless components.

Schaller [10] laid emphasis on the wide capabilities of finite element modeling to assess the dynamic behavior of microelectronic components. However, he faced the drawback in attaining accurate properties of material and boundary conditions related to the system. Thus he noted the value of laboratory testing. He modeled lead wires as stiffness components or beam elements. He increased the effects of components by increasing the board's modulus of elasticity and density 20 in those regions. After analyzing the wedge locks and connectors, he modeled them as torsional springs and springs respectively.

Veilleux [11] confronted with the controlling of the destructive resonant amplitude of printed circuit boards in electronic systems. He compared isolation, extensional damping and shear damping techniques for decrease in the value of resonant amplitude. He carried out his studies by performing vibration tests and revealed that the shear damping techniques offers the foremost solution in controlling the vibration.

Pitarresi [12] employed different approaches of finite element modeling for PCB vibrations and showed comparison of the results obtained with the outcomes of experiment.

Lau and Keely [13] conducted an investigation on the lead dynamics with and without solder joints. They used the method of finite element analysis for obtaining the values natural frequencies, and validated their results by performing vibration tests on a Laser Doppler Vibrometer. Results revealed that the fundamental frequency of the soldered lead is at least five times higher than the unsoldered lead. This proved the significance of the quality of solder joint in affecting the fatigue life of a component.

Ham and Lee [14] also investigated the effect of vibration on lead wire fatigue life. By constructing a fatigue test set-up, they applied a constant frequency vibration load and measured the electrical resistance in the lead. Depending on these measurements, they obtained the component's fatigue life. Their study showed that thermal loading is not the only reason for lead fatigue; vibration is also an important issue in an electronic system's fatigue life.

Aglietti and Schwingshackl [15] emphasized the importance of structural dynamic analysis in electronic equipments. They considered three requirements (i) withstanding the required random vibration spectrum, (ii) avoiding coupling, (iii) withstanding launch loads at low frequencies.

McKeown [16] studied vibration problems in electronic equipment by considering the whole system in three levels: component, module and chassis levels. He reviewed available vibration analysis methods for each level. He also stressed out importance of modal testing to avoid inherent assumptions and simplifications included in analytical techniques. He suggested some useful approaches in finite element modeling related to component, board and chassis. He recommended to model leads by using beam elements, and components by using solid elements. He mentioned that the components are usually modeled by smearing the component mass over the printed circuit board. He also noted that this assumption will fail if the component significantly influences stiffness, and when this is the case the component must be modeled separately. He pointed out possible reasons for finite element solution inconsistencies with test results, which are listed as (i) boundary conditions do not match the actual situation, (ii) material types improperly assigned, (iii) total mass of the model does not match total system mass, and (iv) frequency range of the analysis does not match the input environment.

2.1 Objectives of the present work

Based on the literature review and the gap areas identified, the objectives of the present work are formulated as follows:

- To study the effect of boundary condition on mechanical behaviour of Electronics packages.
- Since there is a need to reduce weight of EP, so study by using alternative space qualified materials which suits the requirement of EP design.
- To investigate about the vibration load on mechanical housing of EP for these alternative space qualified materials by Vibration analysis during launch time. Vibration analysis includes:
 - Quasi-static Mode
 - Normal mode analysis
 - Random mode analysis (20-2000 Hz)

Chapter 3

METHODOLOGY AND ANALYSIS PROCEDURE

3.1 Problem Definition

Electronic packages are subjected to high vibration levels during the spacecraft launch, so effective design has to be proposed incorporating all possible design considerations such as material selection, various boundary conditions, and rib thickness etc., a proper design should avoid failure of electronic package due to resonance under vibrational loads.

3.2 Project Methodology

In designing an electronic package, several vital factors are to be considered which includes material selection, selection of boundary conditions, thickness of ribs, layers of PCB, resonating frequency of adjacent components, acceleration levels etc.,

3.2.1 Selection of material

Electronic packaging is a multidisciplinary subject, comprising of material selection, physical configuration, analysis procedure, fabrication process and advancement of a package. The material selection and design emphasis to electronic products vary significantly, depending on the intended application, spacecraft industry, aerospace, defence equipment, industrial equipment etc. In order to achieve successful electronic packaging, it is required to identify the suitable material, relevant field of innovation and arrangement related to the design issues.

Appropriate material selection for the packages of electronic equipments so as to withstand the loads during launch is of great concern nowadays. From a material reliability aspect, important materials issues include high stiffness, high strength, lighter weight, high young's modulus and so on.

Selection of material for making the structure of a component is a significant task in space applications both for complex and simple designs and even in the case of miniature ones.

However the ultimate choice of a material is rather challenging as there are several factors that needs to be analyzed diligently in the first place. Strength may be the basic aspect but there are

other factors as well such as high frequency, low density, high young's modulus, electrical properties (like EMI, EMC etc.) that plays an important role in performance and application of the system.

Hence the requirements need to be identified primarily so as to fulfill the desired purpose in the form of mechanical, thermal, environmental, electrical, and chemical properties. Further on the basis of defined requirements, selection is carried out by making use of elimination method. Process of material selection also employs fabrication method.

The factors such as high young's modulus, low density, tensile strength, flexural strength and fatigue endurance are examined properly for selecting the materials that raise the possibility of a successful design. However there are chances for a design to fail in actual working conditions under the application of load higher than the expected mainly because of the unpredicted vibrations and high induced stresses.

Following points describes major consideration and process of material selection in electronic packaging.

1. It should be space qualified and possess good specific stiffness (E/ρ).
2. Good thermal conductivity and electrical conductivity.
3. It should have radiation shielding properties.
4. It should have thermal coating compatibility.
5. Total mass loss (TML) in vacuum should be low.
6. Material availability, ease of fabrication, design legacy etc.
7. Material cost, which includes not only about cost but also ease of manufacturing the structural materials and environment friendly.

There should be elementary understanding of physical phenomena in electronic packaging technology. During analysis, assumptions considered in analytical model are implemented on the package. For creating a successful design of similar packages, it is beneficial to compare the outcomes of a selected material with other successful known materials so as to finalize the decision.

Avionics systems require reduction in weight, while needing to increase the first mode frequency of the system to decouple the package suite from the systems frequencies, in order to minimize the stress from vibration [17].

Material properties

This section briefly describes the important material properties which are required in electronic packaging technology.

i. Strength

The materials are selected in the design of electronic package is based on tensile strength, compressive strength, and yield strength. Not only strength but it also includes types of loading such as, bending, torsion, axial loading or combination of both. Since many of the pure metals do not meet the specific requirements, hence there is a need to switch to alloys as they possess high strength heat treatment. Alloys are selected on the basis of density, yield strength, tensile strength, etc.

ii. Density

Density of a material is quantitative articulation of the measure of mass contained per unit volume. This property is utilized as a part of area of material and design to reduce the heaviness of package. Low density not only reduces the weight of the design, but it also affects the frequency of mechanical elements. Hence the extent to which it is influenced by mechanical vibration and mechanical shock loading is to be decided on the other factors.

iii. Heat capacity

The heat capacity is defined as the amount of heat which is required to bring a change in temperature by unity and its unit is energy per degree. It is an extensive variable thus a considerable quantity of matter possess high value of heat capacity. For spacecraft applications, considered material should carry out the heat generated within the electronic package and provide an optimum environment for working of electronics. So, the

material should have high heat carrying capacity and materials like AL6061 and AZ31B have good heat carrying capacity.

iv. Fatigue resistance

It is characterized as the loss of physical strength, service life and failure of a material because the structural components are subjected to repeated loads or cyclic loads. Such loads may be the mechanical stress which happens because of mechanical load induced during the service life of the packages. Thermal stresses which occur during the temperature cycle due to vibration and mechanical impact shock loads.

v. Young's modulus

It is a measure of stiffness of the material and is a feature employed to characterise the material. It is defined as the ratio of the stress along an axis to the strain. It is also known as elastic modulus. Higher the value of 'E' of the material, higher the stress carrying capacity and lower the deformation, thereby material is more stiff and it leads to higher first frequency in the package.

Due to the repeated loading on the packages small incremental cracks are formed, and the crack propagation occurs within and accumulates and ultimately leads to the failure of package. The real expectation of the package failure is because of fatigue damage, it is highly sensitive to load, structure of the part, development points of interest, and variety in temperature. Hence it is obliged to analyze and test the materials and configuration design to avoid the fatigue damage. It is required to have a rise in the first fundamental frequency of a spacecraft electronic packages while reduction in weight. This is carried out to decouple the frequencies of the electronic package to that of the spacecraft structural elements which results in preventing resonance.

The advancement in avionic technology and continuous increase in packaging density requires high young's modulus to attain high fundamental frequency for the electronic packages by keeping their weight at optimum levels Reduction in weight also reduces the stresses resulting from vibration shock, loads that can occur during launch environment and service life of the spacecraft electronics. Traditional materials such as AL6061 and AZ31B which are being used in

electronic packaging are not capable of meeting the desired requirements. As a result, new materials are being developed for fulfilling the same objective.

As per the above features, the material to be selected is the one which fulfills the above requirements satisfactorily. Three materials have been observed as per our requirements which are:

- a) Aluminium alloy (AL6061)
- b) Magnesium alloy (AZ31B)
- c) Beryllium-Aluminium alloy (AM162)

Table 3-1: Properties of various materials used in electronic packages

Properties/Material	Aluminium Alloy (AL6061)	Magnesium Alloy (AZ31B)	Beryllium- Aluminium (AM162)
Young's Modulus (GPa)	72	46	193
Poisson's ratio	0.33	0.3	0.17
Density (kg/m ³)	2780	1770	2100
Ultimate Tensile strength (MPa)	320	220	413
Shear strength (MPa)	190	130	345
Coefficient of Thermal Expansion (ppm/°C)	23.6	25.2	13.9
Specific stiffness (GPa/g/cc)	25.89	25.98	91.9
Electrical resistivity (nΩ-m)	39.9	92.2	35.5
Thermal conductivity (W/m.K)	170	70	210
specific heat capacity (J/g °C)	0.896	1	1.4

These three materials suits aptly for the fabrication of electronic packages. The various advantages and disadvantages of each material is discussed below.

Aluminium alloy (AL6061) -Available in tube rods, sheets and other profiles.

Advantages	Disadvantages
<ol style="list-style-type: none"> 1. Good strength to weight ratio 2. Corrosion resistance 3. Ductile in nature 4. Aesthetic appeal 5. Can be recycled economically 	<ol style="list-style-type: none"> 1. Difficult to join 2. low strength to volume 3. Expensive of raw material 4. High coefficient of thermal expansion

Magnesium alloy (AZ31B) - Available in sheet, rods.

Advantages	Disadvantages
<ol style="list-style-type: none"> 1. High specific strength 2. resistance to ageing 3. better electrical and thermal conductivity 4. Good machinability 5. Recyclable 	<ol style="list-style-type: none"> 1. Low stiffness 2. Low elastic modulus 3. High degree of shrinkage

Beryllium-Aluminium alloy (AM162) - Available in extruded bar, rolled sheet.

Advantages	Disadvantages
<ol style="list-style-type: none"> 1. High young's modulus, low density 2. High strength, stiffness and ease of fabrication 3. Light weight and used in spacecraft and aerospace application. 4. Minimizes the stress from vibration. 5. Reduced section thickness 6. Increase fatigue life of electronic packages 7. Design flexibility 8. Higher first mode frequency 	<ol style="list-style-type: none"> 1. Utmost care needs to be taken during machining due to the toxicity of the Be-Al particle, after it gets air-borne. 2. High cost

3.2.2 Need for Modal Analysis:

- a) For the purpose of examining the dynamic interaction between a component and its supporting structure. Dynamic load amplification is considerable when the natural frequency of the supporting structure is near to the operating frequency.
- b) For analysing the influence of changes in design on the dynamic characteristics.
- c) For making use of the modes in a subsequent forced response analysis.
- d) For taking the natural frequencies as a guide to select the proper time or frequency step for transient and frequency response analyses
- e) For the purpose of assessing the degree of correlation between modal test data and analytical results.

Neither the applied load nor the damping properties of the structure exist in normal modes analysis.

3.2.3 Selection of boundary conditions

Electronic packages produce large dynamic displacements in high vibration and shock environment, when their natural frequencies are excited. Due to this large displacement between the EP and PCB, the electronic components mounted on the PCB, in between the components and its connecting leads may generate a significant amount of stress and strain that may result into failure. In order to avoid such type of failure proper selection of boundary condition in between the PCB and EP is important.

The proper selection of BC's to power electronic packaging is not only limited to minimize the displacement, but also to get desired natural frequency levels, to avoid resonance between the EP and spacecraft equipment panels on which they are mounted.

Here the BC's in FE modeling are also known as constraints or restraints to the PCB and package and refers to the screw locations where the packages are mounted to the fixture. In electronic packaging defining these BC's play an important role to avoid the displacement and provide better fixity to the PCB and mechanical housing.

As increasing the BC's to EP the natural frequency goes on increasing, it is not a good practice to select BC's randomly, because of space constraints in spacecraft and also to avoid the

reduction of stiffness of other structure. Increases in the natural frequency generally, is associated with low displacement, low stress and strains. Similarly, a low natural frequency may lead to large displacements, increase in the dynamic stresses and strains on the package. Different cases are studied here to select proper boundary conditions for the EP.

3.2.3.1 EFFECT OF BOUNDARY CONDITIONS (BCs) ON PCB

Case 1) PCB fixed at 4 locations

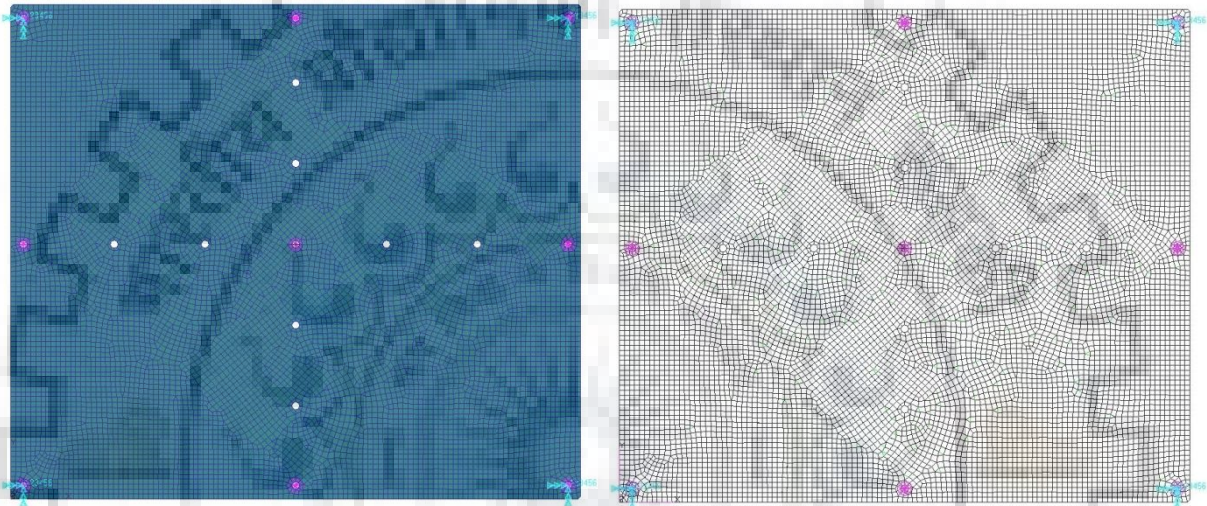


Fig 3.1: FE Model of PCB (a) Solid mesh depiction (b) Wireframe mesh depiction

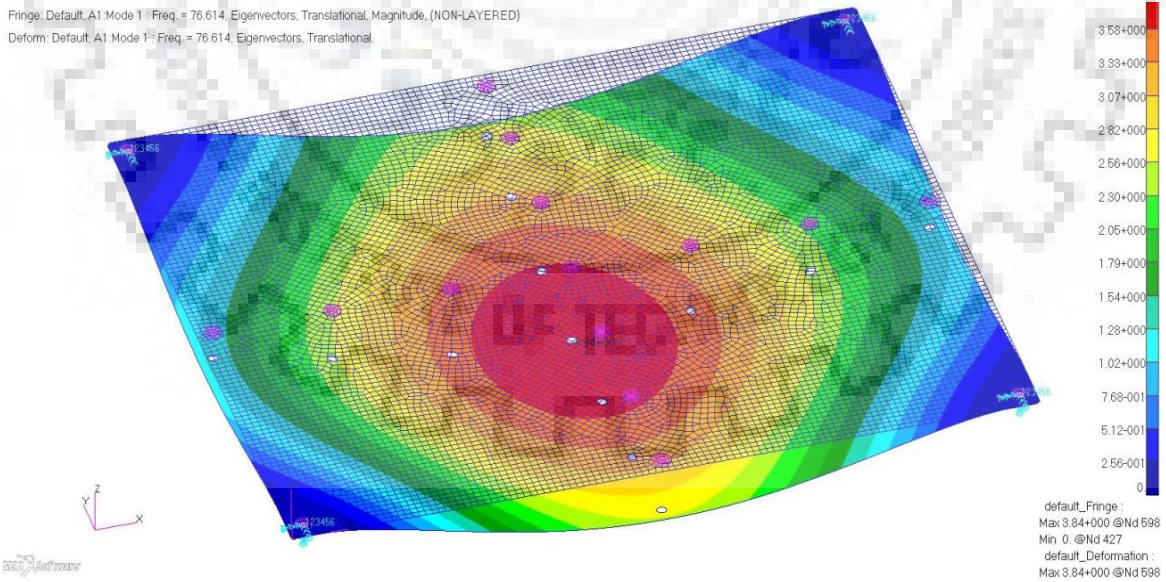


Fig 3.2: 1st Mode behavior of PCB for 4 boundary conditions

Fringe: Default, A1 Mode 2 : Freq. = 146.3, Eigenvectors, Translational, Magnitude, (NON-LAYERED)
Deform: Default, A1 Mode 2 : Freq. = 146.3, Eigenvectors, Translational.

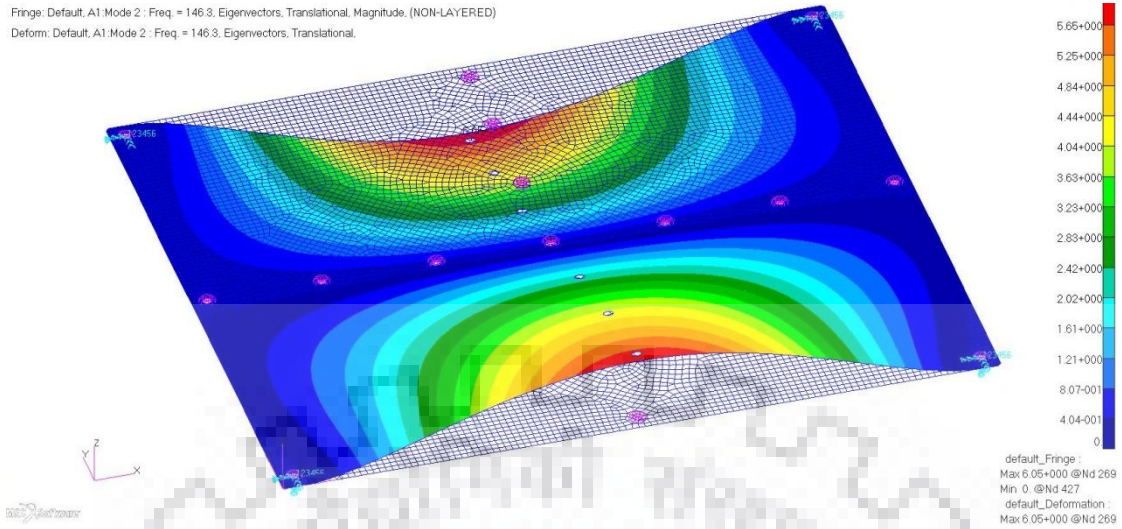


Fig 3.3: 2nd Mode behavior of PCB for 4 boundary conditions

Case 2) PCB fixed at 8 locations.

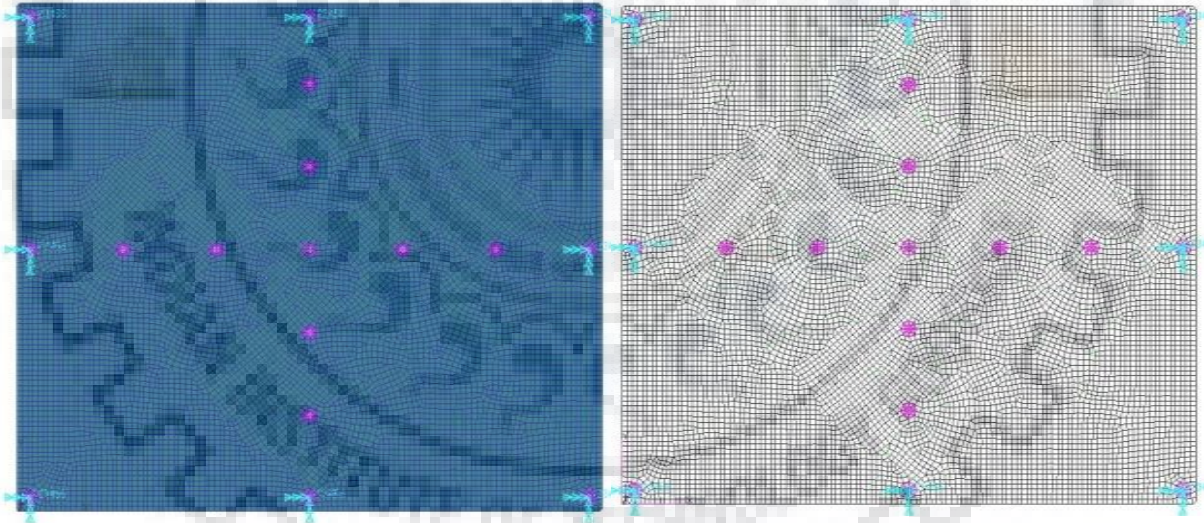


Fig 3.4: FE Model of PCB for 8 Boundary conditions

Fringe: Default, A1 Mode 1 : Freq. = 191.91, Eigenvectors, Translational, Magnitude, (NON-LAYERED)
Deform: Default, A1 Mode 1 : Freq. = 191.91, Eigenvectors, Translational.

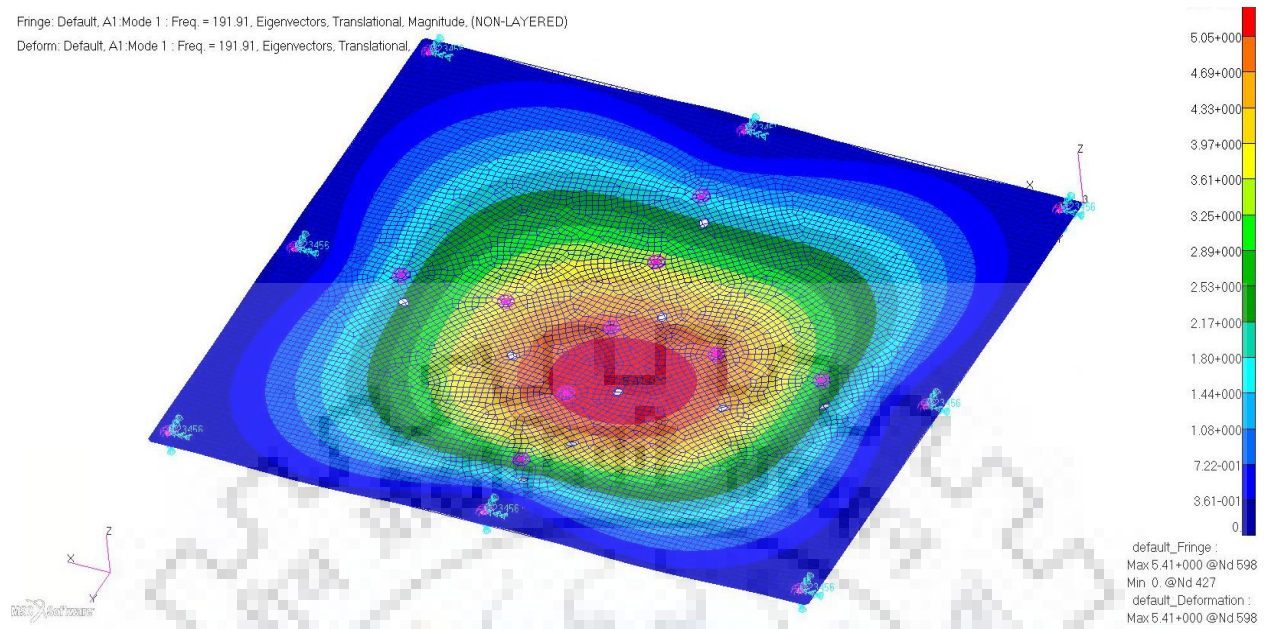


Fig 3.5: 1st Mode behavior of PCB for 8 boundary conditions

Fringe: Default, A1 Mode 2 : Freq. = 313.89, Eigenvectors, Translational, Magnitude, (NON-LAYERED)
Deform: Default, A1 Mode 2 : Freq. = 313.89, Eigenvectors, Translational.

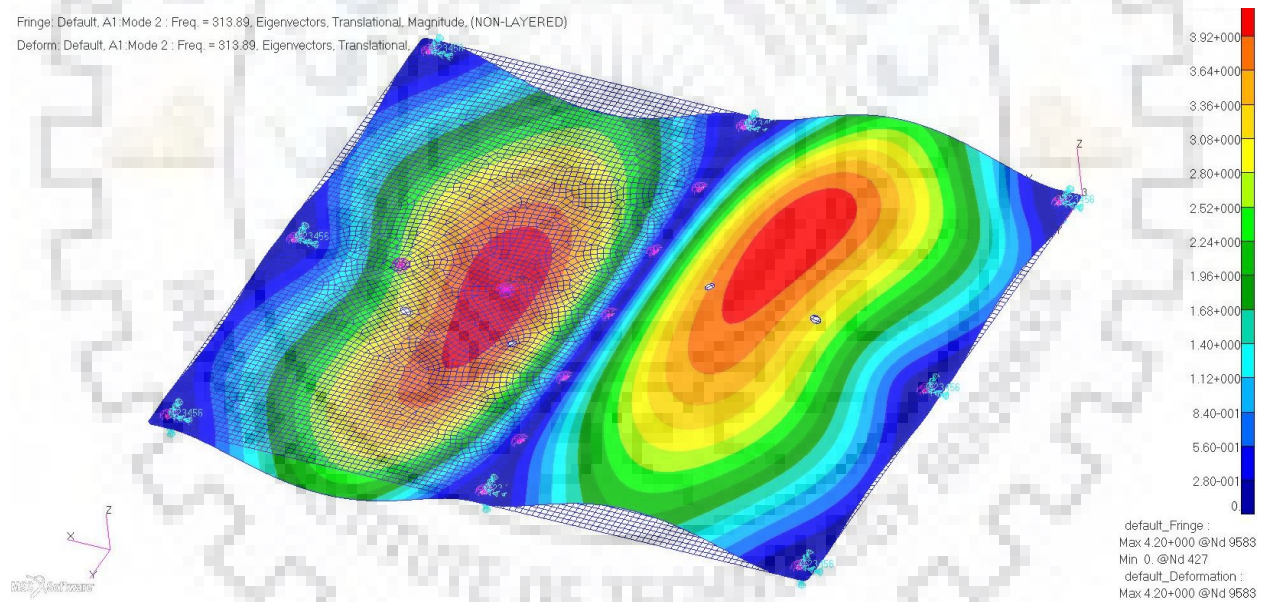


Fig 3.6: 2nd Mode behavior of PCB for 8 boundary conditions

Case 3) PCB fixed at 9 locations

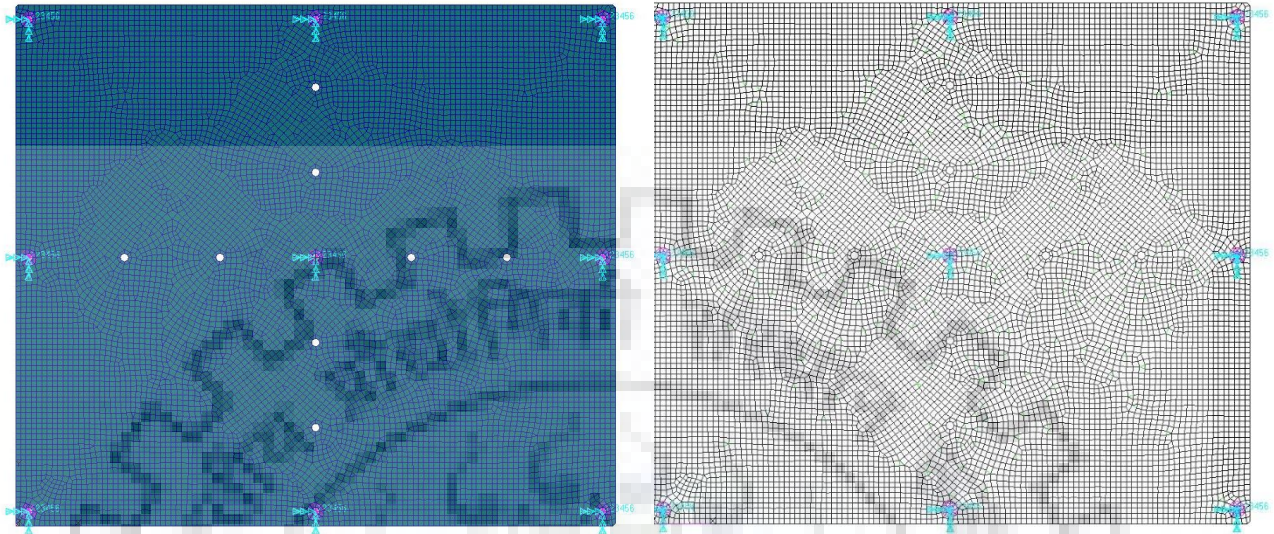


Fig 3.4: FE Model of PCB for 9 boundary conditions

Fringe: Default, A1 Mode 1 : Freq. = 340.89, Eigenvectors, Translational, Magnitude, (NON-LAYERED)
Deform: Default, A1 Mode 1 : Freq. = 340.89, Eigenvectors, Translational.

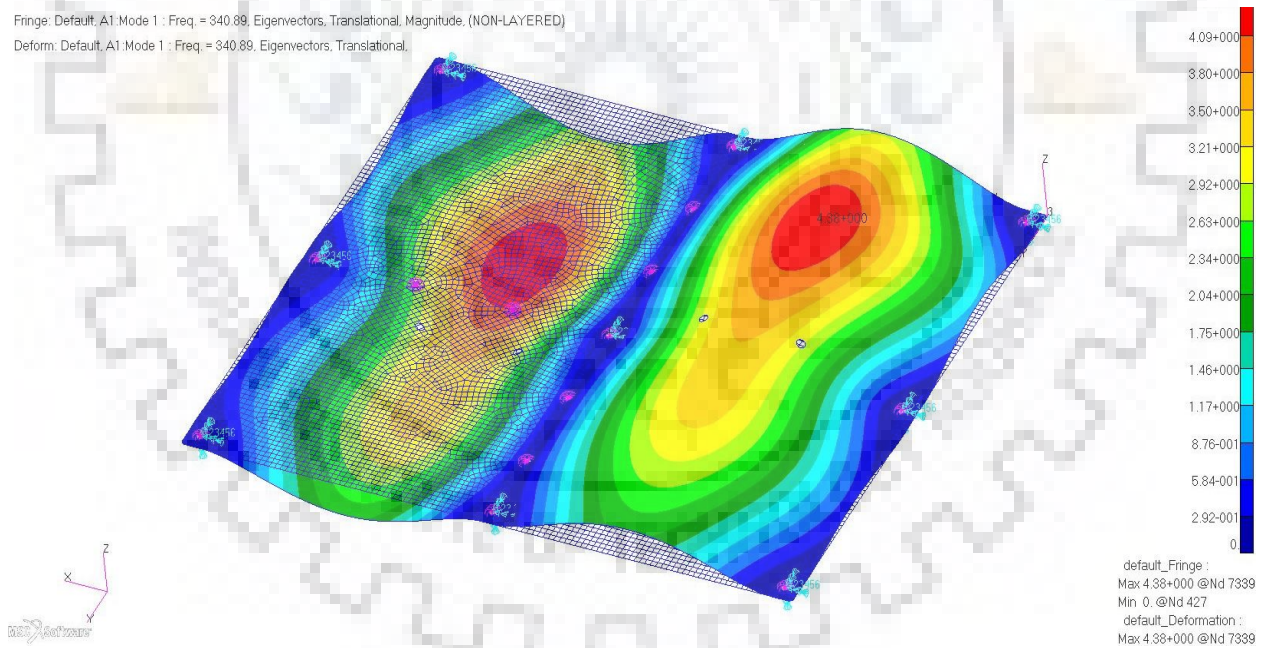


Fig 3.8: 1st Mode behavior of PCB for 9 boundary conditions

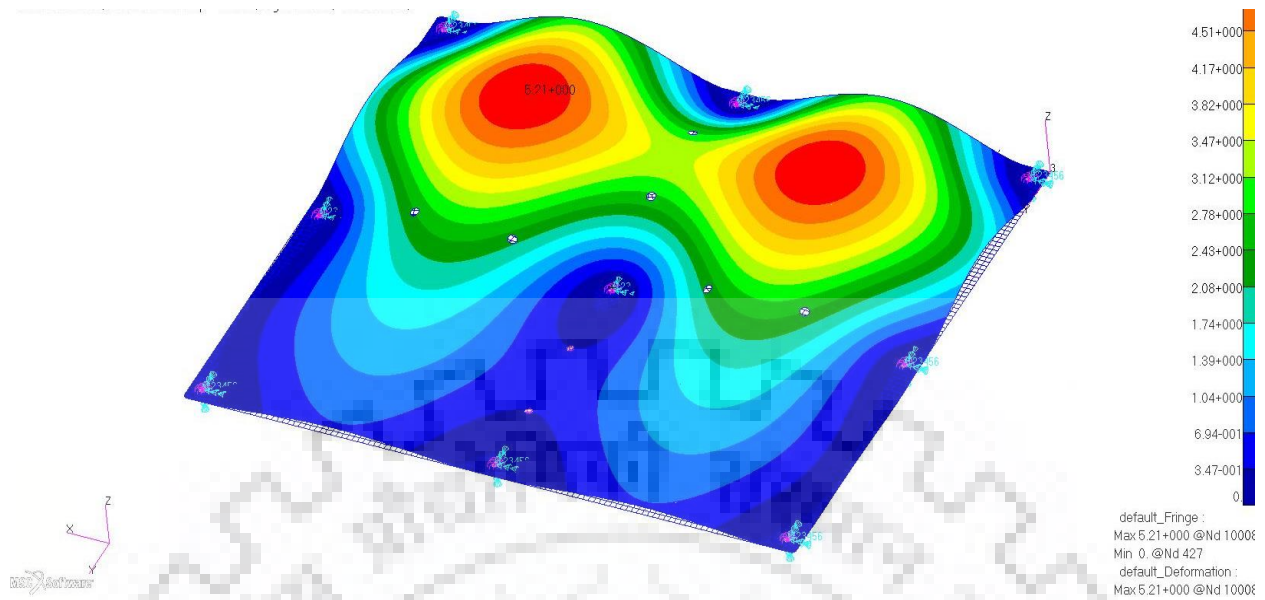


Fig 3.9: 2nd Mode behavior of PCB for 9 boundary conditions

Table 3.2: Modal values of PCB for various boundary conditions

Sl. No.	Modal Values of PCB (Hertz)			
	4 Boundary Conditions	8 Boundary Conditions	9 Boundary Conditions	All Boundary Conditions
1	76.614	191.9	340.89	464.87
2	146.3	313.89	365.92	483.29
3	164.1	364.95	388.57	494.88
4	190.65	387.9	392.38	512.03
5	328.6	505.3	614.78	705.93

From the above obtained values from FE Analysis, we can observe that as the number of boundary conditions increase, fundamental frequency of PCB increases. This increment is because the stiffness of PCB increases as boundary condition increases. So, PCB with 4BCs, 8 BCs, 9 BCs have low fundamental frequency than PCB with 17 BCs which is 464.87 Hertz, which is well above 100 Hertz for designing of Electronic Package.

3.2.3.2 EFFECT OF BOUNDARY CONDITIONS ON TRAY

Case 1) Tray fixed at 4 locations

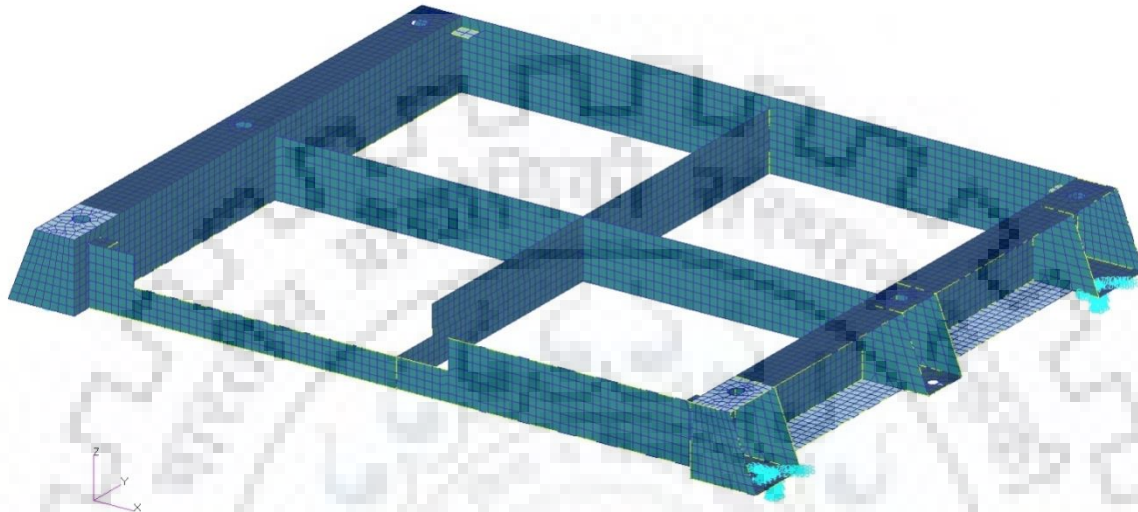


Fig 3.10: FE Model of tray for 4 boundary conditions

Fringe: Default, A1 Mode 1 : Freq = 148.73, Eigenvectors, Translational, Magnitude, (NON-LAYERED)
Deform: Default, A1 Mode 1 : Freq = 148.73, Eigenvectors, Translational,

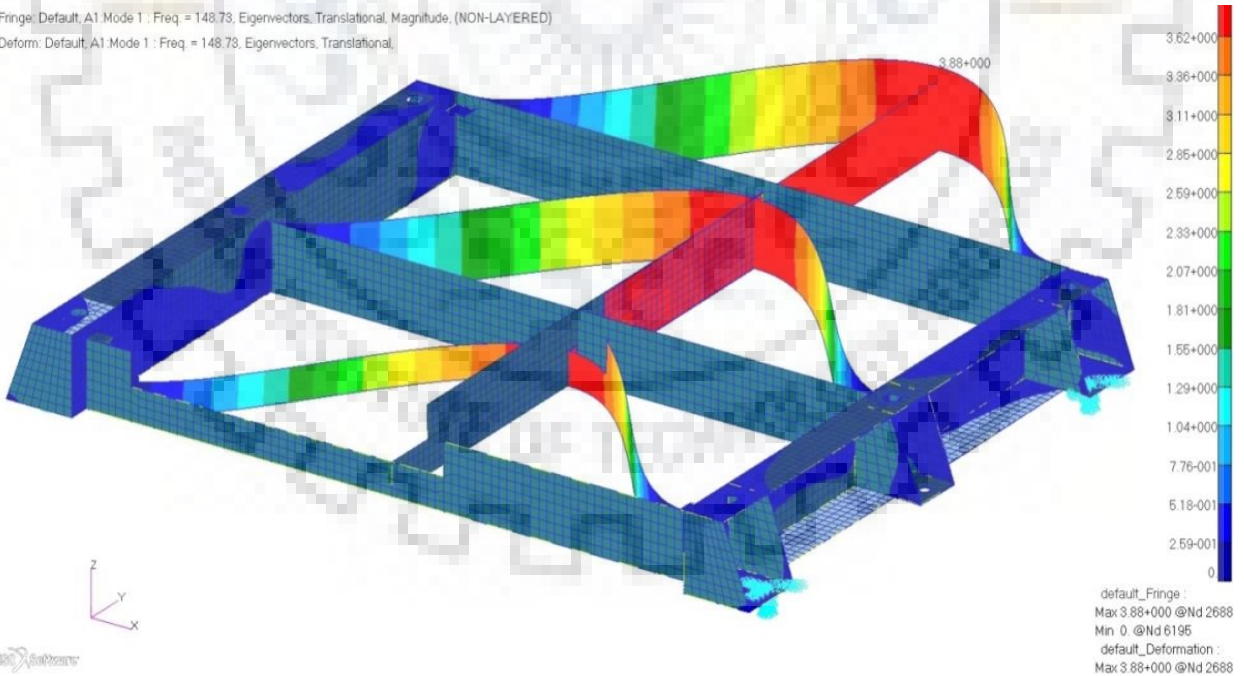


Fig 3.11: 1st Mode behavior of tray for 4 boundary conditions

Case 2) Tray fixed at 6 locations

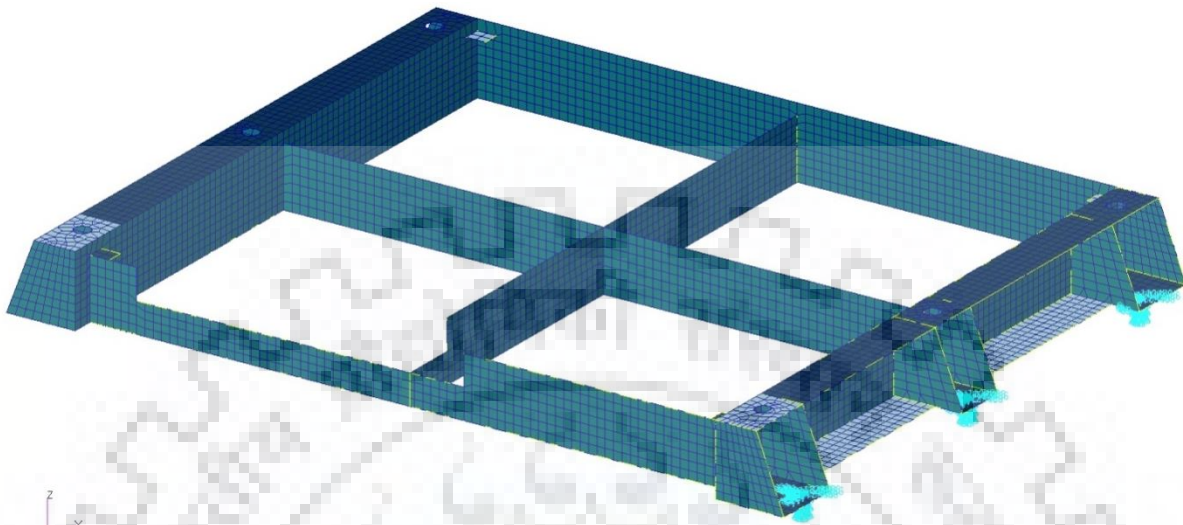


Fig 3.12: FE Model of Tray for 6 boundary conditions

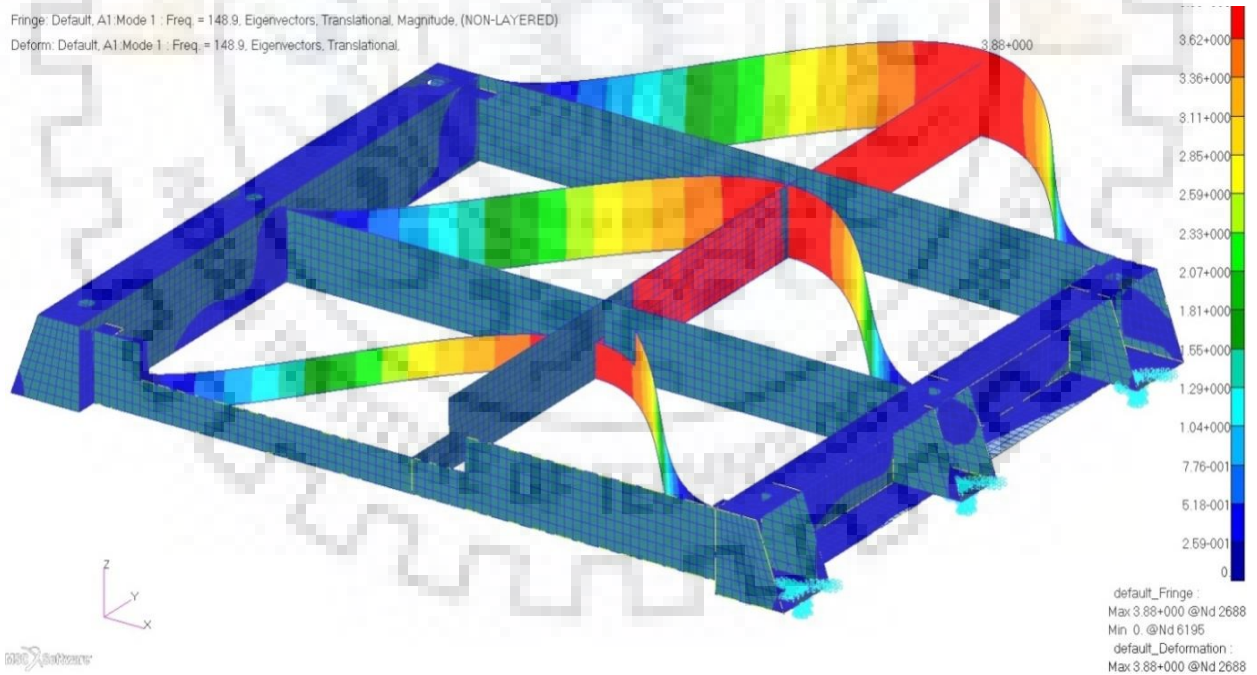


Fig 3.13: 1st Mode behavior of tray for 6 boundary conditions

Table 3.3: Modal values of tray for various boundary conditions

Sl. No.	Modal Values of Tray	
	4 Boundary Conditions (Hertz)	6 Boundary Conditions(Hertz)
1	148.73	148.9
2	508.64	509.19
3	530.53	530.77
4	533.64	600.84
5	601.09	634.34

From the above obtained values from FE Analysis, we can observe that as the number of boundary conditions increase, fundamental frequency or the first modal frequency increases. This increment is because the stiffness of module increases as the number of boundary conditions increase.

So, module with 6 screw locations i.e., 6 BCs is preferred over 4 BCs, as the fundamental frequency of module with 6 BCs is 148.9 Hertz, which is well above 100 Hertz for designing of Electronic Package module.

3.2.3.3 Behavior of Module with PCB

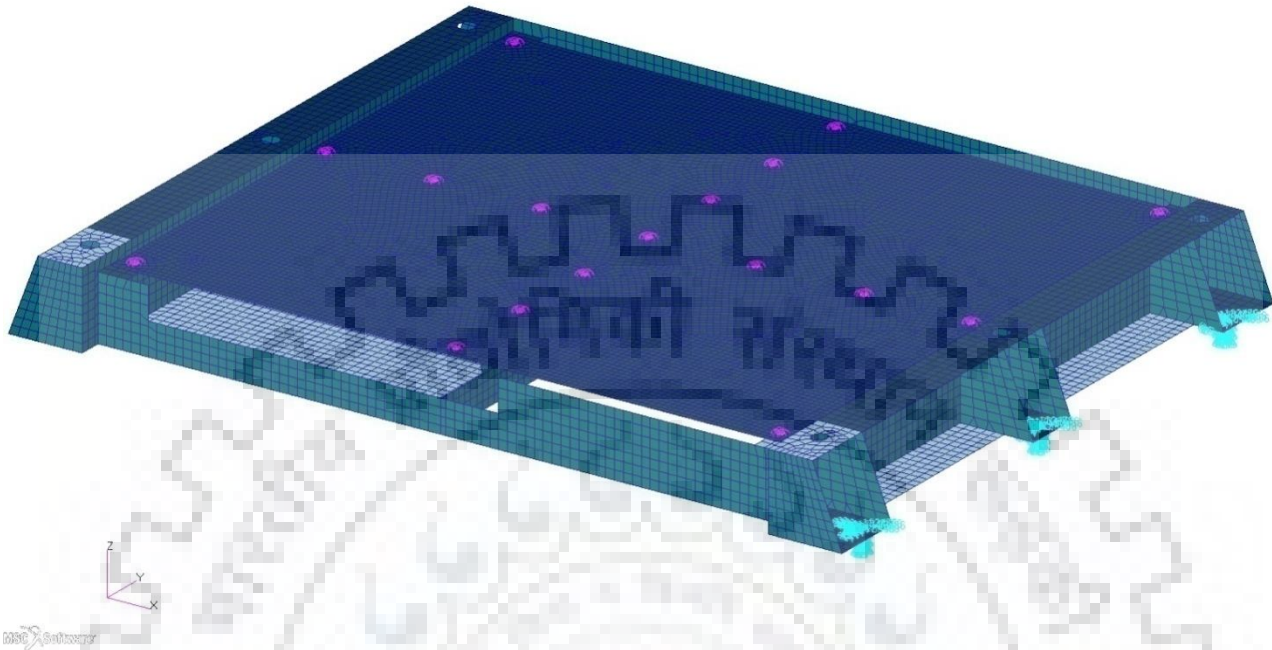


Fig 3.14: FE Model of tray assembled with PCB with screw connections

Fringe: Default, A1 Mode 1 : Freq. = 436.4, Eigenvectors, Translational, Magnitude, (NON-LAYERED)
Deform: Default, A1 Mode 1 : Freq. = 436.4, Eigenvectors, Translational.

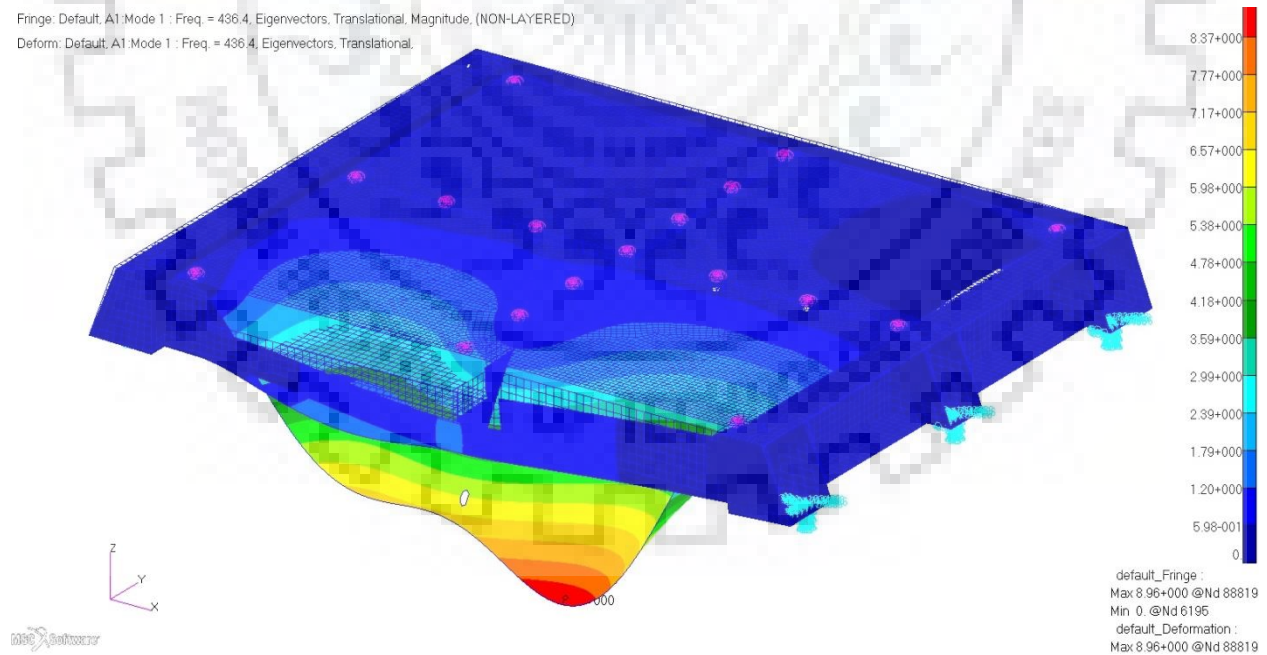


Fig 3.15: 1st modal behavior of tray assembled with PCB with screw connections

3.2.4 Effect of rib thickness

Vibration testing experience with damping techniques has shown that damping can be quite effective for PCBs with low natural frequencies, below about 50 Hz. However, the tests show that stiffening ribs usually work even better. When the natural frequencies are well above about 100 Hz damping is not a very effective means for reducing the transmissibility. High operating temperatures also tend to reduce the damping properties and effectiveness of viscoelastic materials. Constrained layer damping strips take away valuable space that could be used for mounting additional electronics. When this space is already lost, experience has shown that it is often much better to use the space for bonding stiffening ribs to the PCB, instead of constrained layer damping strips.

Stiffening ribs will increase the natural frequency, which will more rapidly reduce the dynamic displacements, because displacements are inversely related to the square of the natural frequency.

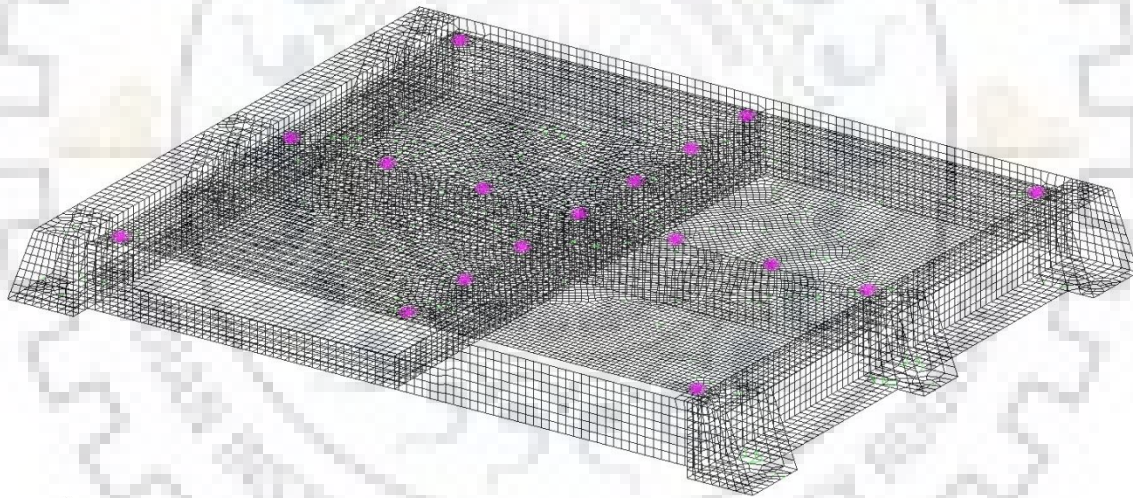


Fig 3.16: FE Model of tray assembled with PCB with screw connections in wireframe view

From the FE analysis values Table 4.4, it can be inferred that as the rib thickness increases, the moment of inertia increases because the depth of cross section increases according to,

$$I = \frac{bd^3}{12} \text{ For rectangular cross – section}$$

Where, I = Moment of Inertia,

d = Depth of rib,

b = Breadth of rib.

Fringe: Default, A5, Mode 1 : Freq. = 437.03, Eigenvectors, Translational, Magnitude, (NON-LAYERED)
 Deform: Default, A5, Mode 1 : Freq. = 437.03, Eigenvectors, Translational.

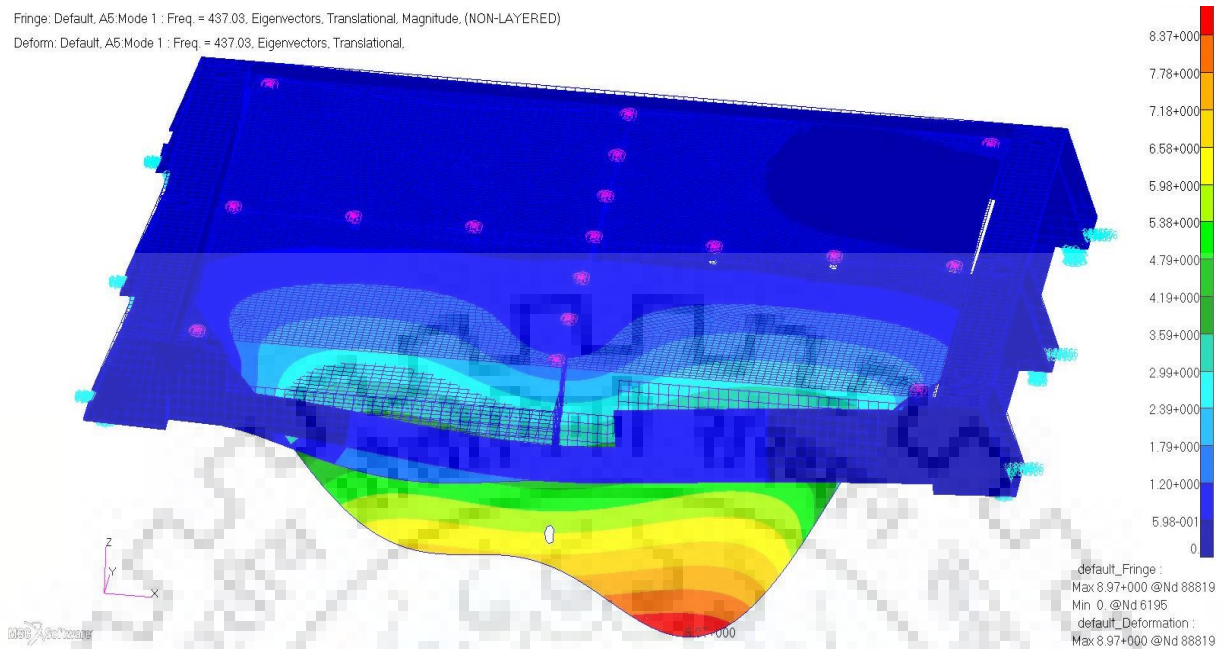


Fig 3.17: 1st mode behavior of tray assembled with PCB with screw connections

Table 3.4: Modal values of tray for various rib thickness

Sl. No.	Modal Values in Hertz with Rib Thickness				
	1 mm	1.5 mm	2 mm	2.5 mm	3 mm
1	384.37	491.74	505.29	512.91	517.23
2	419.87	560.76	582.02	589.42	594.54
3	442.81	571.15	602.93	613.66	616.11
4	469.81	578.75	609.95	617.35	624.92
5	510.59	604.51	724.31	762.18	759.67

It is observed that as the depth of rib increases the moment of inertia of tray increases substantially as I is varying with cube times of depth. But in our case the increase in depth is constrained by the size of tray and also the electronic components which are to be mounted on it. So, breadth is increased which also increases the stiffness of module increases and in turn frequency of the entire module increases. From table, for rib thickness of 2 mm frequency value is 505.29 Hz but for 2.5 mm it raises to 512.91 Hz and for 3 mm thickness corresponds to 517.23 Hz.

3.2.5 Effect of material composition

Table 3.5: Modal values of tray for various rib thickness with various material properties

Sl. No.	Al Alloy (AL6061)		Mg Alloy (AZ31B)		Be – Al Alloy (AM162)	
	1mm	2mm	1mm	2mm	1mm	2mm
1	384.88	425.43	377.05	412.81	404.95	449.33
2	420.6	433.01	405.57	419.36	449.24	459.92
3	443.28	476.45	435.67	465.03	460.47	497.5
4	470.55	490.36	456.5	474.74	502.42	521.62
5	510.15	550.93	499.79	539.22	624.13	648.61

From the above three materials, selection has to be made in such a way that the material suits the functionality specifications. Beryllium Aluminum alloy is almost half dense of the Al Alloy and there is lot of weight saving, and the fundamental frequency values of Be – Al Alloy is high compared to other materials. Also Young's modulus of Be – Al Alloy is 193 GPa which proves to be more stiffer than Al alloy which has a Young's modulus of 70 GPa.

Apart from above considered factors, such as orientation of mounting, placement of package within satellite etc. are also to be considered. So, according to the above carried out analysis, Be – Al Alloy material is chosen for design with rib thickness of 2 mm. PCB of 10 layered FR4 material is used with mounting at 17 locations using M3 screws of 6 length. PCB is mounted onto the module using M4 screws at 6 locations. With the above mentioned pre – requisites FE Modeling and Analysis is carried out which is explained in the subsequent chapters.

Chapter 4

CONCEPTUAL MODELLING OF THE PACKAGE

4.1 Design considerations for PCB

Electronic box provides support to PCBs with respect to its weight, cost, environmental conditions, accessibility and ease of maintenance. For example, in a vacuum environment where there is no air to provide convection heat transfer, heat will often be conducted from the circuit board to a heat exchanger. High-pressure thermal interfaces must then be provided, using materials that have a high thermal conductivity, in order to prevent excessive temperatures from developing in the electronic components mounted on the circuit boards. Screws are ideal for providing high-pressure interfaces.



Fig 4-1: An assembled tray with PCB and electronic components mounted

The response behavior of the boards when subjected to shock and vibrations can be determined by identifying the kind of support provided to the PCBs in the electronic box. If the electronic box is fabricated from light sheet metal and manufacturing tolerances are loose, a loose fit is desirable for the plug-in circuit boards. This will permit easy connector engagement, with a fixed connector position, when there is a substantial mismatch in the mating box connector. This type of installation is not desirable, however, for a system that will be subjected to severe vibration

and shock. A loose circuit board will often develop high acceleration loads, which will lead to high deflections and stresses in the electronic component parts mounted on the circuit boards. The edges of the PCBs should be supported if they will be subjected to severe vibration or shock environments. Availability of board edge guides helps in supporting various kinds of PCBs. These guides are usually fabricated of beryllium copper, but they are also available in a wide range of metals and molded plastics.

It is desirable to have a board edge guide for the purpose of gripping the edge of a PCB strongly. When the edge rotates or translates, deflections are supposed to occur. However, with the firm grip of the edge, deflections are reduced thus increasing the natural frequency of the circuit board. Furthermore, large amount of energy is expected to dissipate under vibration due to the relative motion and friction between the edge guide and edges of the board. This, in turn, will reduce the transmissibility experienced by the printed circuit board during resonance. A tight board edge guide may require tight manufacturing tolerances, plus a floating chassis connector, to permit accurate connector alignment during the circuit board installation, to prevent connector damage.

4.1.1 Transmissibility of PCB

PCBs are available in large number of sizes and shapes along with many different mounting arrangements. In the early stages of a design, these circuit boards must be analyzed to make sure they will function properly in the required environment.

The transmissibility developed by a PCB during resonance will depend on various factors like material of the board, type and number of laminations in multilayer board, natural frequency, mounting type, type of parts of electronic components attached to the circuit board, acceleration G levels, type of conformal coating, type of connector, and the board shape. Slight modifications in the installation geometry of the circuit board can have a sharp effect on the transmissibility and the mode shapes developed at resonance.

Since higher frequencies have smaller deflections, they will also have less damping. This means higher frequencies will usually have higher transmissibilities at resonant conditions.

Some of the factors that should be considered when the transmissibility of a circuit board is being estimated are as follows:

1. The Natural Frequency of the Circuit Board.

A high natural frequency means low displacements and low strains, so the transmissibilities are usually higher. Conversely, a low natural frequency means high displacements and high strains, so the transmissibilities are usually lower.

2. The Input G Force for Sinusoidal Vibration.

A lower input G force means low displacements and low strains, so the transmissibilities are usually higher. A high input G force means high displacements and high strains, so the transmissibilities are usually lower.

3. Ribs.

Riveted and bolted ribs will generally permit some relative motion to occur at the high-pressure interface between the ribs and the circuit board, which will dissipate energy and reduce the transmissibility at resonance. Welded, cast, and cemented ribs are usually stiffer than riveted and bolted ribs, so that they raise the resonant frequency more, but they do not provide as much damping.

4. Circuit Board Supports.

Circuit board edge guides that grip the edges of the board firmly provide a high-pressure interface that will dissipate energy and lower the transmissibility. If mounting bolts are used to fasten the boards, high-pressure interfaces in the bolt areas will tend to dissipate energy. More mounting bolts will dissipate more energy and increase the stiffness at the same time.

5. Circuit Board Connectors.

Circuit board connectors, such as the edge type or the pin-and-socket type, will provide some damping that will tend to reduce the transmissibility. A longer connector will provide more support to the circuit board edge while providing additional damping.

6. Type of Electronic Component Part.

Large electronic component parts that are in intimate contact with the circuit board will tend to dissipate more energy than small electronic component parts. This is because

larger components cover a bigger span on the circuit board, resulting in larger relative deflections at the circuit board interface over a larger area, so the damping is slightly greater.

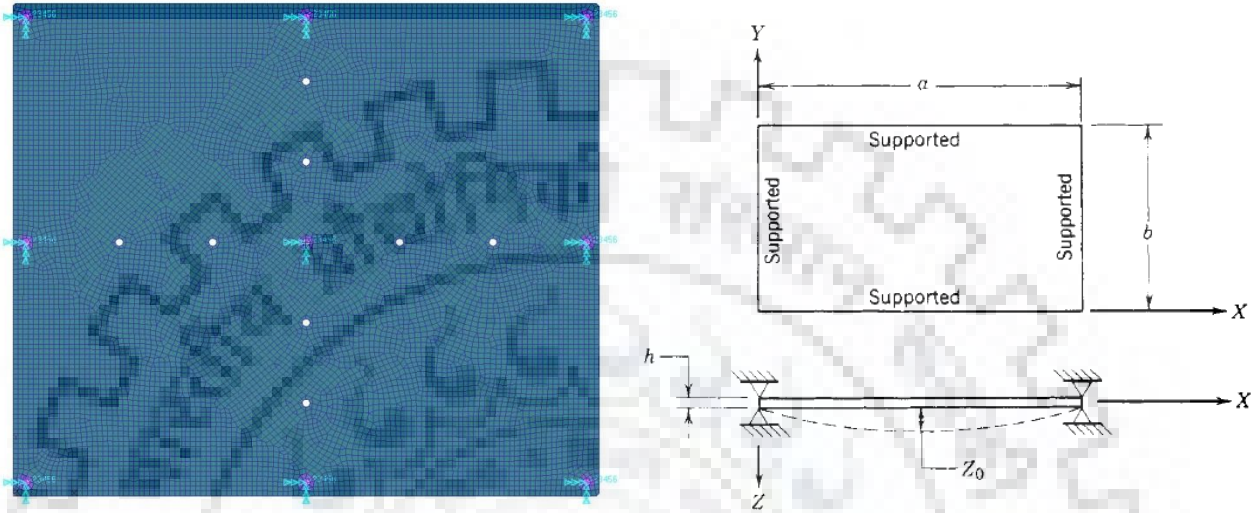


Fig 4-2: FE Model of PCB and approximation of PCB as mathematical model

Test data show the transmissibility of a PCB can generally be related to the square root of the natural frequency of the board. For rectangular boards, the transmissibility will normally range from about 0.50 to 2.0 times the square root of the natural frequency, depending on many factors.

Derivation of natural frequency of a PCB using trigonometric series

Consider a flat, rectangular plate, with four simply supported edges and a uniformly distributed load, being vibrated in a direction perpendicular to the plane of the plate. The deflection curve for the simply supported plate can be represented by a double trigonometric series.

$$Z = \sum_{m,n=1,3,5}^{\infty} \left(A_{mn} \sin \frac{m\pi X}{a} \sin \frac{n\pi Y}{b} \right) \dots\dots\dots \text{(Eqn 4.1)}$$

Extensive vibration test data on PCBs show that most of the damage occurs at the fundamental resonant mode where the displacements and the stresses are the greatest. The above equation 5.1 can then be simplified to the following expression

$$Z = Z_0 \sin \frac{m\pi X}{a} \sin \frac{n\pi Y}{b}$$

The assumed deflection curve must be checked to make sure it meets the geometric deflection boundary conditions. This means the edges of the plate must have a zero deflection and the center of the plate must have the maximum deflection. Then from above eqn 4.1,

- at $X = 0$ and $Y = 0, Z = 0$
- at $X = 0$ and $Y = b, Z = 0$
- at $X = a$ and $Y = 0, Z = 0$
- at $X = a$ and $Y = b, Z = 0$
- at $X = a/2$ and $Y = b/2, Z = Z_0$

The deflection boundary conditions are satisfied: there are no deflections at the edges and the maximum deflection is at the center.

Considering first the slope along the X axis, the required equation can be determined from the partial derivative of Z with respect to X. Then from Eq 4.1,

$$\theta_x = \frac{\partial Z}{\partial X} = Z_0 \frac{\pi}{a} \cos \frac{\pi X}{a} \sin \frac{\pi Y}{b}$$

- at $X = 0$ and $Y = b/2 \theta_x = Z_0 \frac{\pi}{a}$
- at $X = a/2$ and $Y = b/2 \theta_x = 0$
- at $X = a$ and $Y = b/2 \theta_x = -Z_0 \frac{\pi}{a}$

The slope boundary conditions are satisfied at the edges and at the center of the plate along the X axis. The same check can be made for the slope along the Y axis. The total strain energy V of the vibrating plate can be represented in the following form

$$V = \frac{D}{2} \int_0^a \int_0^b \left[\left(\frac{\partial^2 Z}{\partial X^2} \right)^2 + \left(\frac{\partial^2 Z}{\partial Y^2} \right)^2 + 2\mu \left(\frac{\partial^2 Z}{\partial X^2} \right) \left(\frac{\partial^2 Z}{\partial Y^2} \right) + 2(1 - \mu) \left(\frac{\partial^2 Z}{\partial X \partial Y} \right)^2 \right] dX dY \dots \dots \dots \text{(Eqn 4.2)}$$

Where,

$$D = \frac{Eh^3}{12} / (1 - \mu^2) = \text{Plate stiffness factor}$$

E = modulus of elasticity, h = plate thickness, μ = Poisson's ratio

The total kinetic energy T of the vibrating plate can be represented in the following form

$$T = \frac{\rho\Omega^2}{2} \int_0^a \int_0^b Z^2 dX dY \dots\dots\dots \text{(Eqn 4.3)}$$

$\rho = W/abg = \vartheta h/g =$ mass per unit area

$W =$ total weight of plate (lb), $\vartheta =$ material density, $a =$ length of plate, $b =$ width of plate

$h =$ plate thickness, $g =$ acceleration of gravity, $\Omega =$ circular frequency

Performing the operations on Eqn 4.1 required by Eqn 4.2

$$\frac{\partial Z}{\partial X} = Z_0 \frac{\pi}{a} \cos \frac{\pi X}{a} \sin \frac{\pi Y}{b} \dots\dots\dots \text{(Eqn 4.4)}$$

$$\frac{\partial^2 Z}{\partial X^2} = -Z_0 \frac{\pi^2}{a^2} \sin \frac{\pi X}{a} \sin \frac{\pi Y}{b} \dots\dots\dots \text{(Eqn 4.5)}$$

$$\left(\frac{\partial^2 Z}{\partial X^2}\right)^2 = Z_0^2 \frac{\pi^4}{a^4} \sin^2 \frac{\pi X}{a} \sin^2 \frac{\pi Y}{b} \dots\dots\dots \text{(Eqn 4.6)}$$

$$\frac{\partial Z}{\partial Y} = Z_0 \frac{\pi}{b} \sin \frac{\pi X}{a} \cos \frac{\pi Y}{b} \dots\dots\dots \text{(Eqn 4.7)}$$

$$\frac{\partial^2 Z}{\partial Y^2} = -Z_0 \frac{\pi^2}{b^2} \sin \frac{\pi X}{a} \sin \frac{\pi Y}{b} \dots\dots\dots \text{(Eqn 4.8)}$$

$$\left(\frac{\partial^2 Z}{\partial Y^2}\right)^2 = Z_0^2 \frac{\pi^4}{b^4} \sin^2 \frac{\pi X}{a} \sin^2 \frac{\pi Y}{b} \dots\dots\dots \text{(Eqn 4.9)}$$

From Eqn 4.5 and 4.8

$$\left(\frac{\partial^2 Z}{\partial X^2}\right)^2 \left(\frac{\partial^2 Z}{\partial Y^2}\right)^2 = Z_0^2 \frac{\pi^4}{a^2 b^2} \sin^2 \frac{\pi X}{a} \sin^2 \frac{\pi Y}{b} \dots\dots\dots \text{(Eqn 4.10)}$$

From Eqn 4.4 and 4.7

$$\frac{\partial^2 Z}{\partial X \partial Y} = Z_0 \frac{\pi^2}{ab} \cos \frac{\pi X}{a} \cos \frac{\pi Y}{b}$$

$$\left(\frac{\partial^2 Z}{\partial X \partial Y}\right)^2 = Z_0^2 \frac{\pi^4}{a^2 b^2} \cos^2 \frac{\pi X}{a} \cos^2 \frac{\pi Y}{b} \dots \dots \dots (\text{Eqn 4.11})$$

Since these equations must be integrated, the following relations are used:

$$\int_0^a \sin^2 \frac{\pi X}{a} dX = \frac{a}{2}$$

$$\int_0^b \sin^2 \frac{\pi Y}{a} dY = \frac{b}{2} \dots \dots \dots (\text{Eqn 4.12})$$

Following Eq. 4.2 and integrating Eq. 4.6 using Eq. 4.12,

$$\int_0^a \int_0^b \left(\frac{\partial^2 Z}{\partial X^2}\right)^2 dX dY = Z_0^2 \frac{\pi^4}{a^4} \left(\frac{ab}{4}\right) \dots \dots \dots (\text{Eqn 4.13})$$

Following Eq. 4.2 and integrating Eq.4.9 using Eq. 4.12,

$$\int_0^a \int_0^b \left(\frac{\partial^2 Z}{\partial Y^2}\right)^2 dX dY = Z_0^2 \frac{\pi^4}{b^4} \left(\frac{ab}{4}\right) \dots \dots \dots (\text{Eqn 4.14})$$

Following Eq. 4.2 and integrating Eq. 4.10 using Eq. 4.12,

$$\int_0^a \int_0^b \left(\frac{\partial^2 Z}{\partial X^2}\right) \left(\frac{\partial^2 Z}{\partial Y^2}\right) dX dY = Z_0^2 \frac{\pi^4}{a^2 b^2} \left(\frac{ab}{4}\right) \dots \dots \dots (\text{Eqn 4.15})$$

Following Eq. 4.2 and integrating Eq. 4.11 using Eq. 4.12,

$$\int_0^a \int_0^b \left[\left(\frac{\partial^2 Z}{\partial X \partial Y}\right)^2\right] dX dY = Z_0^2 \frac{\pi^4}{a^2 b^2} \left(\frac{ab}{4}\right) \dots \dots \dots (\text{Eqn 4.16})$$

Substituting Eqn4.13-4.16 into Eq. 4.2 for the strain energy of the vibrating plate,

$$V = \frac{D}{2} \left(\frac{abZ_0^2\pi^4}{4} \right) \left(\frac{1}{a^4} + \frac{1}{b^4} + \frac{2\mu}{a^2b^2} + \frac{2(1-\mu)}{a^2b^2} \right)$$

$$V = \frac{D}{2} \left(\frac{abZ_0^2\pi^4}{4} \right) \left(\frac{1}{a^4} + \frac{1}{b^4} + \frac{2\mu}{a^2b^2} \right) \dots \dots \dots \text{(Eqn 4.17)}$$

The kinetic energy of the vibrating plate can be determined from the deflection (Eq. 4.1) along with the kinetic energy

$$Z^2 = Z_0^2 \text{Sin}^2 \frac{\pi X}{a} \text{Sin}^2 \frac{\pi Y}{a} \dots \dots \dots \text{(Eqn 4.18)}$$

Substituting Eq.4.12 into Eq.4.18 for the integration, we have

$$\int_0^a \int_0^b [Z^2] dXdY = Z_0^2 \frac{ab}{4} \dots \dots \dots \text{(Eqn 4.19)}$$

Substituting Eq. 4.19 into Eq. 4.3 for the kinetic energy of the vibrating plate, we have

$$T = \frac{\rho\Omega^2}{2} \left(Z_0^2 \frac{ab}{4} \right) \dots \dots \dots \text{(Eqn 4.20)}$$

Since the strain energy of the vibrating plate must equal the kinetic energy at resonance, if there is no energy dissipated, then Eq.4.17 must be equal to Eq. 4.20

$$\frac{D}{2} \left(\frac{abZ_0^2\pi^4}{4} \right) \left(\frac{1}{a^2} + \frac{1}{b^2} \right)^2 = \frac{\rho\Omega^2}{2} \left(Z_0^2 \frac{ab}{4} \right)$$

$$\Omega^2 = \frac{\pi^4 D}{\rho} \left(\frac{1}{a^2} + \frac{1}{b^2} \right)^2$$

Solving for the natural frequency of the rectangular plate, we have

$$fn = \frac{\Omega}{2\pi} = \frac{\pi}{2} \sqrt{\frac{D}{\rho}} \left(\frac{1}{a^2} + \frac{1}{b^2} \right) \dots \dots \dots \text{(Eqn 4.21)}$$

4.1.2 Analysis of PCB by analytical method

From the above equation 4.21 we can estimate the natural frequency of the PCB using empirical relations.

Consider, a PCB fixed at 4 corner locations using M3 screws then we can calculate fundamental frequency as below,

$$a = 9 \text{ inches}$$

$$b = 8 \text{ inches}$$

$$g = 386 \text{ in/s}^2$$

$$h = 0.086614 \text{ inches}$$

$$E = 2.0 \times 10^6 \text{ lb/in}^2$$

$$\mu = 0.136$$

$$W = 1.1023 \text{ lb}$$

$$D = \frac{Eh^3}{12(1-\mu^2)} = \frac{2.0 \text{ E6 X}(0.086614)^3}{12(1-0.136^2)} = 110.337 = \text{Plate stiffness factor}$$

$$\rho = \frac{W}{gab} = \frac{1.1023}{386 \times 9 \times 8} = 3.966 \times 10^{-5}$$

$$fn = \frac{\Omega}{2\pi} = \frac{\pi}{2} \sqrt{\frac{D}{\rho} \left(\frac{1}{a^2} + \frac{1}{b^2} \right)}$$

$$fn = \frac{\pi}{2} \sqrt{\frac{110.337}{3.966 \times 10^{-5}} \left(\frac{1}{64^2} + \frac{1}{81^2} \right)}$$

$$fn = 73.281 \text{ Hz}$$

4.1.3 Modeling of PCB

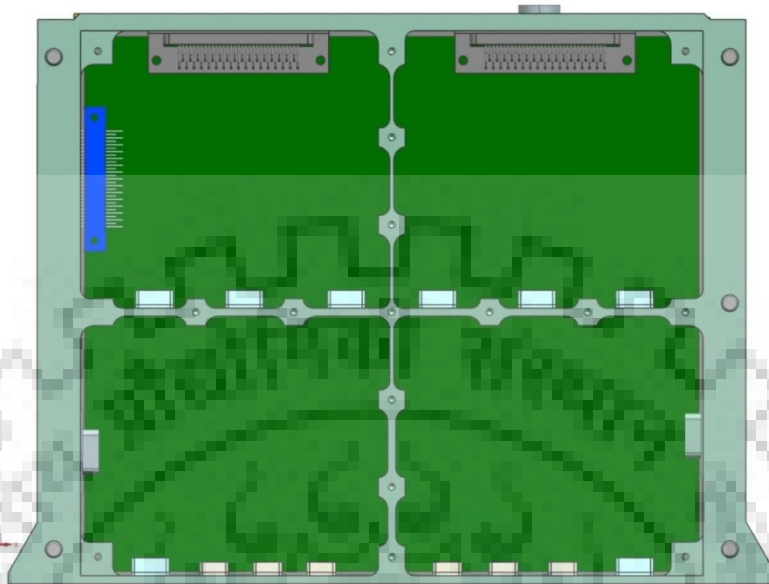


Fig 4-3: Front view of the package

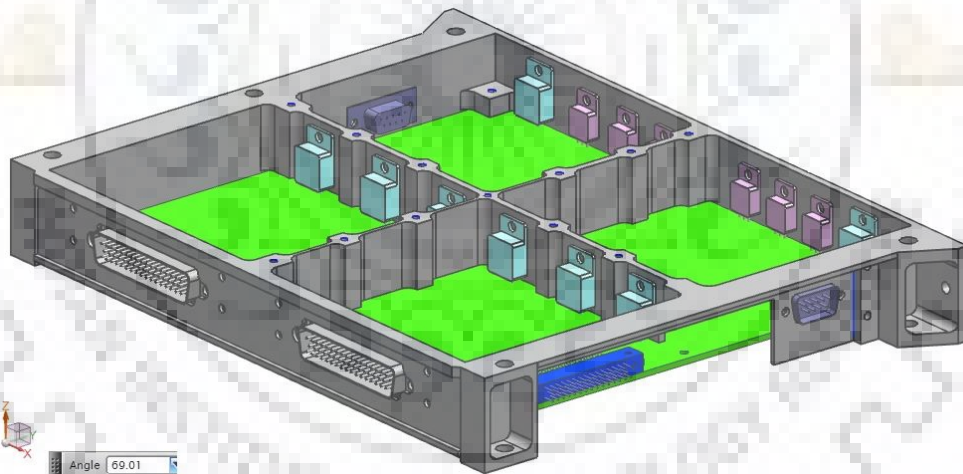


Fig 4-4: Isometric view of the package

In designing of PCB, FR4 material is used with thickness of 2.2 mm. PCB is mounted onto the tray at four corners using a PCB seating provision and the remaining part is mounted on the ribs. Also, in the above figure 4-3 and 4-4 we can see the accommodation of mosfets and diodes.

4.2 Design Considerations for Tray

The package of electronic equipment depends on the shape and space available that leads to the development of different configurations to meet the desired conditions. Usually the box of rectangular type is employed as it is not so expensive to fabricate, mounting is simple, and plug-in modules such as printed circuit boards (PCBs) conform readily to this shape. First of all, it is essential to take into account the different modes of vibration before performing computerized analysis for the purpose of determining frequency response characteristics of the chassis. Various bending and torsional modes can be examined to determine whether coupling may occur. Preliminary dynamic loads can also be determined to check the buckling of panels, shearing of rivets, or cracking of welds.

Torsional vibration modes are often a source of trouble in an electronic chassis. These modes, which are generally ignored or overlooked, can result in low resonant frequencies. This in turn can lead to large deflections and stresses that can substantially reduce the fatigue life of the structure.

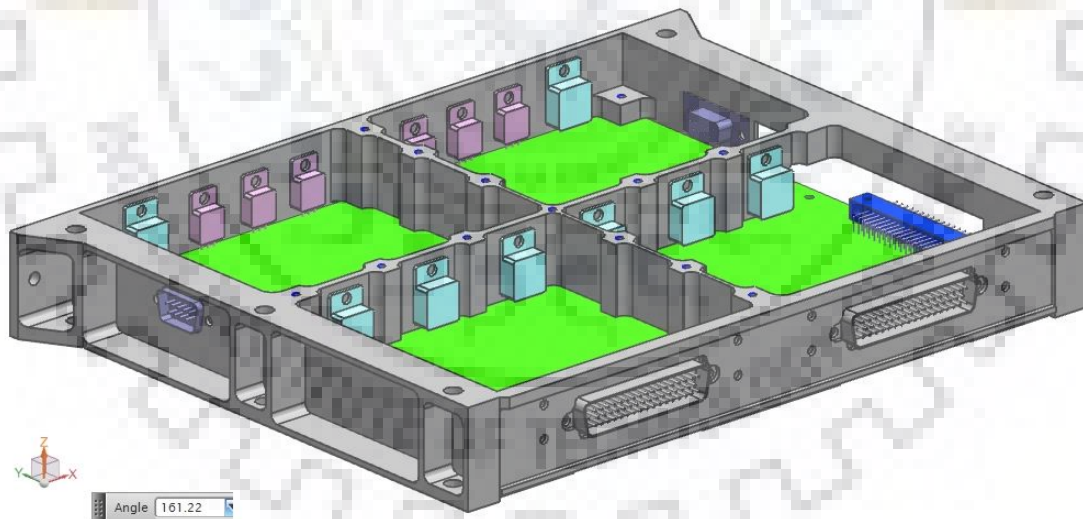


Fig 4-5: Depiction of PCB and Tray

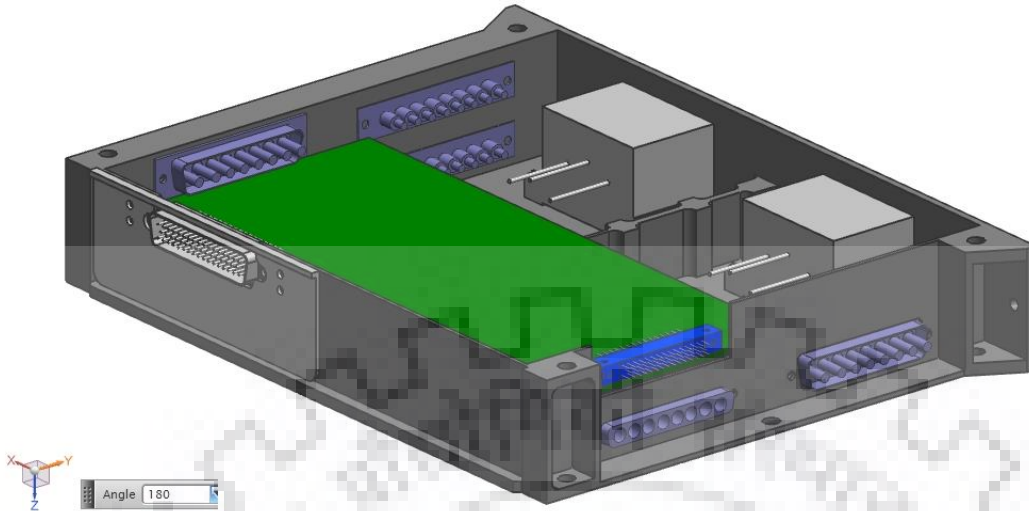


Fig 4.6: Representation of tray with electronic components

Taking into account the dynamic response characteristics the dynamic loads developed in a chassis can be determined. The response characteristics of a chassis are influenced by the type of mount. The inertia load produced at resonance is maximum at the center of a uniformly loaded chassis whereas minimum at the supporting ends by taking into account the vibration input to be sinusoidal. The transmissibility at the supporting ends is unity when no relative motion exist between the chassis and the supports. A good approximation for the dynamic load can be obtained with a sinusoidal load distribution acting along the chassis.

The tray is made of Beryllium - Aluminium alloy as material and in modeling PCB is mounted on the tray. Rib thickness of 3 mm is used and proper provisions are made for connections of pin connectors, Relays, Mosfets and diodes.

4.3 Three dimensional modeling of electronic package

There are two type of packages. One is horizontal mounting and second one is vertical mounting packages. Fig 4.7 and Fig 4.8 shows both packages consists of 4 trays of different sizes which are modeled using Unigraphics- 8.5 Version. Stacks are placed one beside the other, and are mounted to the deck using titanium or stainless steel screws. Pin-Connectors, Plug connectors, Transistors, Diodes, Mosfets etc. are placed at appropriate locations and all the stacks are held together using studs at six locations. Cover plates are used at the ends of each exposed tray to avoid interference and damage to the package.

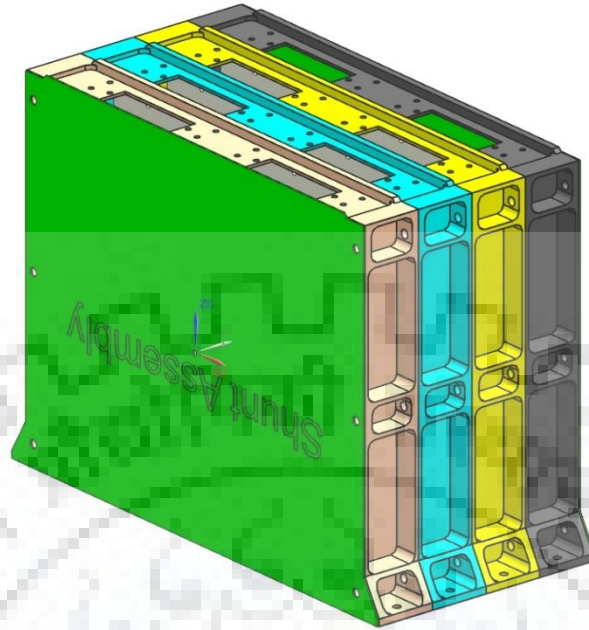


Fig 4-7: Isometric view of integrated vertical stacked module

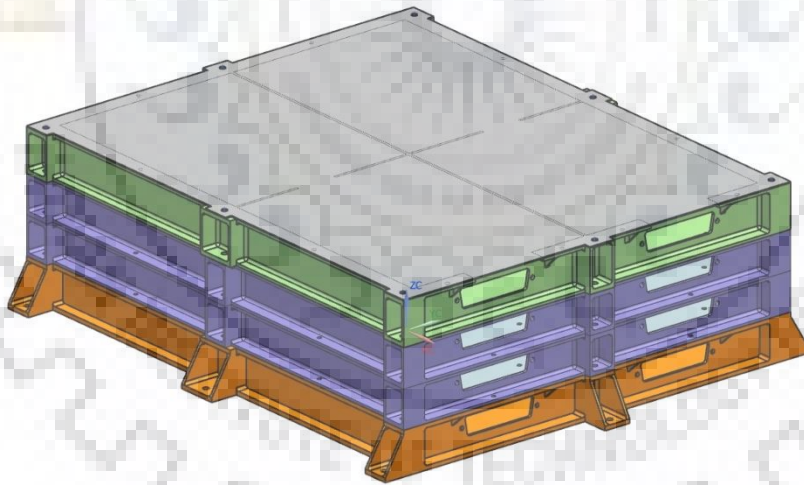


Fig 4-8: Isometric view of integrated horizontal stacked module

Chapter 5

FINITE ELEMENT MODELING

5.1 Overview

In the finite element method, the actual continuum or body of matter, such as a solid, liquid or gas are considered as assembly of subdivisions called finite elements. It is considered that these elements are interconnected at specified joints called as nodes or nodal points which usually lie on the element boundaries. The variation of the field variable (e.g., displacement, stress, temperature, pressure, or velocity) inside a finite element is assumed to be approximated by a simple function as the actual variation of the field variable inside the continuum is unknown.

These approximating functions are also known as interpolation models that are defined with respect to the values of the field variables at the nodes. After writing the field equations (like equilibrium equations) for the whole continuum, it is found that the new unknowns are the values of the field variable at the nodes. These unknown values of nodal field variable are determined by resolving the field equations that are in terms of matrix equations. This leads to defining of field variable while assembling the elements by approximating functions.

Advantages of finite element modeling of the package,

1. Easy modifications of geometry in the model.
2. Efficiently manage heavy, complex analysis models through assembly.
3. Simplify the geometry editing process by direct modelling process.
4. Product development cost is decreased by reduction in time and the changes in the design can be adjusted afterwards.

5.2 Steps in FEM

In problems of a continuum, the solution using the finite element method commonly is in a stepwise process i.e. in proper sequence. Referring to the problems of static structural, the stepwise procedure is:

Step (i): Structure Discretization

The primary step in this method is to split the structure into subdivisions or elements. Thus modelling of structure is done with appropriate finite elements. The factors that needs to be decided are number, type, size, and arrangement of the elements.

Step (ii): Selecting appropriate interpolation or displacement model

In complex structures, prediction of the displacement solution under any specified load conditions is not accurate. Thus a suitable solution is assumed within an element for the purpose of approximating the unknown solution. This assumed solution must satisfy specific convergence requirements however it should be simple from a computational point of view. Generally the solution is in the form of a polynomial.

Step (iii): Deriving element stiffness matrices and load vectors

The stiffness matrix [k(e)] and the load vector P(e) of element are now derived with the help of either equilibrium conditions or a suitable variational principle.

Step (iv): Assembly of element equations to find the overall equilibrium equations

The stiffness matrices and the load vectors of a particular element are combined appropriately such that the overall equilibrium equation is expressed as

$$[K] \Phi = P \dots\dots\dots (Eqn 5.1)$$

Where,

[K] is the assembled stiffness matrix,

Φ is the vector of nodal displacements, and

P is the vector of nodal forces for the complete structure.

Step (v): Solving the unknown nodal displacements

Considering boundary conditions of the problem, there emerges a need to modify overall equilibrium equations. After modification, the equilibrium equations can be stated as $[K]\Phi = P$.

It is very easy to solve vector ϕ in linear problem whereas this is not the case in nonlinear problems. Here a series of steps are performed to obtain the solution alongwith the modification of the stiffness matrix $[K]$ and/or the load vector P in each step.

Step (vi): Computing stresses and strains of elements

As per the necessity the stresses and strains of elements can be determined by employing suitable equations of solid or structural mechanics from the known nodal displacements Φ

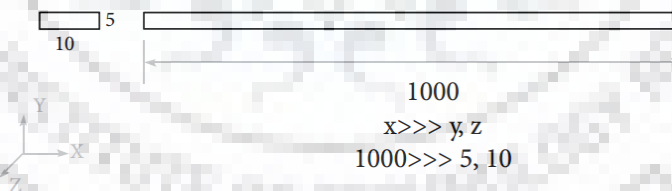
5.3 Selection of Type of Element

Elements are selected on the basis of following factors:

5.3.1 Geometry Size and Shape

According to dominant dimensions, the geometry can be classified as 1D, 2D, or 3D, consequently appropriate selection of element is done.

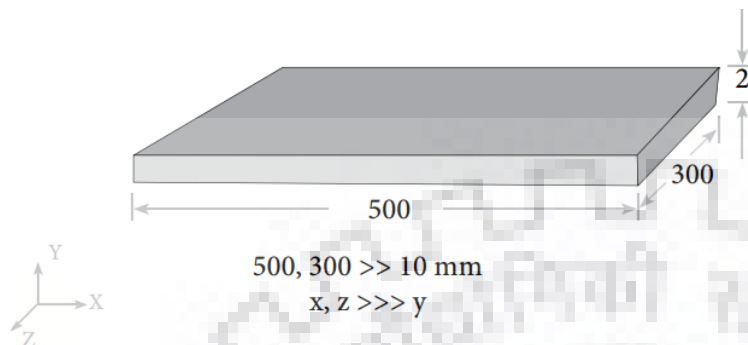
1D Element: This element is employed for geometries which have one dimension very large in size as compared to the other two dimensions.



1D element is represented by a line. During formation of element by joining two nodes, only one dimension out of the three dimensions is known to the software. The user is supposed to allocate the remaining two dimensions, cross section area, and section as input data.

Practical example: Long shaft, rod, beam, column, column, spot welding, bolted joints, pin joints, joints, bearing modeling, modeling, etc.

2D Element: This is used when two dimensions are extremely large with respect to the third one.



2D meshing is done on a mid-surface of the part. 2D elements are planar. Due to the formation of 2D elements, 2 out of the 3 required dimensions are known to the software. The user has to give the third dimension i.e. thickness as an additional input data. It is required to extract the mid surface followed by meshing on the same to depict the geometry in proper manner.

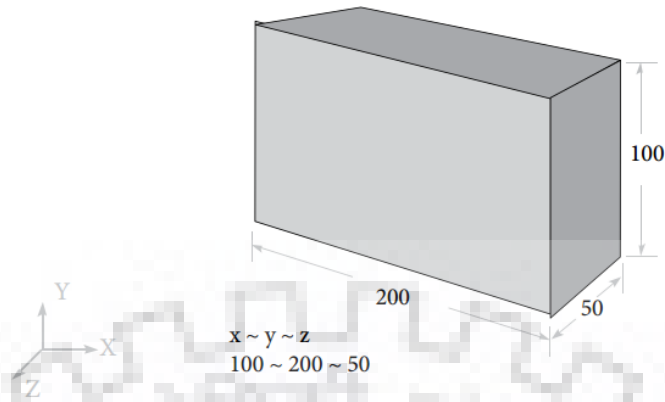


Practical example: All sheet metal parts, plastic components like instrument panels, etc. In general, 2D general, 2D meshing is used for parts having a width / thickness ratio > 20 .

2D meshing can result in a higher approximation if it is used for –

- variable part thickness
- Surfaces that are not planar and have different features on the two sides.

3D Element: This element is employed when all the three dimensions are large with respect to each other.



Practical examples: Transmission casing, clutch housing, connecting rod, crank shaft etc.

5.3.2 Based On the Type of Analysis

Structural and fatigue analysis - Quad, hex elements are preferred over tries, tetras and pentas.

Crash and nonlinear analysis - Priority is given to mesh flow lines and brick elements over tetrahedron.

Mold flow analysis – Triangular element are preferred over quadrilateral elements.

Dynamic analysis – When the geometry falls within the category of 2D and 3D geometry, 2D shell elements are preferable over 3D due to the fact that the shell elements are less stiff due to which the mode shapes are attained with accuracy and with a lesser number of nodes and elements.

5.4 Basic Requirements of Electronic Package

- **External environment conditions:** Surface mounting needs equipment use requirement, service life prerequisite, ecological conditions, surface finish, maintenance and repair contemplations, electrical interconnection, resistance to thermal stress and mechanical vibration.
- **Interior environment conditions:** The enclosure of electronic components or the package comprises of electronic modules, interconnections which provides electrical and thermal interface between the external and internal environment.

- **Component requirements:** Electronic parts, modules and subassemblies require immense protection from mechanical vibration, mechanical stresses, and thermal stresses including impact of temperature caused by heat generation and vibration loads.
- **Component environments:** Modules and subassembly housing characterize the interface between the environment of a particular electronic component and the internal package.

5.5 FE Model of the PCB

Electronic industries make various types of printed circuit boards. Most commonly used material is epoxy having laminated layers of Cu on one or both the sides of the board to serve as electrical conductors. The overall thickness of printed circuit board ranges from 0.006 -0.125 inches. The size of the board scan ranges from 2 -16 inches.

A wide variety of shapes can be obtained, varying from small squares to the large circular plates and triangles which depend on the shape of the electronic box employed for supporting the circuit boards. As the electronic equipments are packed as per each and every inch of space in airplanes, missiles and even in television sets, therefore the circuit board shape depends on the the geometry of the available space.

The electronic industry considers rectangular PCB to be the most commonly used due to its flexibility to the modular plug-in type of assembly, that makes use of an electrical connector along the bottom edge of the circuit board. PCBs get heated up as it consists of a large number of components which exhaust heat at high power, so there is a need to dissipate this heat. For this purpose, Al and Cu possessing high thermal conductivities are bonded to the epoxy fiberglass circuit boards to serve as heat sinks.

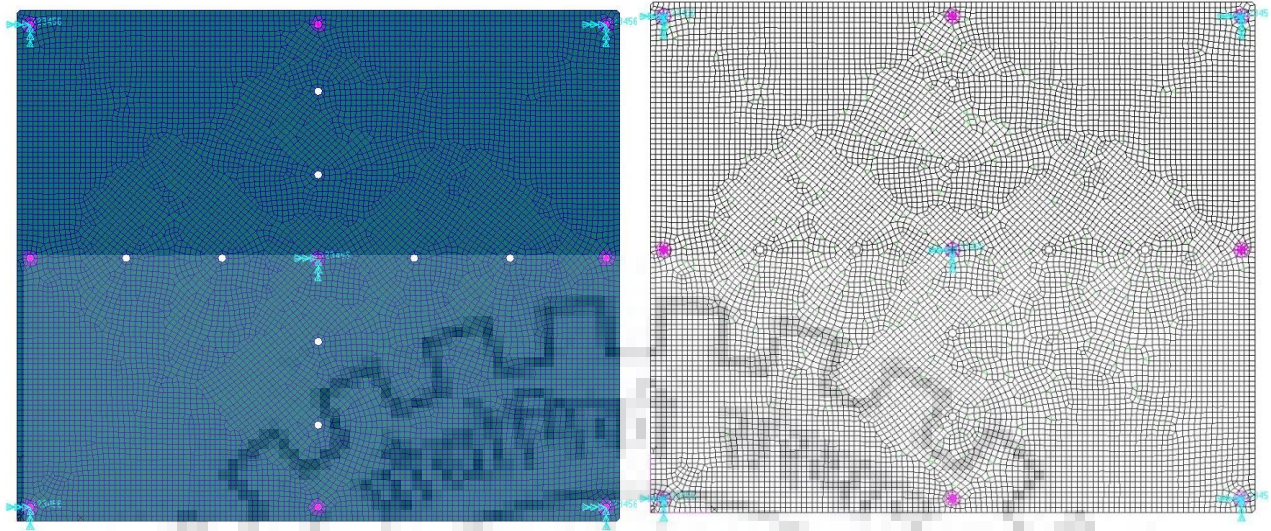


Fig 5-1: FE Model of PCB

5.6 FE Model of the Package Assembly

Package housing should work as a protection and support box to the electronic components and PCB's. Determining the natural frequency of the package and PCB followed by their comparison is essential. In case the natural frequency for both comes out to be equal or near to each other, it may lead to coupling of their transmissibility and cause the package to vibrate at extreme levels, and resonance exist. This may lead failure of the package and sub components. Hence the electronic package is designed in such a way that resonance should not be exists at extreme level. Hence package is designed according to the octave rule. Ribs, connectors are considers to add extra stiffness to the package.

If the ribs are not designed properly, they will not increase the stiffness of the package. Ribs are placed in such a way that the entire load of the PCB and their trays load directly support properly. The total lug locations of the modules are constrained by utilizing multi point constraints (MPC) are joined with the help of RBE2 elements by generating node at the centre of the holes by constraining the surrounding elements of the hole for even distribution of load.

FE software is used for the purpose of generation of electronic package and to perform analysis for estimating the dynamic characteristics. This leads to the reduction in cost consumed in developing the product by reduction in time as well as preventing the modifications in design at

further stages. Besides this the structure reliability can also be assessed. The shell elements are available in MSC NASTRAN/PATRAN and UG-NX FE software that are used to generate three dimensional and two dimensional mesh. Both packages are modeled by using 3D tetra mesh. Fig 5.2 and Fig 5.3 shows the FE model of both package.

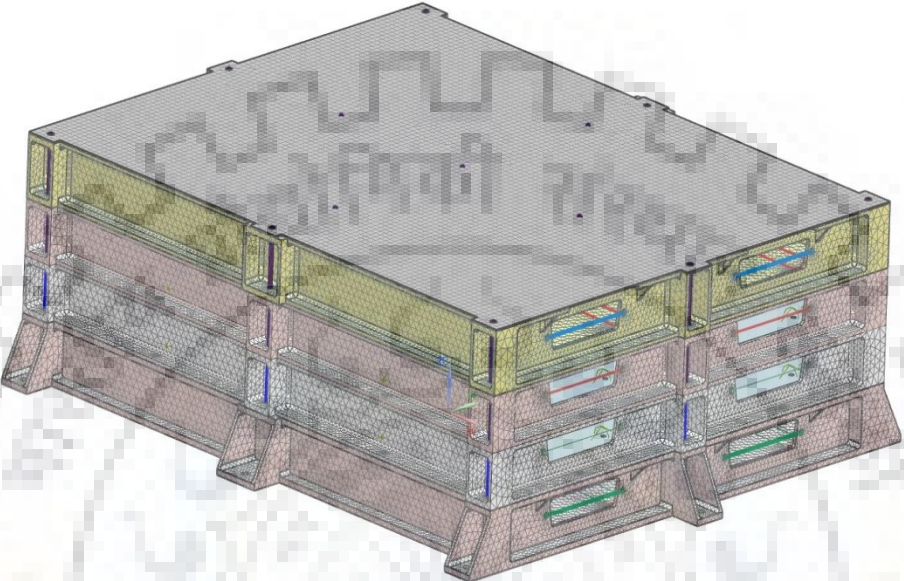


Fig 5-2: FE Model of horizontal mounting package

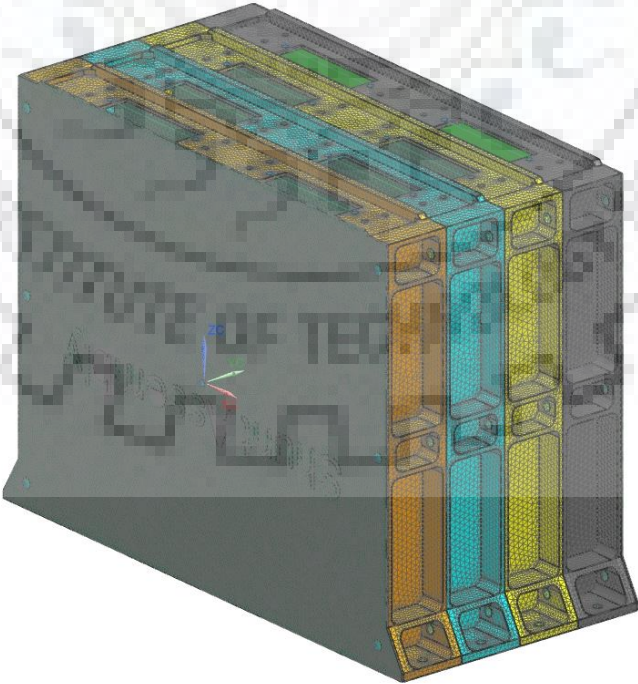


Fig 5-3: FE Model of vertical mounting package

Table 5.1: Finite element details used in FE model

Component	Material	Element property for FE simulation
Tray cover	Al-6061/AZ31B/AM162	3-D ,CTETRA(4)
Tray	Al-6061/AZ31B/AM162	3-D ,CTETRA(4)
PCB	FR-4	2-D, CQUAD(4)
Converters, Relays or any electronic component	-	PMASS, concentrated mass
Stud	SS-304/Ti	RBE2
Fasteners	SS-304/Ti	RBE2

All degrees of freedom of lug locations are arrested using MPC (Multi Point Constrain) Connections by making use of RBE2 elements at holes for distributing the load evenly. The nodes around the periphery of the hole are dependent on the central node. All such independent central nodes are arrested. Each tray is modeled using 3D shell element which consists of tetrahedral (CTETRA) elements. Ribs are modeled to support the PCB in bottom side to add the extra stiffness to the structure.

5.6.1 Screws and Studs modeled as Bars

Bars are characterized by long and slender members. Modeling complex cross-sections sections excluding the geometry modeling is flexible which makes the use of bars very beneficial. Bar elements help in obtaining stress and deflection results with great accuracy. Studs and rods are basically two dimensional bars that are excellent in the case of plane problems.

The studs are employed to connect PCB and trays. There are many connectors present in Electronic packages and these connectors are connected with tray with the help of screws. These screws gave stiffness to the assembly and enhance the frequency so these screws are modeled by using rigid bar elements (RBE2) and constrained using the multi-point constraints (MPC). Studs

also modeled by using rigid bar elements (RBE2) or beam element. Fig 5.4 shows beam element and RBE2 element that is used in both packages.

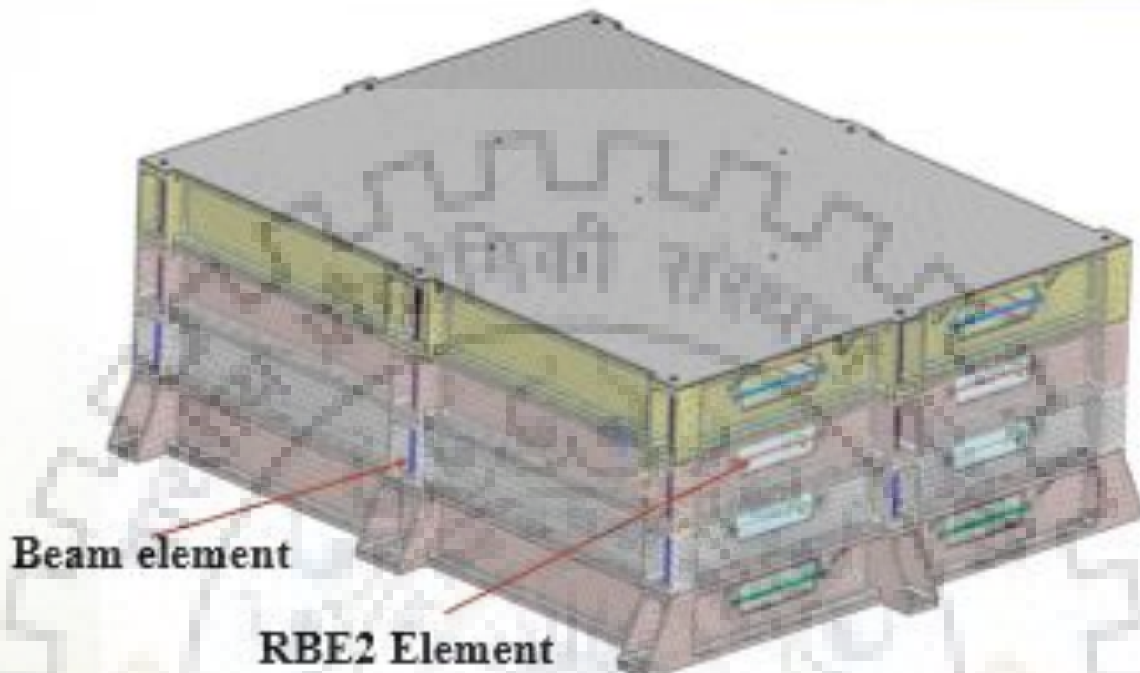


Fig 5-4: Elements used in FE Modeling

5.6.2 Tray modeled as 3D elements and PCB Modeled as 2D Shell elements

Each tray is modeled using 3D element which consists of CTETRA elements. Ribs are modeled to support the PCB in bottom side to add the extra stiffness to the structure. All such four stacks in both packages are assembled one after the other and held together using a stud which is clamped on the two sides. Similarly studs are clamped at 6 and 8 locations to avoid transverse movements of package under external loading.

The shells are basically two dimensional elements representing the three dimensional space. For three dimensional structures of lesser thickness such as body panels, injection molded plastic, sheet metal or any component that has negligible thickness as compared to the other dimensions, shells are the best substitute. Stresses are determined on the upper and lower surfaces likewise at

the mid plane whereas deflections are defined at the nodes. Therefore the analyst is provided with the capability to compare the results pertaining to membrane effects against bending effects.

Fig 5.5 and Fig 5.6 shows FE model of tray and PCB.

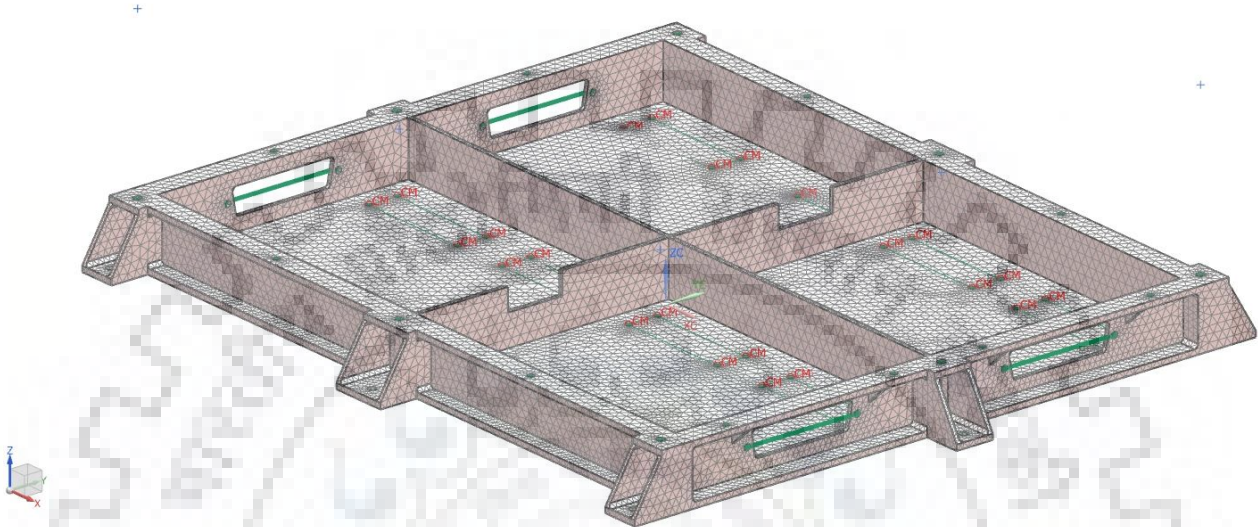


Fig 5-5: FE modeling of tray

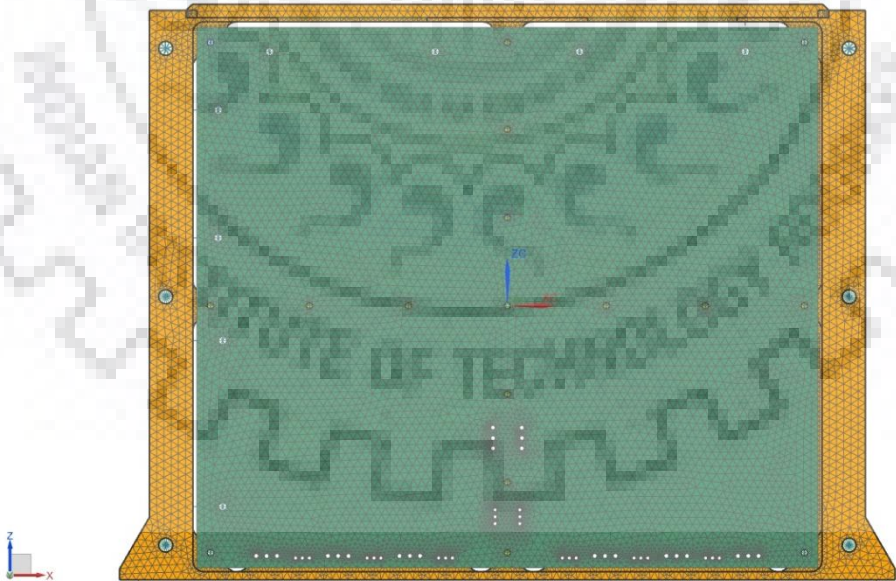


Fig 5-6: FE modeling of tray with PCB

5.7 General Mesh Generations

The main concern in discretization of physical model is finite element mesh. Mesh is the process of creating finite elements from surface, curves or solids. The method of finite element is a numerical technique to solve boundary value problems.

Traditionally mesh creation process start from the coarse mesh, this gives a large discretization error and takes more iteration to get a desired final mesh. Usually analyst do not account the material properties and boundary conditions of the module and begins from the mesh, which requires a more step for optimise the accuracy and result, it consumes more time [15]. The method used for mesh generation usually depends on the geometry and physical problem of the structure. It is left to use the analyst to select the best method. In general, good quality of mesh is required to define the correct mesh density value, which is important parameter in FEM because of its relationship to accuracy and computational time.

Finite element method involves different types of element that can be used when meshing a structure. If the structure is three dimensional in nature tetrahedral, wedge or hexahedral elements are used. If the structure is two dimensional then shell elements i.e. CQUAD or elements of triangular shape are employed. During analysis, elements size for meshing is significant, hence too coarse mesh may give results that are not satisfy with result. To ensure that the element size and mesh is used better enough, mesh refinement study be performed.

A good mesh can be ensuring by perceptual convergence and it should be below 5% when computing the mode frequencies. Too fine mesh will lead to high computational time which is not economic. Therefore in finite element analysis, the density of the mesh i.e. element size and shape plays an important role in influencing the accuracy of results. If the choice of element size is very small, it may give accurate results but requires more computational time to analyse the structure. If the structure to be meshed is complicated and there is a risk of stress concentration. Mesh density required will be depending on the boundary conditions, stress gradients, type of loading.

Whereas large element size i.e. coarse mesh may affect the results. Hence appropriate element size is selected based on the structure and solution required. Better mesh cannot be obtained directly from the meshing method. Extra steps are necessary to optimise the mesh [15].

5.8 Mesh refinement and verification

A mesh refinement study was made on different modules of the package and assembly of power package. The mid surface of the PCBs and all trays is meshed in UG-NX and they are verified within the software. Mesh verification and equivalence options used to make a model error free. Equivalence has been done to find the duplicate elements, free edges, duplicate nodes etc. If any free edges are found those are modified by moving nodes or splitting the edges of elements and duplicate elements and nodes were deleted automatically through software.

The package is meshed using the data from the refinement study. 2D and 3D elements were used to mesh the package. Meshing errors usually occur at hole location and in complex geometrical locations, which were difficult to avoid, hence structure is divided into small surfaces to maintain the continuity of the mesh, the optimal element size was maintained to entire package assembly. Several iterations are carried out to finalise the mesh size, the mesh is finalised for an element size of 3 mm.

Chapter 6

ANALYSIS AND RESULTS

6.1 Overview

The whole package assembly is simulated for different types of analysis like linear static analysis to find out the package strength and to determine the regions that are critical for further analysis. This is followed by Normal modal analysis to determine the dynamic characteristics of the package such as natural frequency and mode shapes of the package. Lastly the frequency response analysis is conducted for determining the package transmissibility and as a result it reduces the vibrations which get into the package. All these analysis are carried out for different parameters such as different materials, different thickness to determine which materials will give more satisfactory results such as minimum stress, displacement, higher first fundamental frequency, thereby increase in the life of the package.

6.2 Significance of Linear Static and Modal Analysis in Fe Software

6.2.1 Linear Static Analysis

Linear static analysis is the most basic type of analysis. The term “linear” means that the computed response-displacement or stress is linearly related to the force applied. The term “static” means that the forces do not vary with time.

The static analysis equation is:

$$[K]\{u\} = \{f\} \dots\dots\dots (Eqn 6.1)$$

Where, [K] represents the system stiffness matrix (generated automatically by MSC/NASTRAN, which is based on the geometry and properties), f represents the vector of applied forces, and u represents the vector of displacements that MSC/NASTRAN computes. After computing the displacements, MSC/NASTRAN calculates element forces, stresses, reaction forces, and strains.

Linear static analysis is carried out for different materials (AL6061, AZ31B and AM162 materials); aim of the analysis is to know at which material minimizes the displacement and the strength at the worst loading condition. Analysis is carried out for several parameters such as

changing the mountings of the packages like vertical and horizontal, changing the materials and load.

The importance of changing the material and mounting orientation is to reduce the mass of the structure and the mass of the package for different materials with varying thickness, AZ31B shows reduced mass compared to the AL6061 and AM162. However electronic package involves other parameters to be achieved, other than mass reduction, such as minimum stress, minimum displacement, increased first fundamental frequency, higher fatigue life of the structure. Hence further analysis needs to be carried out for obtaining stress, displacement and first fundamental frequency.

Quasi-static analysis has been carried out for all three materials i.e. Al6061, AZ31B and AM162 for both type of mounting orientation i.e. horizontal and vertical mounting.

6.2.1.1 Quasi-static analysis for Vertical Mounting package for Al6061, AZ31B and AM162 materials

In Quasi-static analysis, the package is loaded by 25 g loading condition in longitudinal direction and 20 g in both lateral direction by giving fixed constrained at the mounting points. Since vertical mounting package has 8 mounting location so all 8 location has been given fixed constrained and then one by one 25 g and 20 g loading has been done over the package for all three materials i.e. Al6061, AZ31B and AM162. By this loading, for vertical mounting package, maximum displacement and maximum stress value is obtained in both 25 g and 20 g direction for all three materials at the critical locations of the package.

Quasi-static analysis has been carried out for Al6061 material. By the analysis, it is found that the maximum value of displacement and stress is in 20 g loading condition as compare to 25 g loading condition. Fig 6.1 to Fig 6.4 shows the quasi-static analysis for AL6061 material and corresponding maximum displacement and maximum stress is shown in the respective figures.

Sunt Assy_sim1 : quasi Result
 Subcase - Static Loads 1, Static Step 1
 Displacement - Nodal, Magnitude
 Min : 0.000E+000, Max : 5.587E-003, Units = mm
 Deformation : Displacement - Nodal Magnitude

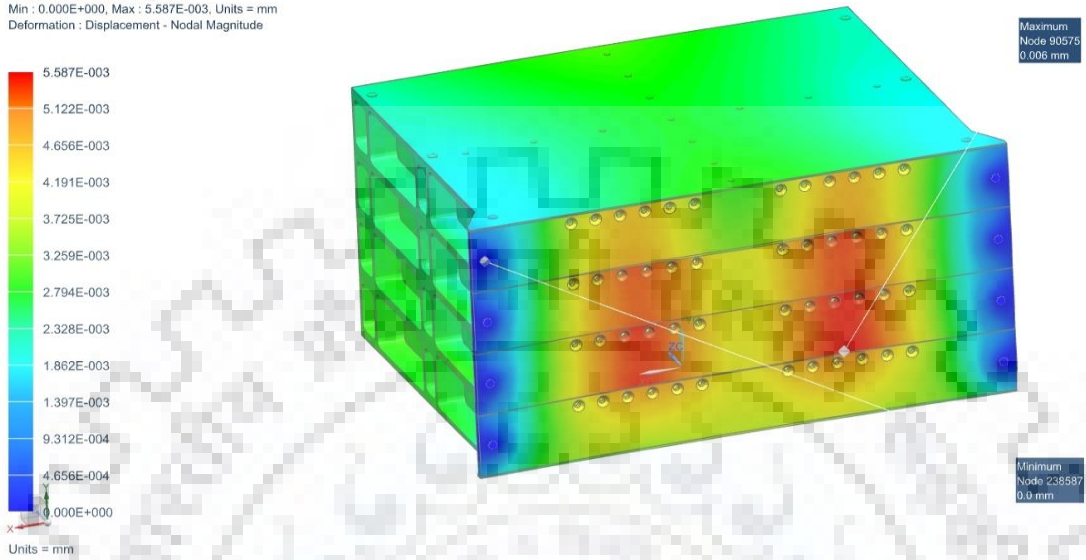


Fig 6-5: Maximum Displacement of Vertical mounting package under 25 g loading for Al6061

Sunt Assy_sim1 : 20g_yaxis Result
 Subcase - Static Loads 1, Static Step 1
 Displacement - Nodal, Magnitude
 Min : 0.0000, Max : 0.1077, Units = mm
 Deformation : Displacement - Nodal Magnitude

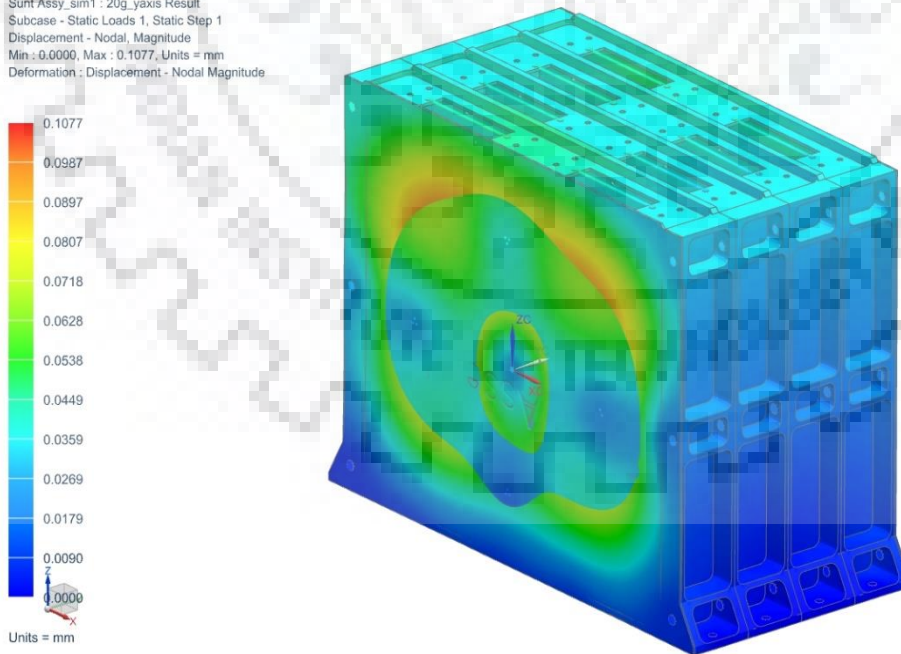


Fig 6-2: Maximum Displacement of Vertical mounting package under 20 g loading for Al6061

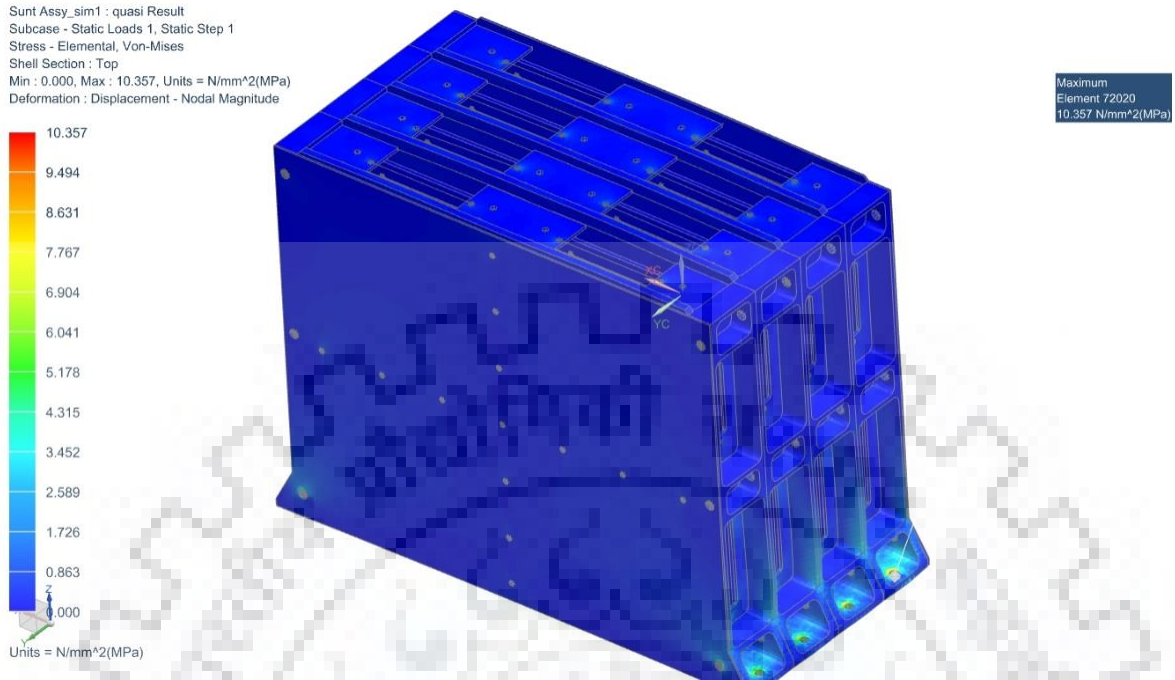


Fig 6-3: Maximum Stress of Vertical mounting package under 25 g loading for Al6061

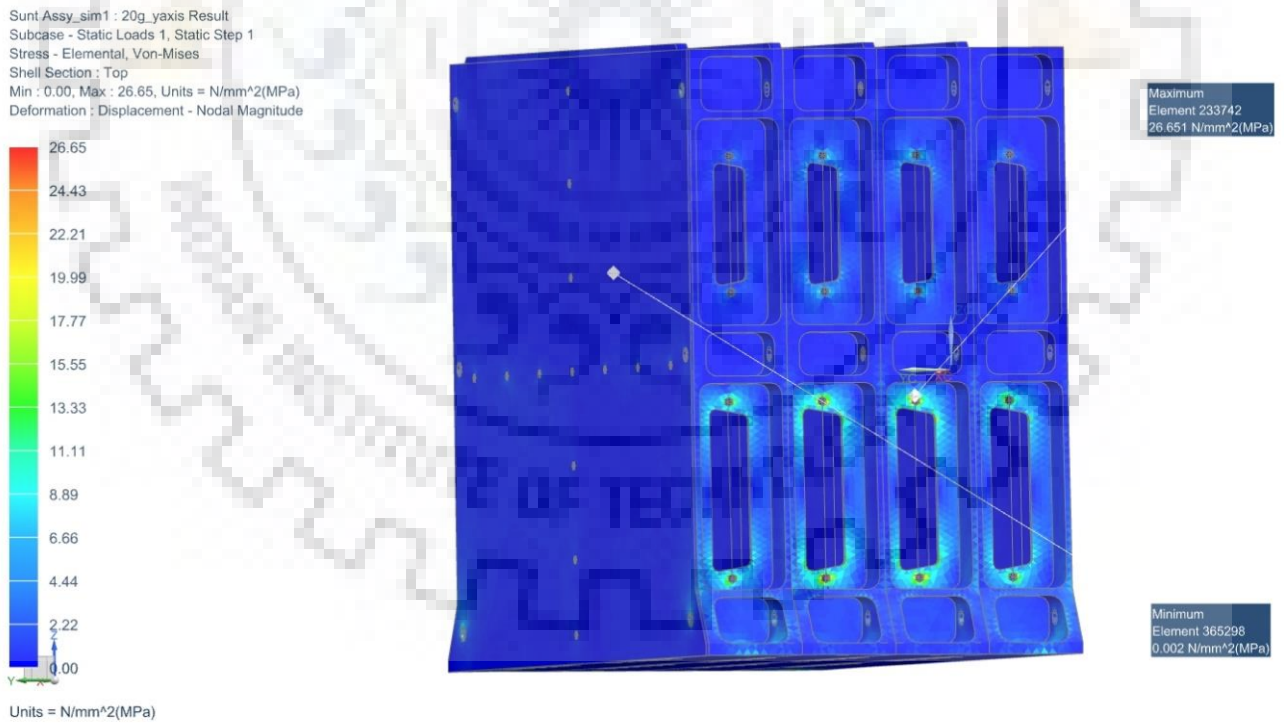


Fig 6-4: Maximum Stress of Vertical mounting package under 20 g loading for Al6061

The fig 6.1 to fig 6.4 shows the maximum displacement and maximum stress of vertical mounting packages under 20 g and 25 g inertial loading for AL6061 material. In UG-NX each element takes 20 g and 25 g loading when respective inertial load is applied over the entire package leading to a uniform load distribution. It can be observed that maximum displacement occurs at node 139214 for vertical mounting package which is 0.1 mm under 20 g loading. The maximum displacement is concentrated on the top plate of the module and the displacement is gradually less as we move down towards the mounting plane. This is because the package is held to the deck by the help of 8 screws which holds the package rigidly. The displacement values obtained are very less and the package can withstand the load without losing its structural integrity. It can also be observed that maximum stress is 26.65 MPa under 20 g loading for Al6061 material. The maximum stress is concentrated on the connector mounting location.

Now, Quasi-static analysis has been carried out for AZ31B material for vertical mounting package. By the analysis, it is found that the maximum value of displacement and stress is in 20 g loading condition as compare to 25 g loading condition. Fig 6.5 to Fig 6.8 shows the quasi-static analysis for AZ31B material and corresponding maximum displacement and maximum stress is shown in the respective figures.

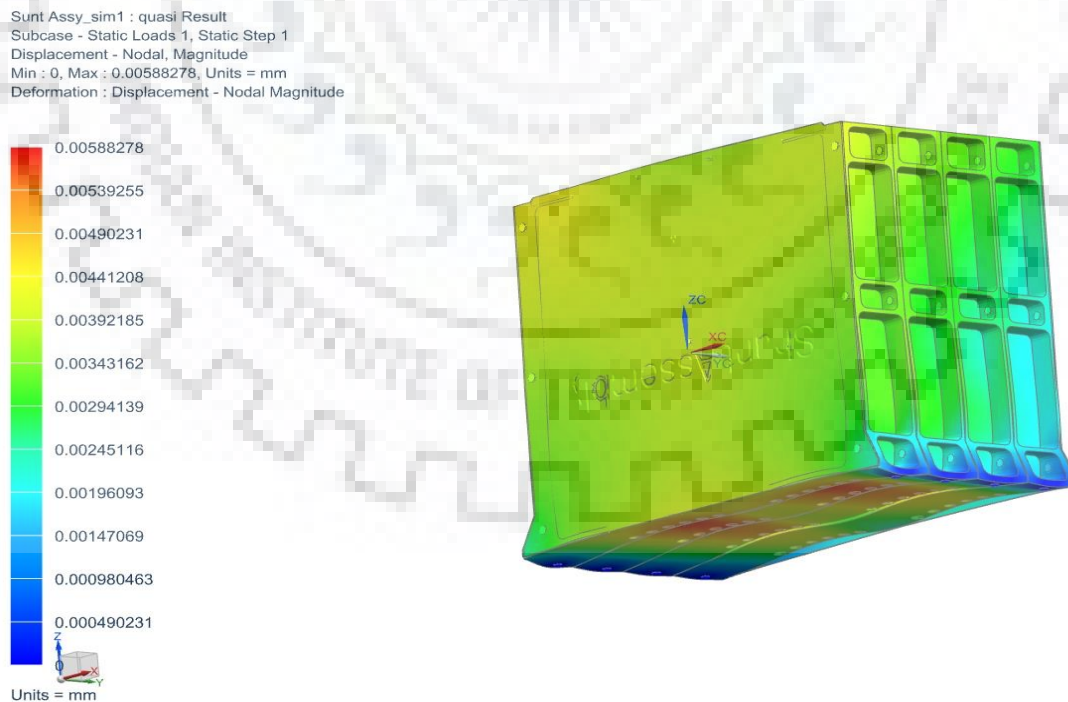


Fig 6-5: Maximum Displacement of Vertical mounting package under 25 g loading for AZ31B

Sunt Assy_sim1 : 20g_yaxis Result
 Subcase - Static Loads 1, Static Step 1
 Displacement - Nodal, Magnitude
 Min : 0.0000, Max : 0.1065, Units = mm
 Deformation : Displacement - Nodal Magnitude

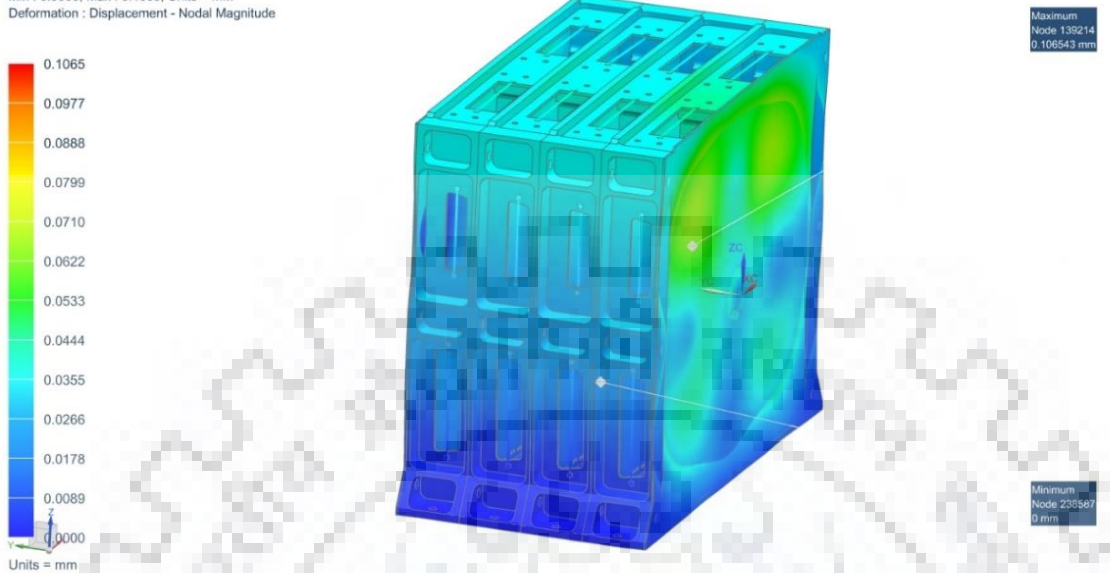


Fig 6-6: Maximum Displacement of Vertical mounting package under 20 g loading for AZ31B

Sunt Assy_sim1 : quasi Result
 Subcase - Static Loads 1, Static Step 1
 Stress - Elemental, Von-Mises
 Shell Section : Top
 Min : 0.000, Max : 8.379, Units = N/mm²(MPa)
 Deformation : Displacement - Nodal Magnitude

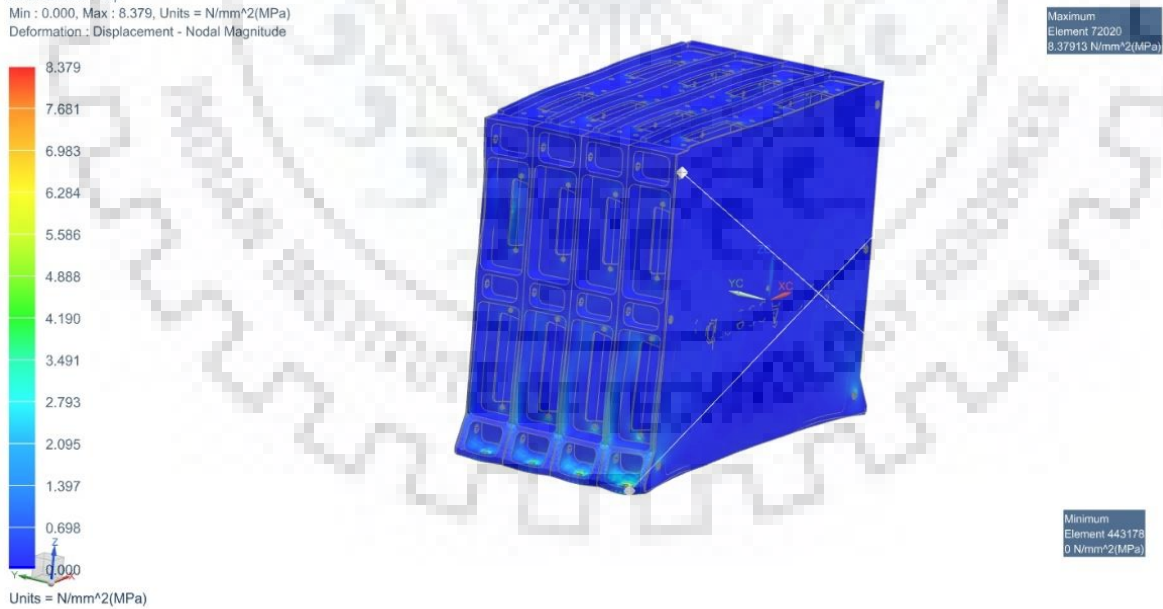


Fig 6-7: Maximum Stress of Vertical mounting package under 25 g loading for AZ31B

Sunt Assy_sim1 : 20g_yaxis Result
Subcase - Static Loads 1, Static Step 1
Stress - Elemental, Von-Mises
Shell Section : Top
Min : 0.00, Max : 23.61, Units = N/mm²(MPa)
Deformation : Displacement - Nodal Magnitude

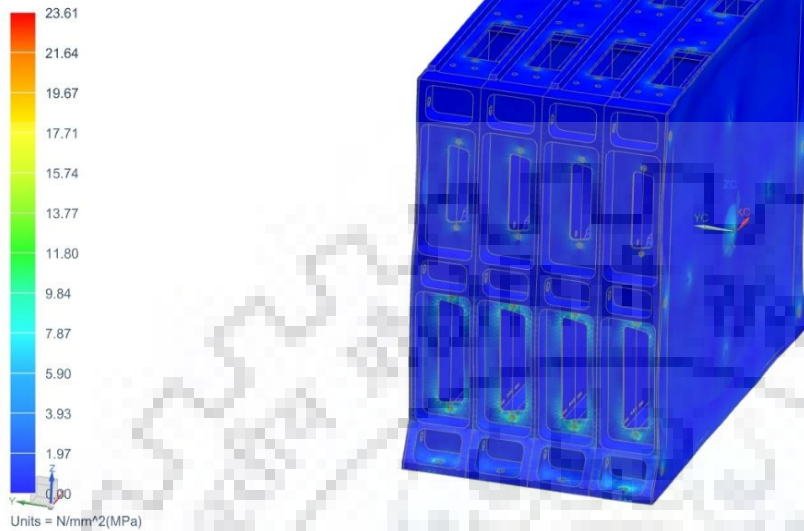


Fig 6-8: Maximum Stress of Vertical mounting package under 20 g loading for AZ31B

The fig 6.5 to fig 6.8 shows the maximum displacement and maximum stress of vertical mounting packages under 20 g and 25 g inertial loading for AZ31B material. In UG-NX each element takes 20 g and 25 g loading when respective inertial load is applied over the entire package leading to a uniform load distribution. It can be observed that maximum displacement occurs at node 139214 for vertical mounting package which is 0.1 mm under 20 g loading. The maximum displacement is concentrated on the top plate of the module and the displacement is gradually less as we move down towards the mounting plane. This is because the package is held to the deck by the help of 8 screws which holds the package rigidly. The displacement values obtained are very less and the package can withstand the load without losing its structural integrity. It can also be observed that maximum stress is 23.61 MPa under 20 g loading for AZ31B material. The maximum stress is concentrated on the connector mounting location.

Now, Quasi-static analysis has been carried out for AM162 material for vertical mounting package. By the analysis, it is found that the maximum value of displacement and stress is in 20 g loading condition as compare to 25 g loading condition. Fig 6.9 to Fig 6.12 shows the quasi-static analysis for AM162 material and corresponding maximum displacement and maximum stress is shown in the respective figures.

Sunt Assy_sim1 : quasi Result
Subcase - Static Loads 1, Static Step 1
Displacement - Nodal, Magnitude
Min : 0, Max : 0.00215484, Units = mm
Deformation : Displacement - Nodal Magnitude

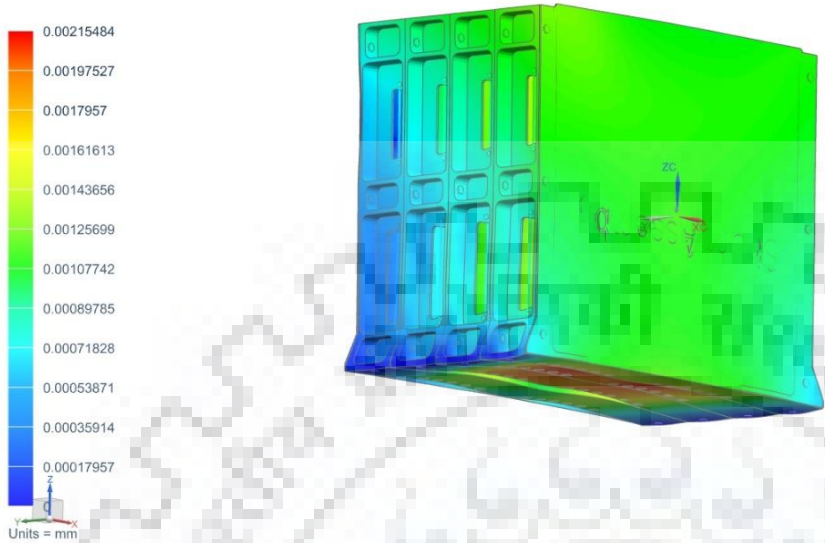


Fig 6-9: Maximum Displacement of Vertical mounting package under 25 g loading for AM162

Sunt Assy_sim1 : 20g_yaxis Result
Subcase - Static Loads 1, Static Step 1
Displacement - Nodal, Magnitude
Min : 0.0000, Max : 0.0311, Units = mm
Deformation : Displacement - Nodal Magnitude

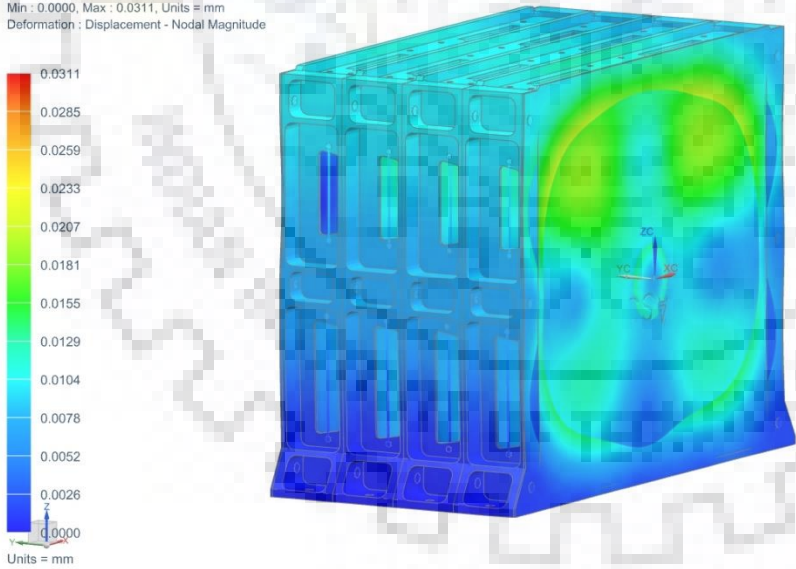


Fig 6-10: Maximum Displacement of Vertical mounting package under 20 g loading for AM162

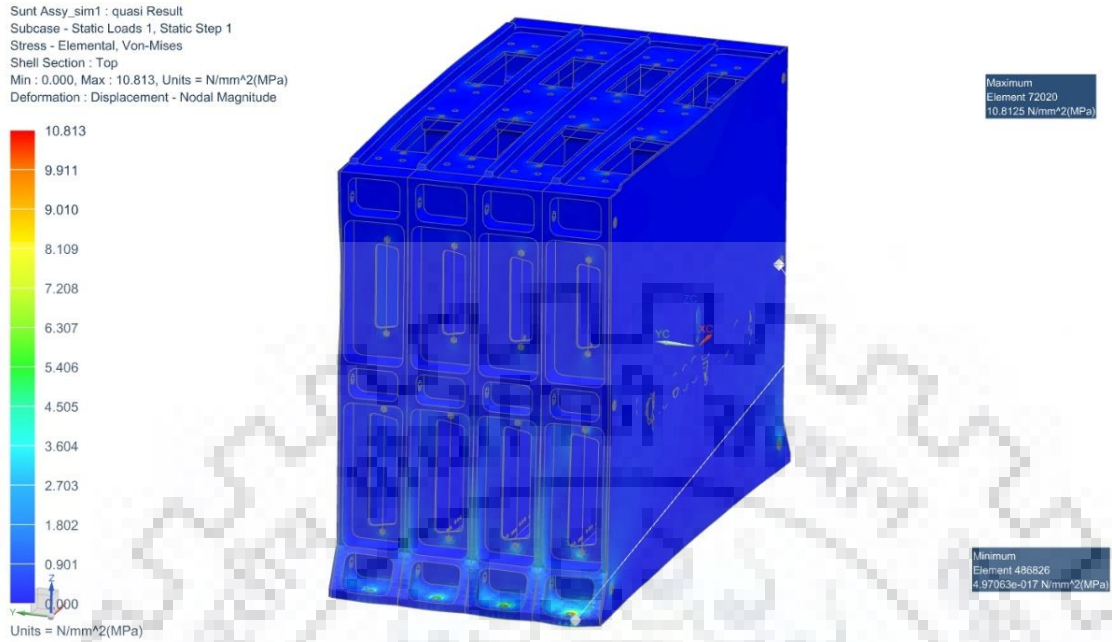


Fig 6-11: Maximum Stress of Vertical mounting package under 25 g loading for AM162

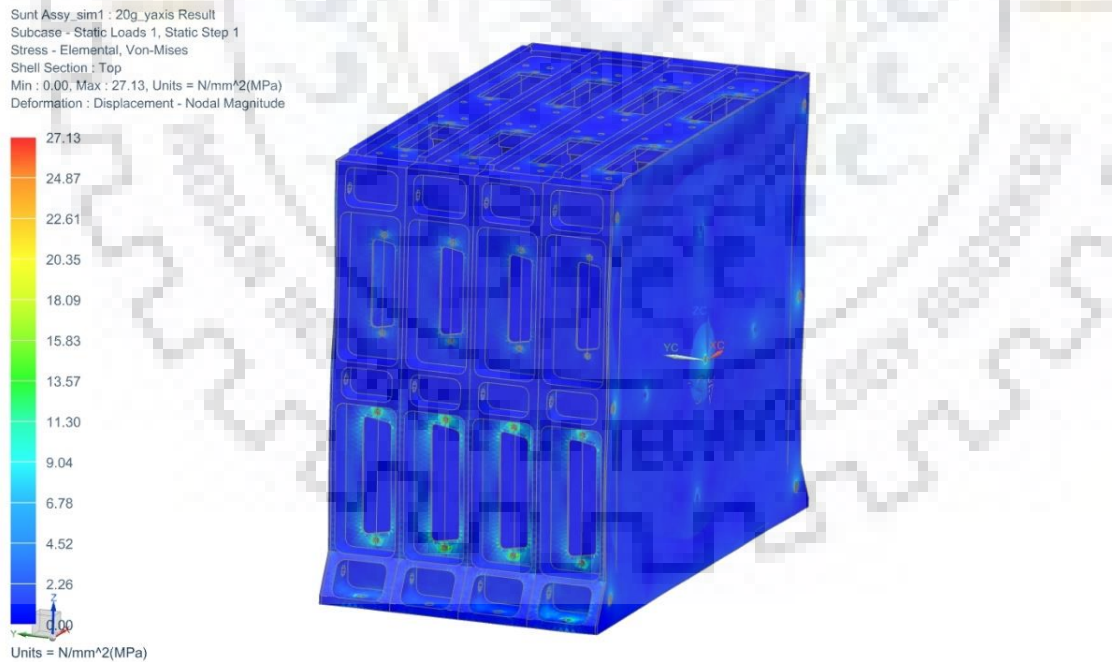


Fig 6-12: Maximum Stress of Vertical mounting package under 20 g loading for AM162

The fig 6.9 to fig 6.12 shows the maximum displacement and maximum stress of vertical mounting packages under 20 g and 25 g inertial loading for AM162 material. In UG-NX each element takes 20 g and 25 g loading when respective inertial load is applied over the entire package leading to a uniform load distribution. It can be observed that maximum displacement occurs at node 139214 for vertical mounting package which is 0.031 mm under 20 g loading. The maximum displacement is concentrated on the top plate of the module and the displacement is gradually less as we move down towards the mounting plane. This is because the package is held to the deck by the help of 8 screws which holds the package rigidly. The displacement values obtained are very less and the package can withstand the load without losing its structural integrity. It can also be observed that maximum stress is 27.13 MPa under 20 g loading for AM162 material. The maximum stress is concentrated on the connector mounting location.

Table 6.1: Comparison of maximum Stress and displacement of vertical mounting package for Al6061, AZ31B and AM162 materials

Load direction / Materials		Al6061	AZ31B	AM162
25g (Z-direction)	Displacement (mm)	0.0055	0.0058	0.0021
	Stress (MPa)	10.35	8.379	10.813
20g (Y-direction)	Displacement (mm)	0.1077	0.1065	0.0311
	Stress (MPa)	26.65	23.51	27.13
20g (X-direction)	Displacement (mm)	0.00489	0.0044	0.00178
	Stress (MPa)	6.58	8.618	13.45

By comparison, it is observed that the maximum value of displacement and stress of vertical mounting package for all materials is in 20 g direction. By this analysis, it is observed that maximum value of displacement is least for AM162 material and highest for Al6061 material and maximum value of stress is least for AZ31B and highest for AM162 material for vertical mounting package.

6.2.1.2 Quasi-static analysis for Horizontal Mounting package for Al6061, AZ31B and AM162 materials

In Quasi-static analysis, the package is loaded by 25 g loading condition in longitudinal direction and 20 g in both lateral direction by giving fixed constrained at the mounting points. Since horizontal mounting package has 8 mounting location so all 8 location has been given fixed constrained and then one by one 25 g and 20 g loading has been done over the package for all three materials i.e. Al6061, AZ31B and AM162. By this loading, for horizontal mounting package, maximum displacement and maximum stress value is obtained in both 25 g and 20 g direction for all three materials at the critical locations of the package.

Quasi-static analysis has been carried out for Al6061 material. By the analysis, it is found that the maximum value of displacement and stress is in 20 g loading condition as compare to 25 g loading condition. Fig 6.13 to Fig 6.16 shows the quasi-static analysis for AL6061 material and corresponding maximum displacement and maximum stress is shown in the respective figures.

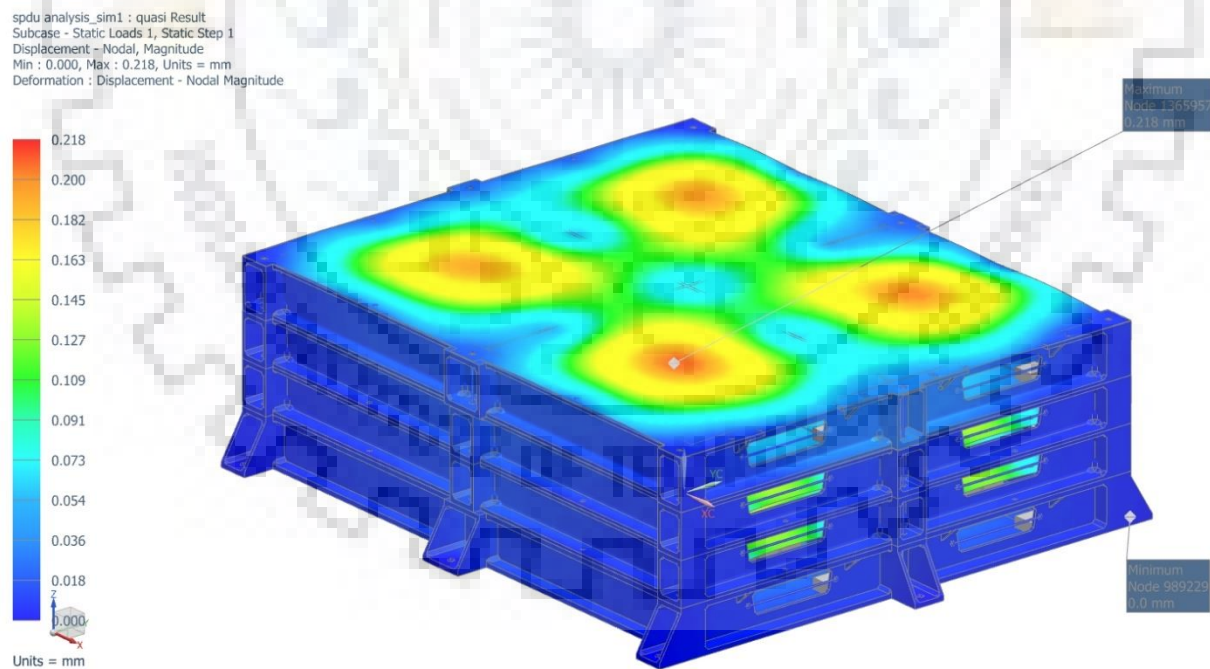


Fig 6-13: Maximum Displacement of horizontal mounting package under 25 g loading for Al6061

spdu analysis_sim1 : 20g_yaxis Result
Subcase - Static Loads 1, Static Step 1
Displacement - Nodal, Magnitude
Min : 0.0000, Max : 0.0531, Units = mm
Deformation : Displacement - Nodal Magnitude

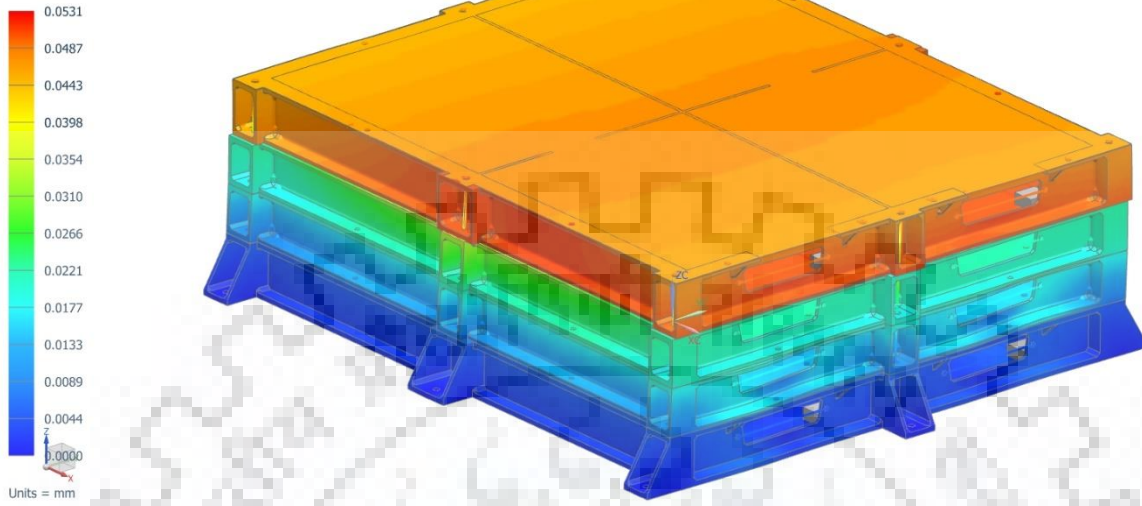


Fig 6-14: Maximum Displacement of horizontal mounting package under 20 g loading for Al6061

spdu analysis_sim1 : quasi Result
Subcase - Static Loads 1, Static Step 1
Stress - Elemental, Von-Mises
Shell Section : Top
Min : 0.00, Max : 76.09, Units = N/mm^2(MPa)
Deformation : Displacement - Nodal Magnitude

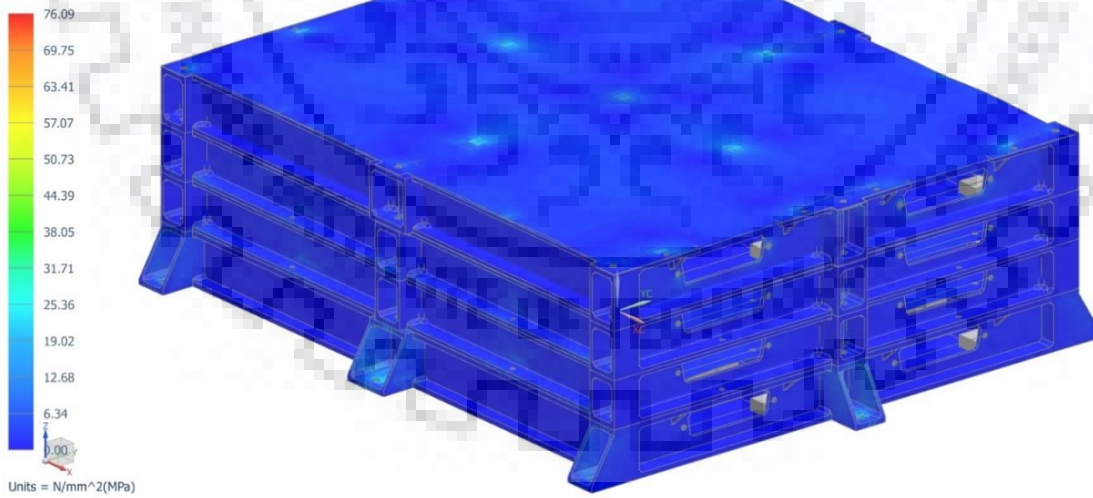


Fig 6-15: Maximum Stress of horizontal mounting package under 25 g loading for Al6061

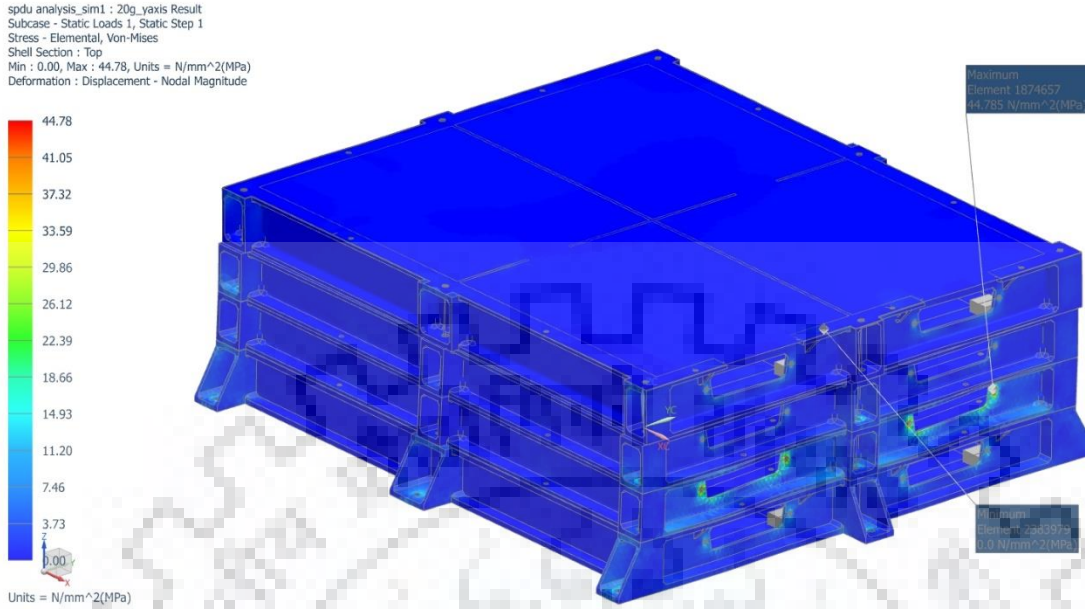


Fig 6-16: Maximum Stress of horizontal mounting package under 20 g loading for Al6061

The fig 6.12 to fig 6.16 shows the maximum displacement and maximum stress of vertical mounting packages under 20 g and 25 g inertial loading for AL6061 material. In UG-NX each element takes 20 g and 25 g loading when respective inertial load is applied over the entire package leading to a uniform load distribution. It can be observed that maximum displacement occurs at node 1365957 for horizontal mounting package which is 0.218 mm under 25 g loading. The maximum displacement is concentrated on the top plate of the module and the displacement is gradually less as we move down towards the mounting plane. This is because the package is held to the deck by the help of 8 screws which holds the package rigidly. The displacement values obtained are very less and the package can withstand the load without losing its structural integrity. It can also be observed that maximum stress is 76.09 MPa under 25 g loading for Al6061 material. The maximum stress is concentrated on the lugs at the mounting location.

Now, Quasi-static analysis has been carried out for AZ31B material for horizontal mounting package. By the analysis, it is found that the maximum value of displacement and stress is in 20 g loading condition as compare to 25 g loading condition. Fig 6.17 to Fig 6.20 shows the quasi-static analysis for AZ31B material and corresponding maximum displacement and maximum stress is shown in the respective figures.

spdu analysis_sim1 : quasi Result
Subcase - Static Loads 1, Static Step 1
Displacement - Nodal, Magnitude
Min : 0.000, Max : 0.291, Units = mm
Deformation : Displacement - Nodal Magnitude

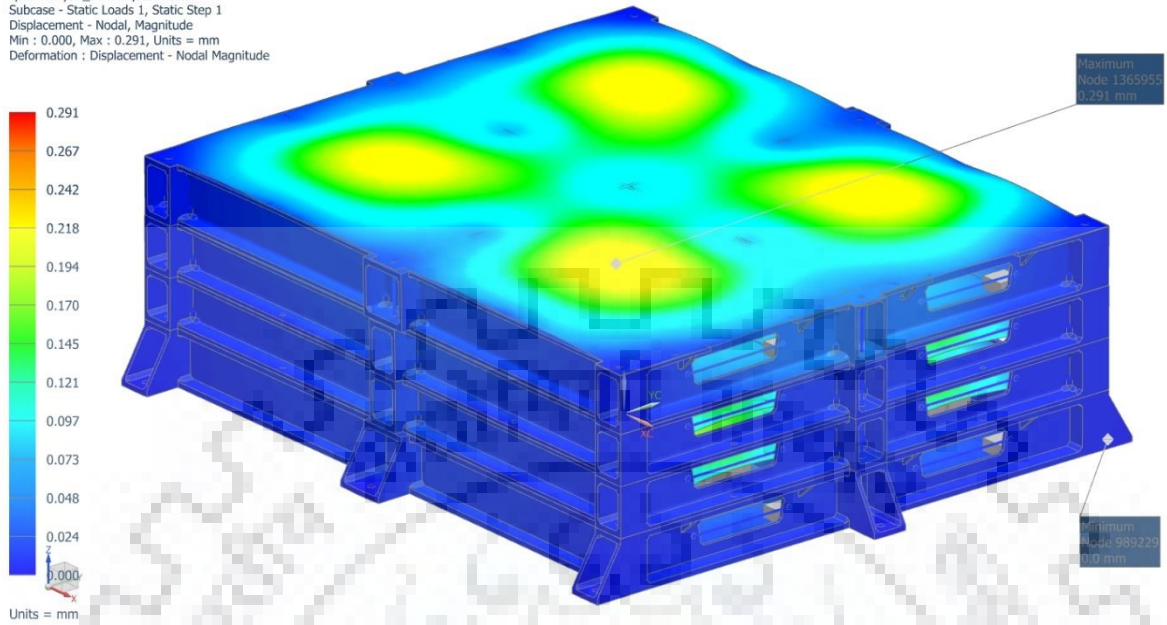


Fig 6-17: Maximum Displacement of horizontal mounting package under 25 g loading for AZ31B

spdu analysis_sim1 : 20g_yaxis Result
Subcase - Static Loads 1, Static Step 1
Displacement - Nodal, Magnitude
Min : 0.0000, Max : 0.0686, Units = mm
Deformation : Displacement - Nodal Magnitude

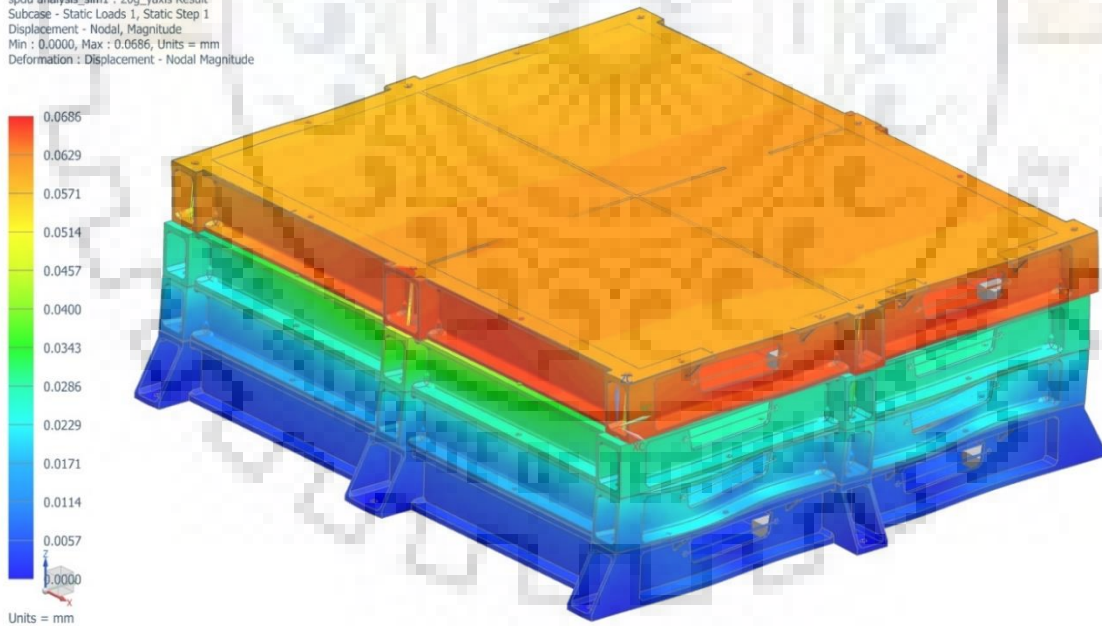


Fig 6-18: Maximum Displacement of horizontal mounting package under 20 g loading for AZ31B

spdu analysis_sim1 : quasi Result
Subcase - Static Loads 1, Static Step 1
Stress - Elemental, Von-Mises
Shell Section : Top
Min : 0.00, Max : 69.39, Units = N/mm²(MPa)
Deformation : Displacement - Nodal Magnitude

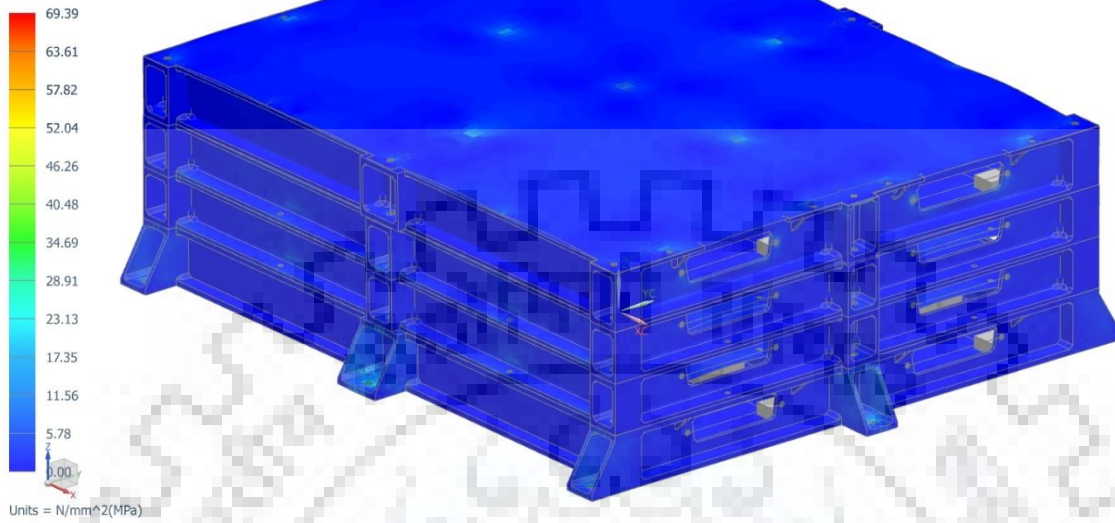


Fig 6-19: Maximum Stress of horizontal mounting package under 25 g loading for AZ31B

spdu analysis_sim1 : 20g_yaxis Result
Subcase - Static Loads 1, Static Step 1
Stress - Elemental, Von-Mises
Shell Section : Top
Min : 0.00, Max : 40.06, Units = N/mm²(MPa)
Deformation : Displacement - Nodal Magnitude

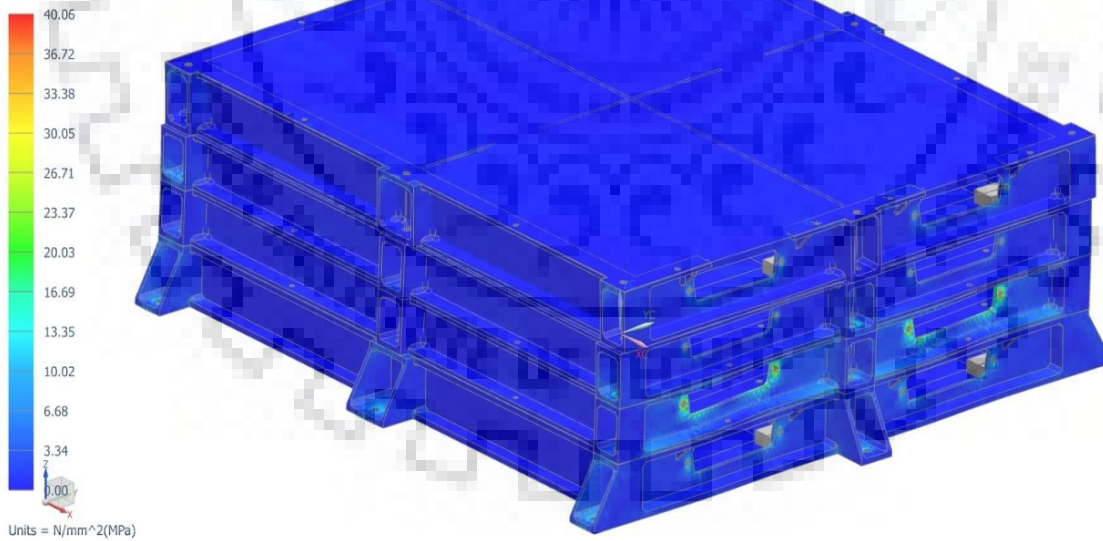


Fig 6-20: Maximum Stress of horizontal mounting package under 20 g loading for AZ31B

The fig 6.17 to fig 6.20 shows the maximum displacement and maximum stress of vertical mounting packages under 20 g and 25 g inertial loading for AZ31B material. In UG-NX each element takes 20 g and 25 g loading when respective inertial load is applied over the entire package leading to a uniform load distribution. It can be observed that maximum displacement occurs at node 1365957 for horizontal mounting package which is 0.291 mm under 25 g loading. The maximum displacement is concentrated on the top plate of the module and the displacement is gradually less as we move down towards the mounting plane. This is because the package is held to the deck by the help of 8 screws which holds the package rigidly. The displacement values obtained are very less and the package can withstand the load without losing its structural integrity. It can also be observed that maximum stress is 69.39 MPa under 25 g loading for AZ31B material. The maximum stress is concentrated on the lugs at the mounting location.

Now, Quasi-static analysis has been carried out for AM162 material for horizontal mounting package. By the analysis, it is found that the maximum value of displacement and stress is in 20 g loading condition as compare to 25 g loading condition. Fig 6.21 to Fig 6.24 shows the quasi-static analysis for AM162 material and corresponding maximum displacement and maximum stress is shown in the respective figures.

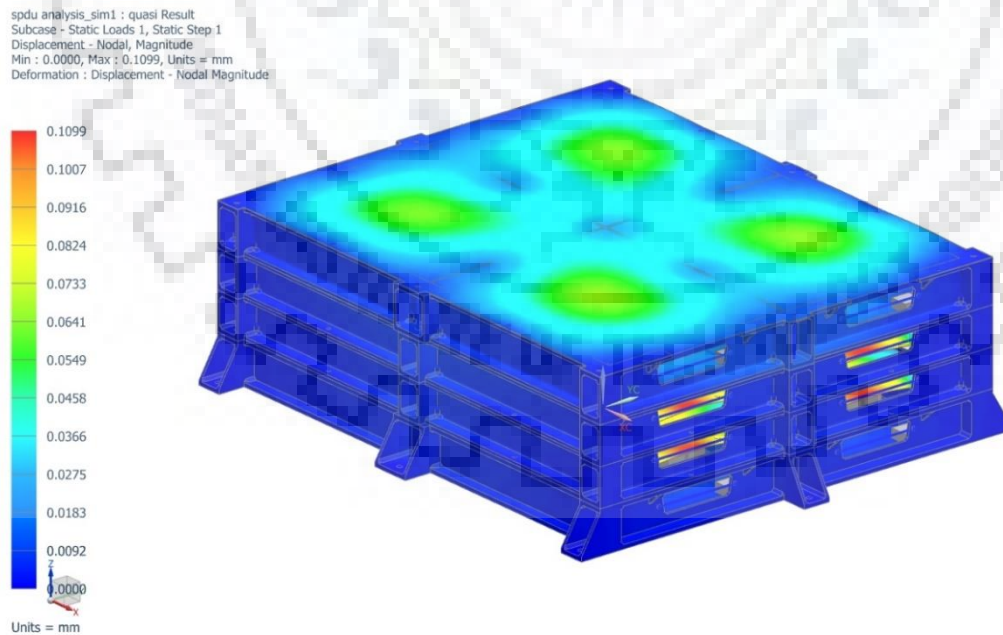


Fig 6-21: Maximum Displacement of horizontal mounting package under 25 g loading for AM162

spdu analysis_sim1 : 20g_yaxis Result
Subcase - Static Loads 1, Static Step 1
Displacement - Nodal, Magnitude
Min : 0.0000, Max : 0.0170, Units = mm
Deformation : Displacement - Nodal Magnitude

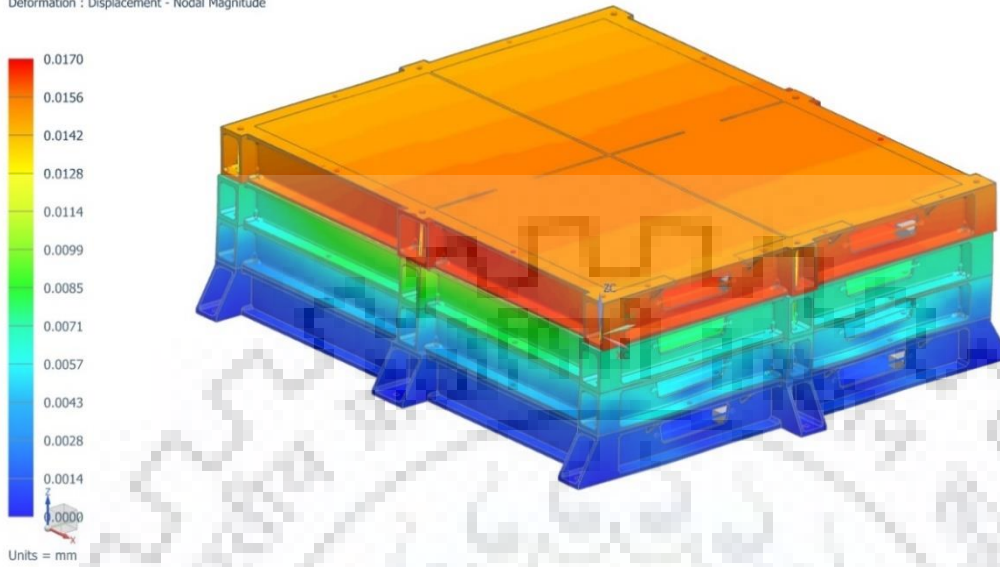


Fig 6-22: Maximum Displacement of horizontal mounting package under 20 g loading for AM162

spdu analysis_sim1 : quasi Result
Subcase - Static Loads 1, Static Step 1
Stress - Elemental, Von-Mises
Shell Section : Top
Min : 0.00, Max : 75.77, Units = N/mm²(MPa)
Deformation : Displacement - Nodal Magnitude

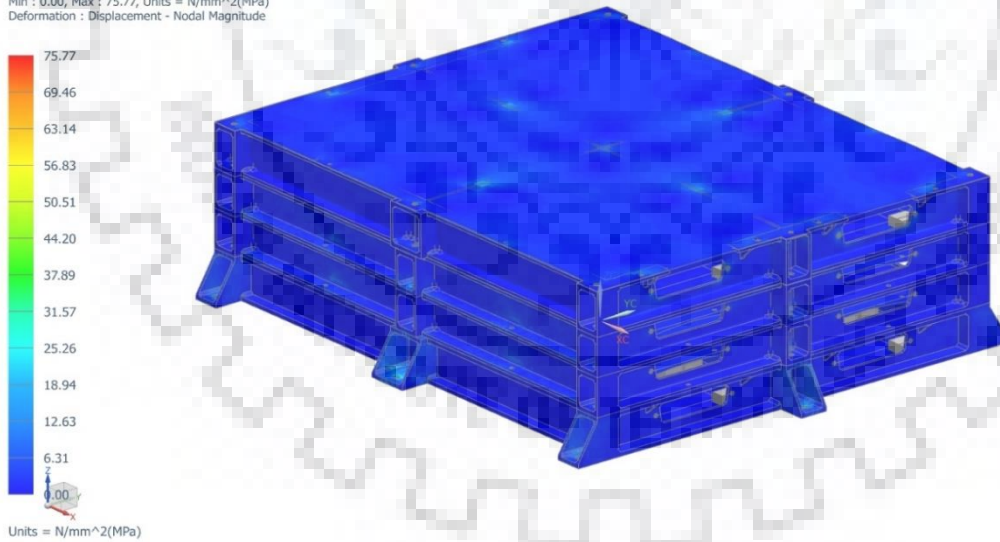


Fig 6-23: Maximum Stress of horizontal mounting package under 25 g loading for AM162

spdu analysis_sim1 : 20g_yaxis Result
Subcase - Static Loads 1, Static Step 1
Stress - Elemental, Von-Mises
Shell Section : Top
Min : 0.00, Max : 46.34, Units = N/mm²(MPa)
Deformation : Displacement - Nodal Magnitude

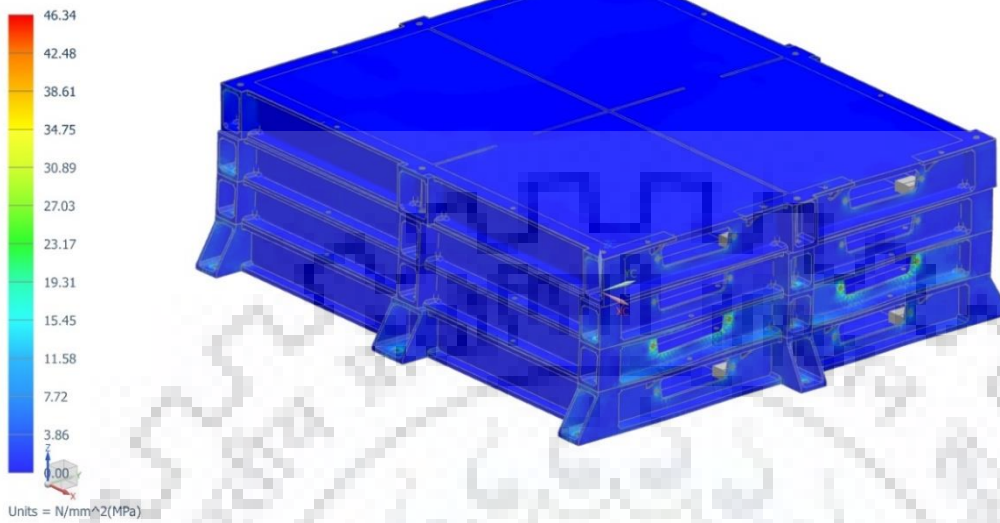


Fig 6-24: Maximum Stress of horizontal mounting package under 20 g loading for AM162

The fig 6.21 to fig 6.24 shows the maximum displacement and maximum stress of vertical mounting packages under 20 g and 25 g inertial loading for AM162 material. In UG-NX each element takes 20 g and 25 g loading when respective inertial load is applied over the entire package leading to a uniform load distribution. It can be observed that maximum displacement occurs at node 1365957 for horizontal mounting package which is 0.11 mm under 25 g loading. The maximum displacement is concentrated on the top plate of the module and the displacement is gradually less as we move down towards the mounting plane. This is because the package is held to the deck by the help of 8 screws which holds the package rigidly. The displacement values obtained are very less and the package can withstand the load without losing its structural integrity. It can also be observed that maximum stress is 75.77 MPa under 25 g loading for AM162 material. The maximum stress is concentrated on the lugs at the mounting location.

Table 6.2: Comparison of maximum Stress and displacement of horizontal mounting packages for Al6061, AZ31B and AM162 materials

Load direction / Materials		Al6061	AZ31B	AM162
25 g (Z-direction)	Displacement (mm)	0.218	0.291	0.1099
	Stress (MPa)	76.09	69.39	75.77
20 g (Y-direction)	Displacement (mm)	0.0531	0.0686	0.017
	Stress (MPa)	44.78	40.06	46.34
20 g (X-direction)	Displacement (mm)	0.0473	0.0613	0.0153
	Stress (MPa)	31.37	27.63	32.97

By comparison, it is observed that the maximum value of displacement and stress of horizontal mounting package for all materials is in 25g direction. By this analysis, it is observed that maximum value of displacement is least for AM162 material and highest for AZ31B material and maximum value of stress is least for AZ31B and highest for Al6061 material for horizontal mounting package.

6.2.2 Factor of safety

Factor of Safety is defined as the the ratio of the actual strength to the required strength. The allowable stress is determined by the yield strength of a given material isolated by a subjective FOS, depending on the material and the required utilization. The term FOS is used to determine the structural ability of a package ahead of excepted loads. Spacecraft and aerospace structural outline is still done all around utilizing code based plan then probabilistic methodologies. FoS is a factor connected to computations to make up for errors that can come about because of streamlining things.

FOS is given by equation.

$$F O S = \frac{\text{Yield stress}}{\text{Working Stress}} \dots\dots\dots (Eq-6.2)$$

Margin of safety, is needed with a specific end goal to guarantee the safety of the structure. In engineering the margin of safety is the factor of safety minus one. In spacecraft and aerospace structural components, the margin of safety is used in the place of factor of safety. The MoS permits the extra stress in the occasion the material is weaker than anticipated.

$$M O S = F O S - 1 \dots\dots\dots (Eq-6.3)$$

For EP it is necessary to calculate the FoS, to determine whether the package will sustain coming loads on the structure without failure. Following table describes the FoS of package for different materials with different thickness. The maximum stress is obtained by applying the unit load to all lug location of the power electronic package assembly. FoS and MoS of different mounting of package for all three materials is shown in Table 6.3.

Table 6-3: Calculations of FOS for maximum stress of both type of mountings for all three materials

Package Mounting	Material	Loading Condition	Von Mises Stress (MPa)	Maximum displacement (mm)	FOS	MOS
Vertical Mounting	Al6061	20g	26.65	0.1077	10.35	9.35
	AZ31B	20g	23.51	0.1065	8.51	7.51
	AM162	20g	27.13	0.0311	10.17	9.17
Horizontal Mounting	Al6061	25g	76.09	0.218	3.63	2.63
	AZ31B	25g	69.39	0.291	2.88	1.88
	AM162	25g	75.77	0.1099	3.64	2.64

By the table, it can be observed that the maximum displacement is least for Be-Al alloy (AM162) material but maximum value of stress is least for magnesium alloy (AZ31B). But for AM162 material, the maximum stress is in safe range. There is enough margin of safety (MOS) for Be-Al alloy (AM162). Therefore, Be-Al alloy (AM162) is the best one among all three material for making the electronic package mechanical housing because mass and displacement of this material is less and it is safe from strength point of view. However electronic package involves other parameters to be achieved, other than mass reduction, minimum stress, minimum displacement such as increased first fundamental frequency, higher fatigue life of the structure. Hence further analysis needs to be carried out for obtaining first fundamental frequency, transmissibility and effect of power spectral density during launch phase of the spacecraft.

6.3 Modal Analysis

With normal mode analysis, natural frequencies and mode shapes of electronic packages are calculated, whereas the natural frequencies are those frequencies at which a structure will tend to vibrate under disturbance. The mode shape is the deformed shape at a specific natural frequency. Normal mode analysis is also known as real Eigen value analysis.

Normal mode analysis lays down the foundation for a detailed understanding of the dynamic characteristics of the structure.

The equation of motion is of the form:

$$[M]\{u\} + [K]\{u\} = 0 \dots\dots\dots (Eq-6.4)$$

Where, [K] and [M] represents the stiffness and mass matrices depicting the elastic and inertial properties of the structure respectively. UG-NX develops these system matrices automatically on the basis of geometry and properties of the FE model.

Each mode shape is similar to a static displaced shape. However, scaling is one significant difference between the mode shape and the static displacement. True displacements are the physical displacements due to the applied loads in quasi-static analysis. All the components of mode shape can be scaled by using a factor since there is no applied load in normal mode

analysis. Similarly, Elementary stresses and reaction forces are calculated by quasi-static analysis.

Fig 6.25 shows the FE Model of electronic package subjected to modal analysis for vertical mounting package and in fig 6.26 shows the modal analysis of electronic package for horizontal mounting package. Since the cover plate is constrained at the center we can observe the behavior of cover plate at the center.

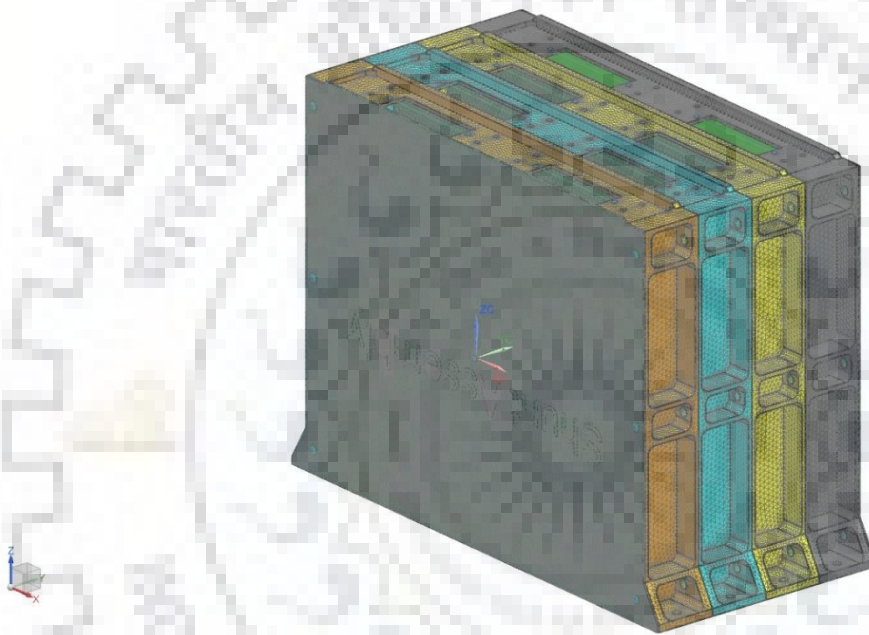


Fig 6.25: FE Model of vertical mounting EP subjected to modal analysis

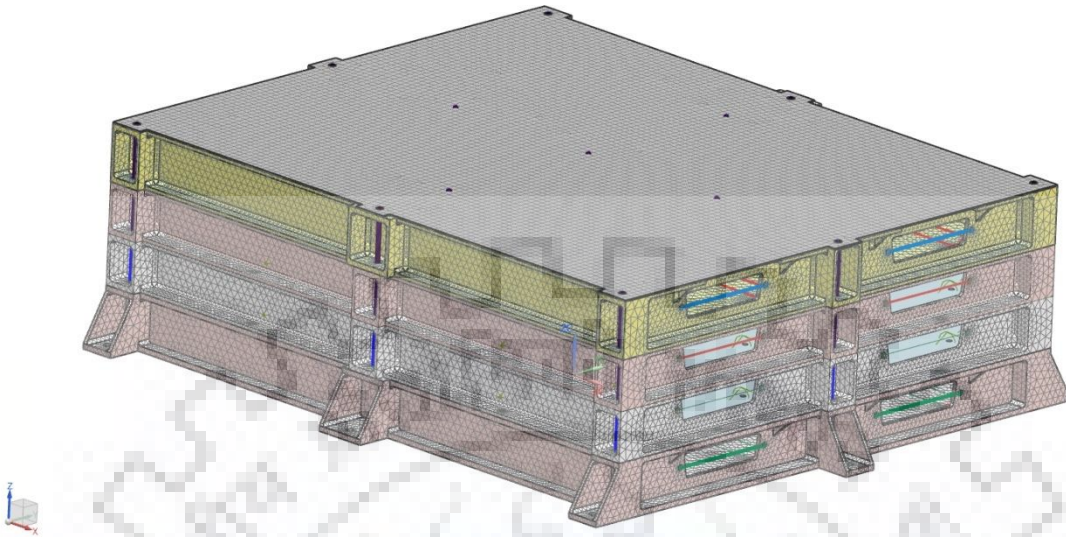


Fig 6.26: FE Model of horizontal mounting EP subjected to modal analysis

Table 6.4: Details of element used in FE model

Component	Material	Element property for FE simulation
Tray cover	Al-6061/AZ31B/AM162	3-D ,CTETRA(4)
Tray	Al-6061/AZ31B/AM162	3-D ,CTETRA(4)
PCB	FR-4	2-D, CQUAD(4)
Converters, Relays or any electronic component	-	PMASS, concentrated mass
Stud	SS-304/Ti	RBE2
Fasteners	SS-304/Ti	RBE2

6.3.1 Fundamental frequency of vertical mounting package for different materials

With normal mode analysis, natural frequencies and mode shapes of vertical mounting electronic package is calculated for all three materials i.e. Al6061, AZ31B and AM162. Simulation has been done from 20 Hz frequency to 2000 Hz frequency. Electronic package has been run by UG-NX software in this frequency range. Electronic package has many modes in this frequency range for all respective materials. The mode shape is the deformed shape at a specific natural frequency. First mode is called as fundamental mode and frequency of this mode is known as fundamental frequency. Fundamental frequency is the main concerned frequency because spacecraft experience 150 Hz frequency during launch phase so for safe working of electronic packages, fundamental frequency should be more than this frequency.

Normal mode analysis has been carried out for all three material for vertical mounting package. By the analysis, the fundamental frequency of vertical mounting package for all three material is obtained. Fig 6.27 to Fig 6.29 shows the fundamental frequency and mode shape on that fundamental frequency for Al6061, AZ31B and AM162 materials.

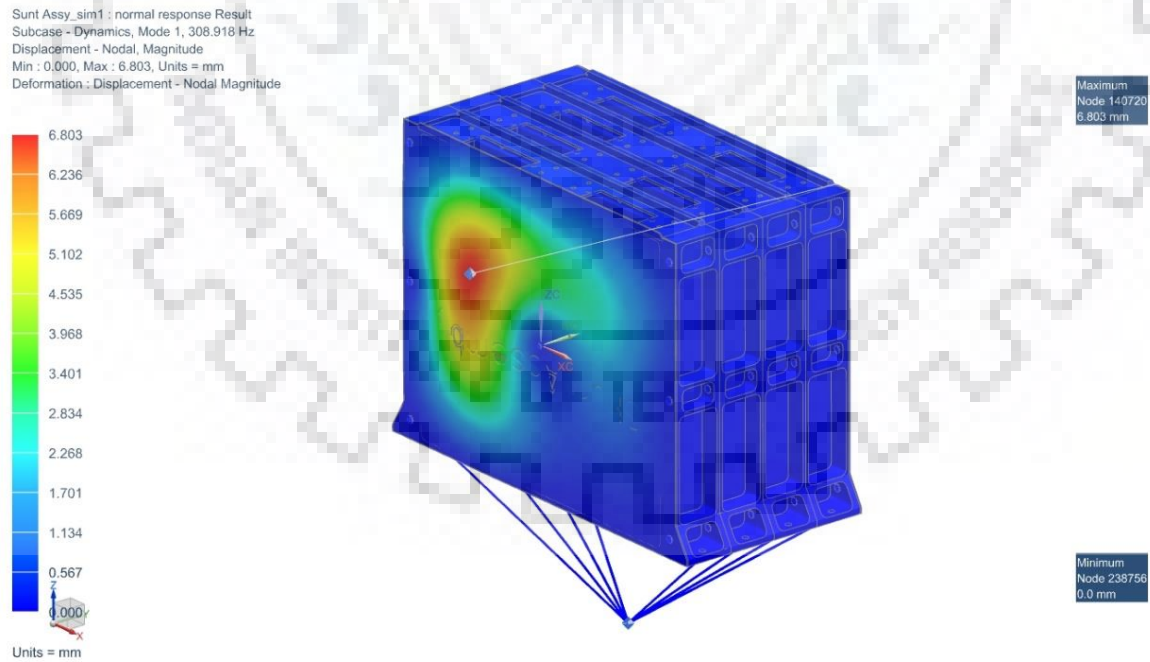


Fig 6-27: Fundamental frequency and mode shape of vertical mounting EP for Al6061

Sunt Assy_sim1 : normal response Result
Subcase - Dynamics, Mode 1, 307.999 Hz
Displacement - Nodal, Magnitude
Min : 0.000, Max : 7.796, Units = mm
Deformation : Displacement - Nodal Magnitude

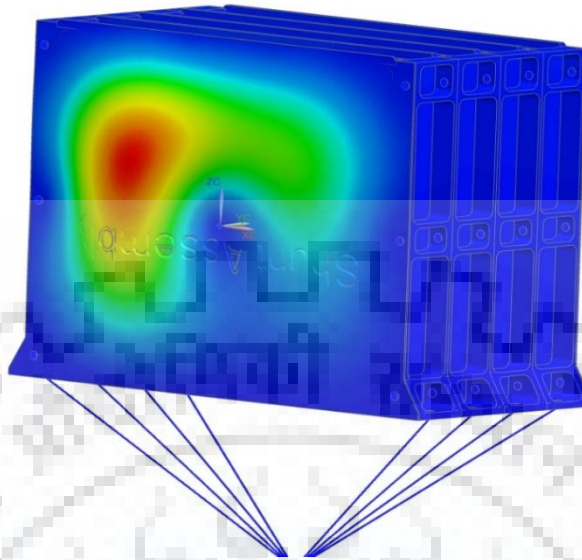


Fig 6-28: Fundamental frequency and mode shape of vertical mounting EP for AZ31B

Sunt Assy_sim1 : normal response Result
Subcase - Dynamics, Mode 1, 563.627 Hz
Displacement - Nodal, Magnitude
Min : 0.000, Max : 7.587, Units = mm
Deformation : Displacement - Nodal Magnitude

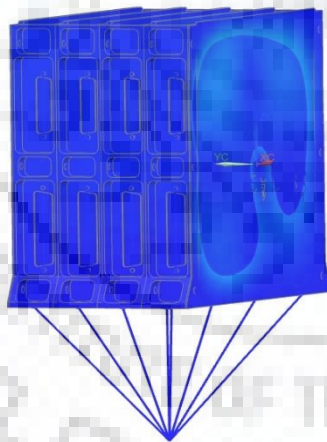
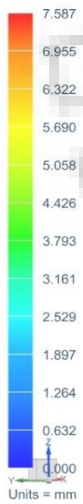


Fig 6-29: Fundamental frequency and mode shape of vertical mounting EP for AM162

6.3.2 Fundamental frequency of horizontal mounting package for different materials

With normal mode analysis, natural frequencies and mode shapes of horizontal mounting electronic package is calculated for all three materials i.e. Al6061, AZ31B and AM162. Simulation has been done from 20 Hz frequency to 2000 Hz frequency. Electronic package has been run by UG-NX software in this frequency range. Electronic package has many modes in this frequency range for all respective materials. The mode shape is the deformed shape at a specific natural frequency. First mode is called as fundamental mode and frequency of this mode is known as fundamental frequency. Fundamental frequency is the main concerned frequency because spacecraft experience 150 Hz frequency during launch phase so for safe working of electronic packages, fundamental frequency should be more than this frequency.

Normal mode analysis has been carried out for all three material for horizontal mounting package. By the analysis, the fundamental frequency of horizontal mounting package for all three material is obtained. Fig 6.30 to Fig 6.32 shows the fundamental frequency and mode shape on that fundamental frequency for Al6061, AZ31B and AM162 materials.

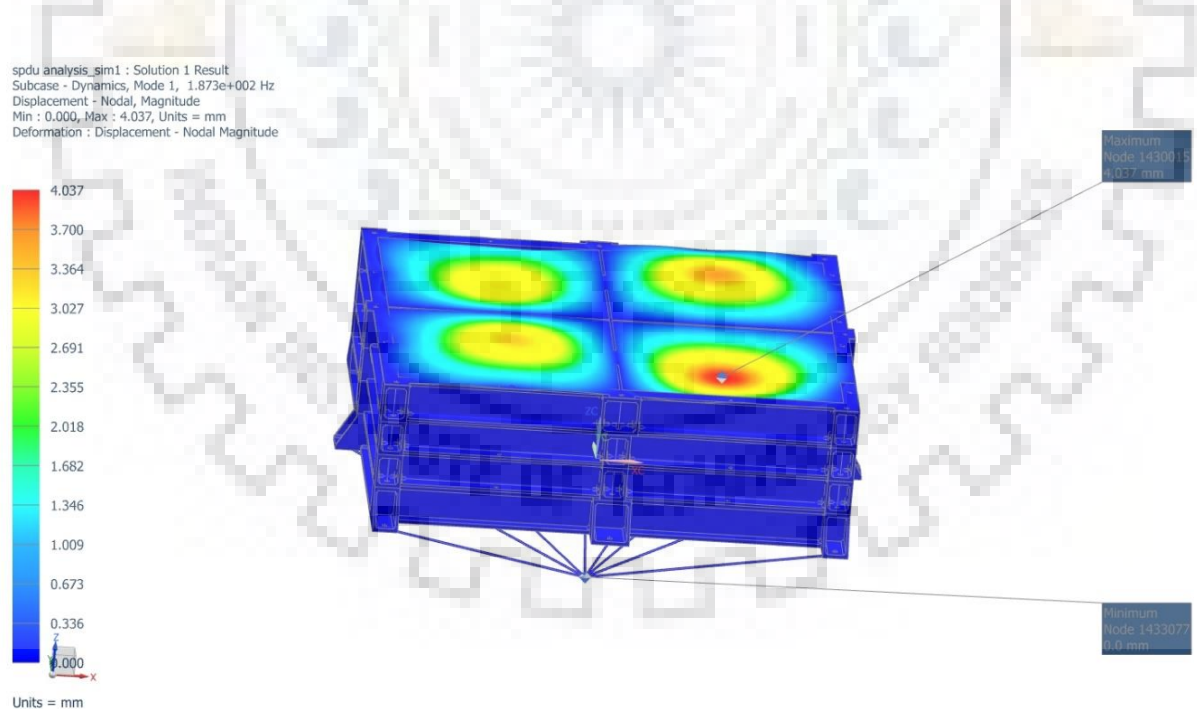


Fig 6-30: Fundamental frequency and mode shape of horizontal mounting EP for Al6061

spdu analysis_sim1 : y_axis_response Result
Subcase - Dynamics, Mode 1, 1.713e+002 Hz
Displacement - Nodal, Magnitude
Min : 0.000, Max : 1.912, Units = mm
Deformation : Displacement - Nodal Magnitude

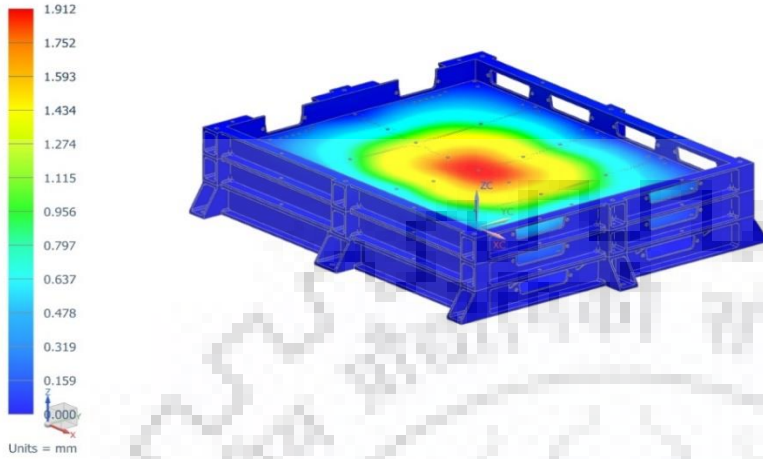


Fig 6-31: Fundamental frequency and mode shape of horizontal mounting EP for AZ31B

spdu analysis_sim1 : Solution 1 Result
Subcase - Dynamics, Mode 1, 2.808e+002 Hz
Displacement - Nodal, Magnitude
Min : 0.000, Max : 1.842, Units = mm
Deformation : Displacement - Nodal Magnitude

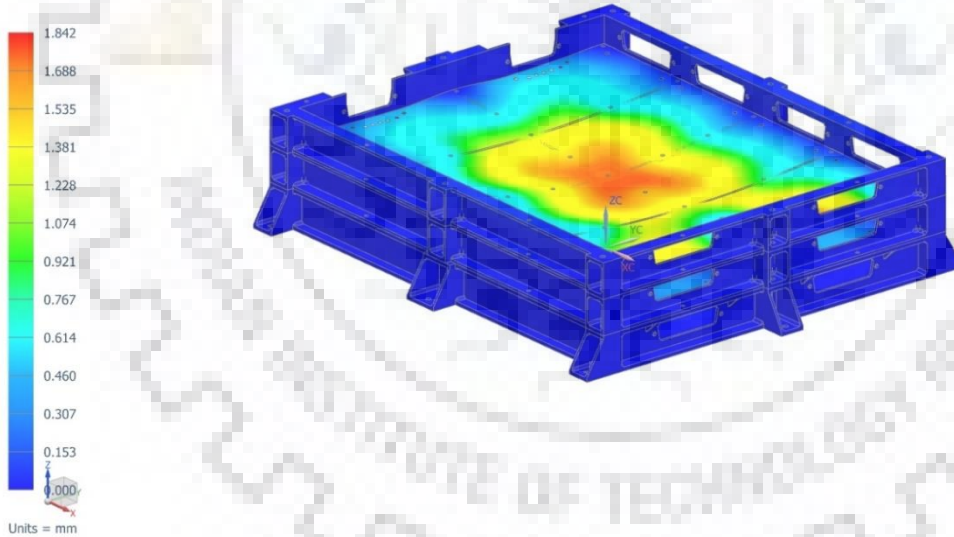


Fig 6-32: Fundamental frequency and mode shape of horizontal mounting EP for AM162

Table 6-5: Comparison of fundamental frequency for different materials

Package Mounting	Material	Fundamental frequency (Hz)
Vertical Mounting	Al6061	308
	AZ31B	307
	AM162	564
Horizontal Mounting	Al6061	187
	AZ31B	171
	AM162	280

By comparison, it is observed that the fundamental frequency is highest for Be-Al alloy (AM162) among all materials for both type of electronics packages and for vertical mounting package, the value of fundamental frequency is 564 Hz and for horizontal mounting package, the value of fundamental frequency is 280 Hz. In both cases, the fundamental frequency is higher than 150 Hz (minimum required at the time of launch of spacecraft). Therefore, Be-Al alloy (AM162) is safer as compare to other material from vibration point of view during launch phase.

6.4 Random Analysis

Random vibration is being specified for acceptance tests, screening tests, and qualification tests by commercial, industrial, and military manufacturers of electronic equipment, because it has been shown that random vibration more closely represents the true environments in which the electronic equipment must operate. This includes airplanes, missiles, automobiles, trucks, trains, and tanks as well as chemical processing plants, steel rolling mills, foundries, petroleum drilling machines, and numerically controlled milling machines. Random vibration has also proved to be a very powerful tool for improving the manufacturing integrity of electronic equipment by screening out defective components and defective assembly methods, which results in a sharp improvement in the overall reliability of the system.

Electronic packaging designers and engineers must understand the fundamental nature of random vibration and fatigue, in order to design, develop, and produce cost-effective and lightweight structures that are capable of operating in the desired environments with a high degree of reliability. They must examine the path that the dynamic load takes as it passes through the structure, to make sure there are no weak links that can cause catastrophic failures. They must also examine the load-carrying capability of the structural elements, to make sure they will not buckle under the expected dynamic loads. They must constantly be on the alert for major structural resonances that can magnify dynamic loads and stresses. If two major structural resonances occur close to one another, they may produce severe dynamic coupling effects that can produce rapid fatigue failures.

6.4.1 Basic Failure modes in Random Vibration

There are four basic failure modes that must be considered and controlled in order to produce a reliable electronic system. These failures are the results of the following conditions:

1. High acceleration
2. High stress levels
3. Large displacement amplitude
4. Electrical signal out of tolerance

Considering high acceleration levels, there are a number of electronic components, such as relays and crystal oscillators that will malfunction electrically when their internal resonances are excited. These components will not suffer catastrophic failures during the vibration; they will just not operate properly. For example, if the relays chatter, the electrical signal may be impaired and an electrical failure can occur. When the resonance is excited in a crystal oscillator, the electronic signal may be distorted enough to produce an electrical failure. Therefore, it is important to use electronic components that will be capable of proper operation in the expected environment. It is also important to locate these sensitive electronic components in areas that will not respond to severe resonant conditions. For example, mount the components at the edges of a plug-in PCB and not at the center.

Considering high stress levels, if they occur in major structural elements, then catastrophic failures can occur. This can usually be avoided by increasing the stiffness of the structure to raise

the resonant frequency. This reduces the dynamic displacements and stresses, so the fatigue life is improved.

Considering large displacement amplitudes, this often results in collision between adjacent PCBs when they are too close together, or when insufficient attention has been given to the placement tolerances. Collision between components on adjacent PCBs can result in broken and cracked components, circuit traces, and solder joints. PCB resonant frequencies must be high enough to limit the dynamic displacements, and positioning tolerances must be controlled to properly locate the PCBs.

Considering electrical signals out of tolerance, this can be caused by relative motion in cables and harnesses, high temperatures, relative motion within some capacitors, resonances within crystal oscillators, a slipping potentiometer, relative motion in a transformer core, and excessive motion in a tube filament.

6.4.2 Random vibration input curve

There are many different types of curves that can be used to show the random vibration input requirements. The most common curve, which is also the simplest, is the white-noise curve shown in Fig. 6.32. Random vibration input and response curves are typically plotted on log-log paper, with the power spectral density, expressed in squared acceleration units per hertz (G^2/Hz), plotted along the vertical axis, and the frequency (Hz) plotted along the horizontal axis. The power spectral density P is often referred to as the mean squared acceleration density, and it is defined by

$$P = G^2 / \Delta f \dots\dots\dots (Eqn 6.5)$$

In the above equation, G is the root mean square (RMS) of the acceleration expressed in gravity units, and Δf is the bandwidth of the frequency range expressed in hertz. Root mean square acceleration levels are related to the area under the random vibration curve. The input RMS acceleration levels can be obtained by integrating under the input random vibration curve, and the output (or response) RMS acceleration levels can be obtained by integrating under the output (or response) random vibration curve. The square root of the area then determines the RMS acceleration level.

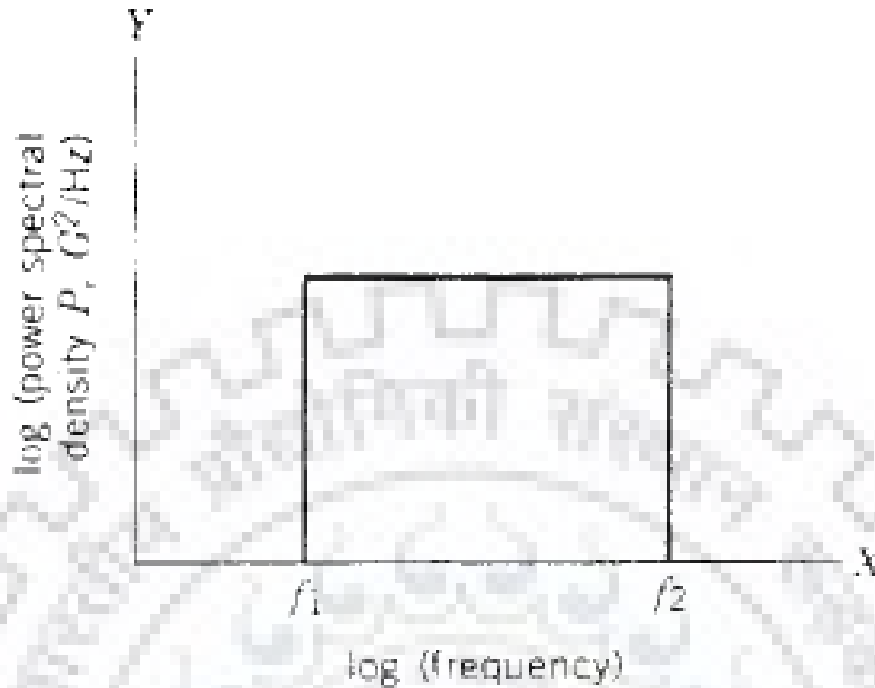


Fig 6-33: White- noise curve with a constant input power spectral density (PSD)

Random vibration environments in the electronics industry normally deal in terms of the power spectral density P (or mean squared acceleration density), which is measured in gravity units so that it is dimensionless. That is, the acceleration is divided by the acceleration of gravity:

$$G = \frac{\text{acceleration}}{\text{gravity}} = \text{dimensionless}$$

An acceleration level of 10 G means that the acceleration has a magnitude that is 10 times greater than the acceleration of gravity. The most common method used for evaluating random vibration is in terms of the power spectral density. However, random vibration can also be expressed in terms of velocity spectral density, and in terms of displacement spectral density. Unit of power spectral density is (acceleration²/frequency) or (g²/Hz).

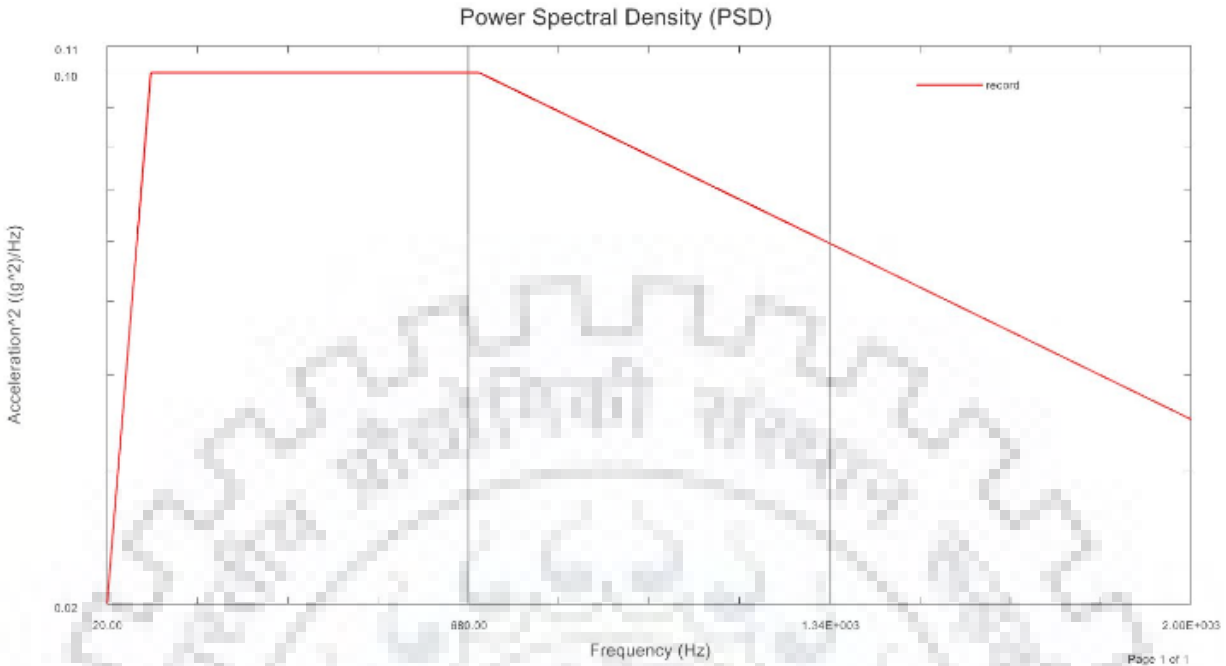


Fig 6-34: Input curve of power spectral density (PSD) used for spacecraft

In frequency response analysis of electronic packages, the entire package is subjected to base excitation from 20 Hz to 2000 Hz frequency range with a damping ratio of 3% and force is applied in the form of enforced motion in all direction one by one with gravity load. This analysis has been carried out with enforced motion in all direction with gravity load for different materials and for different mounting conditions. By this analysis, all the modes has been found out between 20 to 2000 Hz with 3% damping and by response simulation, the complete mass participation of the package between 20 to 2000 Hz has been found in all direction with respective enforced motion.

With the help of mass participation, particular node is identified where the mass participation is maximum and this node is called Global node for all three materials in both EP case. Global node is that node where electronic component can fail. There is the highest probability of electronic component failure at this node because of maximum mass participation. Because of the enforced motion with gravity load, the displacement and stress value can amplify. Because of this frequency range and enforced load, gravitational acceleration also can amplify. Since acceleration is directly proportional to displacement so this can affect displacement and the

output force on the package. So to find out this output force, transmissibility has been found out. Transmissibility is the ration of output parameter to input parameter. Parameter can be in the form of force or acceleration. With the help of transmissibility, output acceleration level has been found out. The package will experience this acceleration level during launch phase.

Therefore, transmissibility and output acceleration level has been found out by frequency response and random analysis respectively and also, root mean square value for stress and displacement has been found out by random analysis that the spacecraft will experience during launch phase. By the results, it can be observed that with critical damping coefficient of 3 %, there is an increase in response values up to a certain limit and then there is a decrease in acceleration level as it reaches to 2000 Hz as it can be observed in transmissibility curves of different materials.

6.4.3 Random analysis for vertical mounting electronic package

In random analysis of vertical mounting package, the entire package is subjected to base excitation from 20 Hz to 2000 Hz frequency range with a damping ratio of 3 % and force is applied in the form of enforced motion in all three direction one by one with gravity load. This analysis has been carried out for Al6061, AZ31B and AM162 material and mass participation has been found at all modes. Then global node is identified for particular material and at this global node, transmissibility and output acceleration curve is obtained. After this, input is given in form of PSD and output response of the vertical mounting package can be seen in PSD curves for all materials. By these curve, root mean square values of output acceleration level (G_{rms}) can be obtained in form of G for Al6061, AZ31B and AM162 material during launch phase. Similarly root mean square values of stress and displacement can be obtained.

Vertical package has the maximum mass participation in Y-direction as compare to other direction. Therefore, Y-direction is the critical direction for output parameters such as transmissibility and output acceleration level (G_{rms}) for all materials. It can be observed that transmissibility and output acceleration level (G_{rms}) value is highest at global node with Y-direction enforced motion.

6.4.3.1 Random analysis of vertical mounting EP with Al6061 material

For vertical mounting package, major mass participation modes for Al6061 material is given in the below table.

Table 6.6: Different modes of frequency and mass participation for Al6061 material with Y-direction enforced motion

Mode No.	Frequency (Hz)	X- Direction (%)	Y- Direction (%)	Z- Direction (%)
Mode 1	308	0.00010	2.63	0.00035
Mode 2	312	0.00005	12.10	0.00010
Mode 3	364	0.00000	0.00057	0.00002
Mode 4	414	0.00090	48.0557	0.00594
Mode 5	428	0.00009	0.2739	0.00003
Mode 6	504	0.00137	0.76163	0.00025
Mode 7	531	0.00064	1.57314	0.00087
Mode 8	557	0.00016	0.39135	0.00049
Mode 9	560	0.00076	0.07035	0.00044
Mode 10	576	0.00000	0.05258	0.00009

By the table, maximum mass participation is in Y-direction and global mode of this package for Al6061 material is mode 2 with frequency 312 Hz. This is called global mode because it is the first mode where mass participation is maximum. This maximum mass participation obtained at 140816 Node of the vertical mounting package for Al6061 material.

This node is be subjected to maximum enforced loading during launch phase, so transmissibility and output acceleration level (G_{rms}) is to be find out at this node.

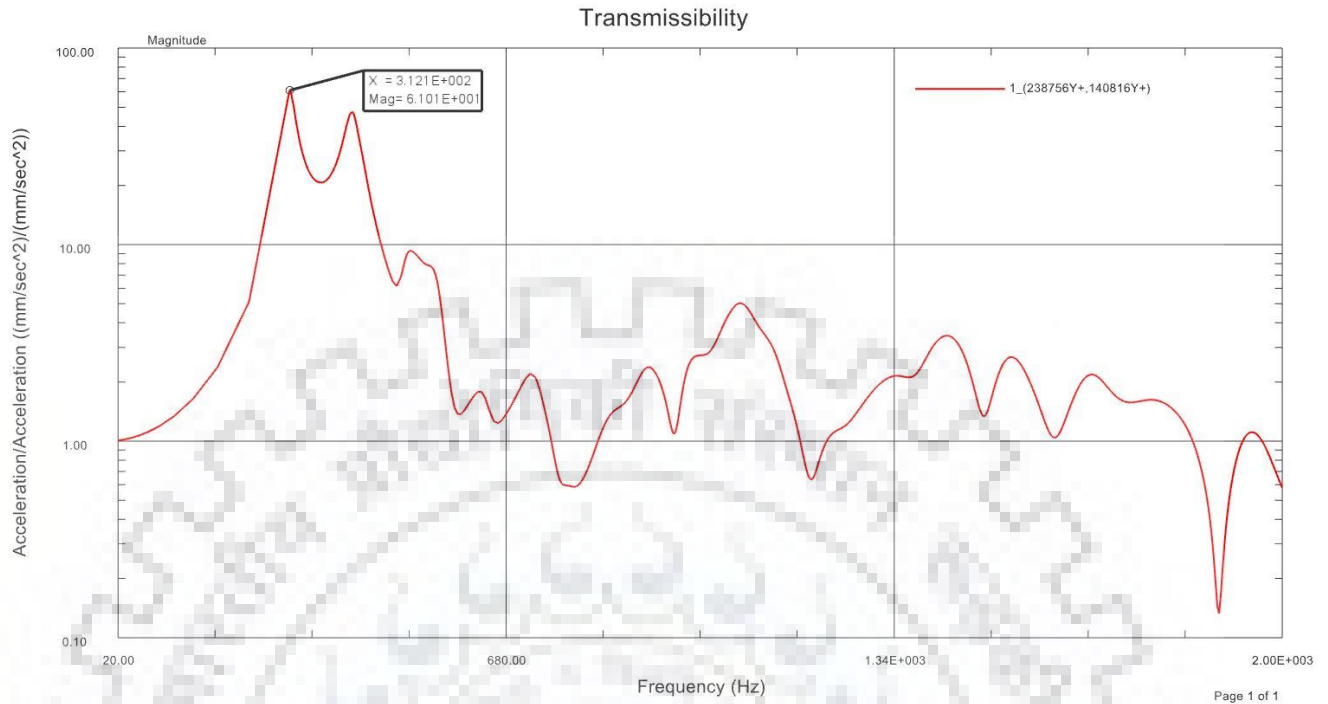


Fig 6-35: Transmissibility of vertical EP at node 140816 for Al6061 material

Fig 6.34 shows frequency versus transmissibility. In the graph, transmissibility is in the form of output acceleration to input acceleration. From the graph, it is observed that the maximum transmissibility of vertical EP with 3 % damping is 61 for Al6061 material. That occurs at 312 Hz. It means, the force or enforced motion that transmits from electronics package to electronic components is 61 times of the input/applied force or enforced motion during launch phase. So cover plate (critical component because node 140816 lie at cover plate) of vertical mounting EP of Al6061 material will experience 61 times force or enforced motion/acceleration as compared to input force or enforced motion/acceleration.

By random analysis, output acceleration level can be observed at this 140816 node for Al6061 material for vertical mounting EP. Input is given in form of power spectral density (PSD) as shown in fig 6.33 and output response can be observed as shown in fig 6.35. Random vibration input and response curves are typically plotted on log-log paper, with the power spectral density, expressed in squared acceleration units per hertz (G^2/Hz), plotted along the vertical axis, and the frequency (Hz) plotted along the horizontal axis. The input RMS acceleration levels can be

obtained by integrating under the input random vibration curve, and the output (or response) RMS acceleration levels can be obtained by integrating under the output (or response) random vibration curve. The square root of the area then determines the RMS acceleration level (G_{rms}).

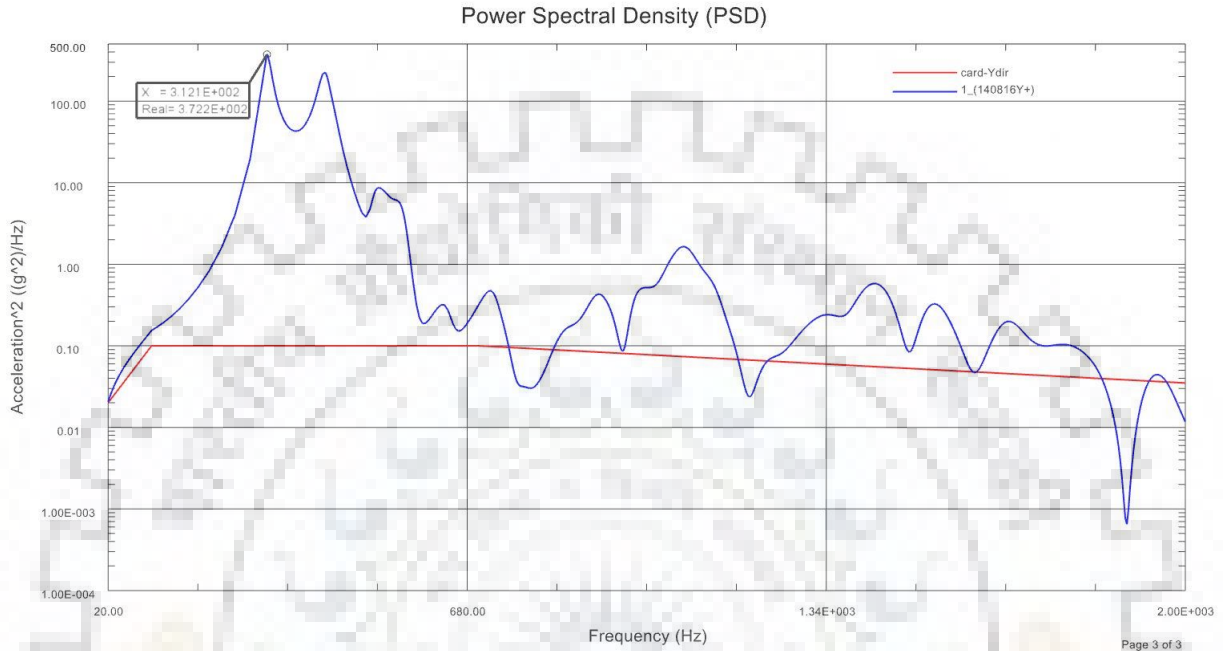


Fig 6-36: PSD curve at node 140816 of vertical mounting EP for Al6061 material

Results from the random analysis for vertical mounting EP (Al6061 material)

- G_{rms} value = 148.9 G
- (Stress)_{rms} value = 34.195 MPa
- (Displacement)_{rms} value = 0.4119 mm

G_{rms} value for Al6061 material vertical mounting EP is 148.9 G, it means output acceleration level has a magnitude that is 148.9 times greater than the acceleration of gravity. By random analysis, (Stress)_{rms} value and (Displacement)_{rms} value for Al6061 material is 34.195 MPa and 0.4119 mm, while maximum stress and displacement value for this material in quasi-static analysis is 27.16 MPa and 0.1055 mm. Similarly, random analysis has been carried out for magnesium alloy (AZ31B) vertical mounting EP and Be-Al alloy (AM162) vertical mounting EP.

6.4.3.2 Random analysis of vertical mounting EP with AZ31B material

For vertical mounting package, major mass participation modes for AZ31B material is given in the below table.

Table 6.7: Different modes of frequency and mass participation of AZ31B material with Y-direction enforced motion

Mode No.	Frequency (Hz)	X- Direction (%)	Y- Direction (%)	Z- Direction (%)
Mode 1	308	0.00005	16.1886	0.00146
Mode 2	311	0.00008	1.07605	0.00014
Mode 3	365	0.00000	0.16653	0.00006
Mode 4	395	0.00036	48.0906	0.01437
Mode 5	429	0.00011	0.06022	0.00002
Mode 6	504	0.00108	0.46464	0.00038
Mode 7	531	0.00084	1.05948	0.00133
Mode 16	809	0.48906	0.16558	0.00934
Mode 31	1033	0.02604	4.65609	0.77901
Mode 43	1173	58.21	0.00225	0.39926

By the table, maximum mass participation is in Y-direction and global mode of this package for AZ31B material is mode 1 with frequency 308 Hz. Maximum mass participation is obtained at 139052 Node of the vertical mounting package for AZ31B material.

This node is be subjected to maximum enforced loading during launch phase, so transmissibility and output acceleration level (G_{rms}) is to be find out at this node.

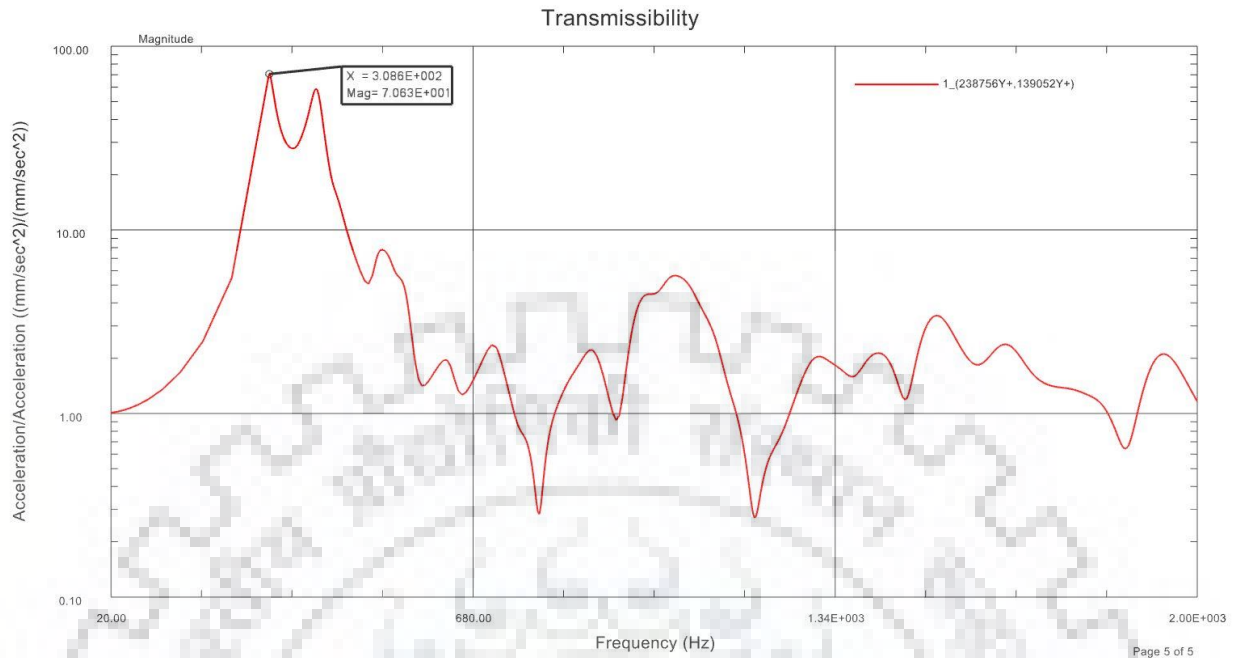


Fig 6-37: Transmissibility of vertical EP at node 139052 for AZ31B material

Fig 6.36 shows frequency versus transmissibility. In the graph, transmissibility is in the form of output acceleration to input acceleration. From the graph, it is observed that the maximum transmissibility of vertical EP with 3 % damping is 70.6 for AZ31B material. That occurs at 308 Hz. It means, the force or enforced motion that transmits from electronics package to electronic components is 70.6 times of the input/applied force or enforced motion during launch phase. So cover plate (critical component because node 139052 lie at cover plate) of vertical mounting EP of AZ31B material will experience 70.6 times force or enforced motion/acceleration as compared to input force or enforced motion/acceleration.

By random analysis, output acceleration level is observed at this 139052 node for AZ31B material for vertical mounting EP. Input is given in form of power spectral density (PSD) as shown in fig 6.33 and output response can be observed as shown in fig 6.37.

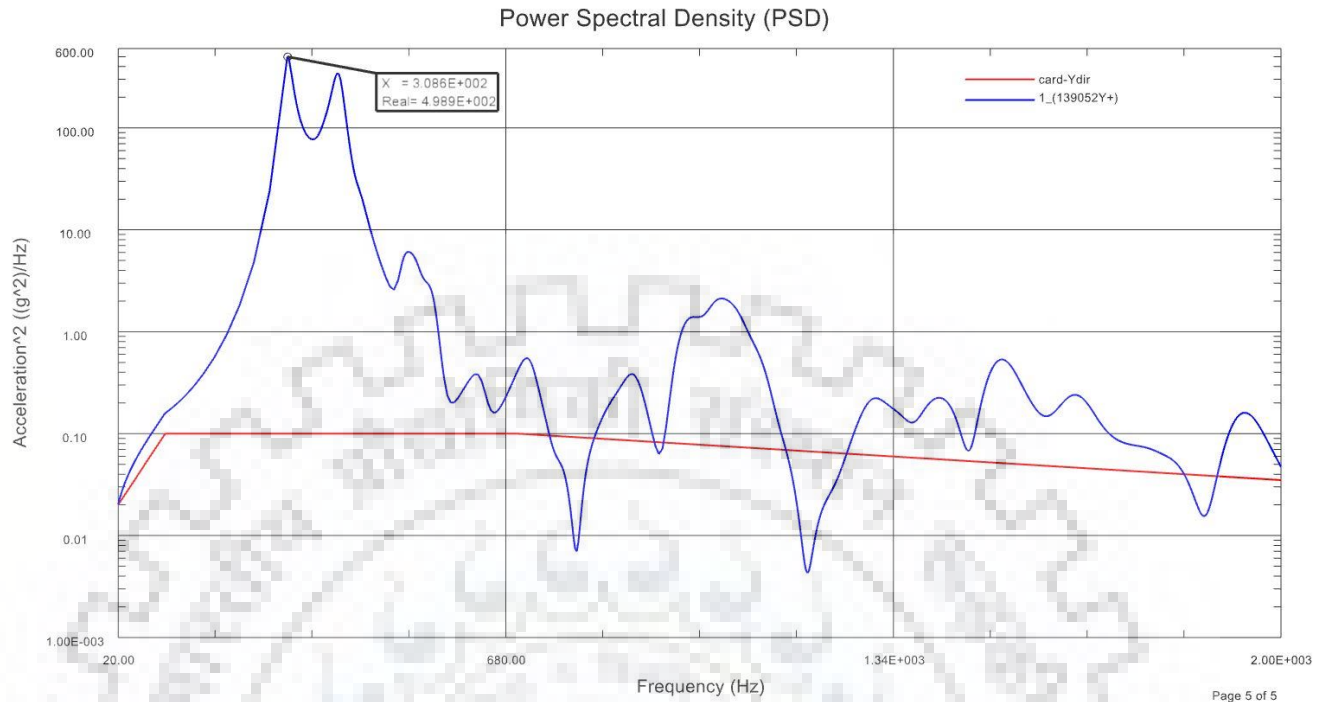


Fig 6-38: PSD curve at node 139052 of vertical mounting EP for AZ31B material

Results from the random analysis for vertical mounting EP (AZ31B material)

- G_{rms} value = 193.6 G
- (Stress)_{rms} value = 25 MPa
- (Displacement)_{rms} value = 0.45 mm

G_{rms} value for AZ31B material vertical mounting EP is 193.6 G, it means output acceleration level has a magnitude that is 193.6 times greater than the acceleration of gravity. By random analysis, (Stress)_{rms} value and (Displacement)_{rms} value for AZ31B material is 25 MPa and 0.45 mm, while maximum stress and displacement value for this material in quasi-static analysis is 20.7 MPa and 0.11 mm. Similarly, random analysis has been carried out for Be-Al alloy (AM162) vertical mounting EP.

6.4.3.3 Random analysis of vertical mounting EP with AM162 material

For vertical mounting package, major mass participation modes for AM162 material is given in the below table.

Table 6.8: Different modes of frequency and mass participation of AM162 material with Y-direction enforced motion

Mode No.	Frequency (Hz)	X- Direction (%)	Y- Direction (%)	Z- Direction (%)
Mode 1	564	0.00001	13.31512	0.00068
Mode 2	568	0.00001	1.71354	0.00013
Mode 3	669	0.00000	0.03844	0.00003
Mode 4	736	0.00017	49.375	0.01036
Mode 7	968	0.00083	1.15449	0.00100
Mode 18	1181	0.02012	1.79010	0.00016
Mode 20	1208	0.10499	1.49015	0.00252
Mode 33	1572	0.04517	0.48050	0.03248
Mode 35	1698	1.61204	0.01541	0.00091

By the table, maximum mass participation is in Y-direction and global mode of this package for AM162 material is mode 1 with frequency 564 Hz. Maximum mass participation is obtained at 140720 Node of the vertical mounting package for AM162 material.

This node is be subjected to maximum enforced loading during launch phase, so transmissibility and output acceleration level (G_{rms}) is to be find out at this node.

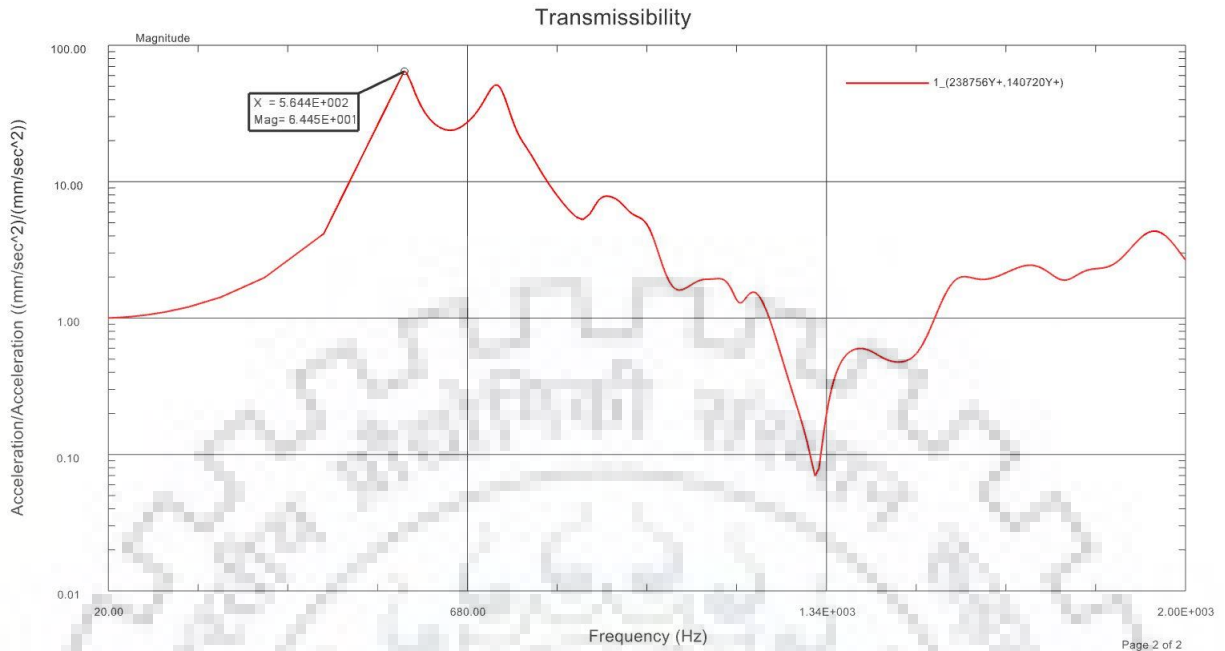


Fig 6-39: Transmissibility of vertical EP at node 140720 for AM162 material

Fig 6.38 shows frequency versus transmissibility. In the graph, transmissibility is in the form of output acceleration to input acceleration. From the graph, it is observed that the maximum transmissibility of vertical EP with 3 % damping is 64.4 for AM162 material. That occurs at 564 Hz. It means, the force or enforced motion that transmits from electronics package to electronic components is 64.4 times of the input/applied force or enforced motion during launch phase. So cover plate (critical component because node 140720 lie at cover plate) of vertical mounting EP of AM162 material will experience 64.4 times force or enforced motion/acceleration as compared to input force or enforced motion/acceleration.

By random analysis, output acceleration level is observed at this 140720 node for AM162 material for vertical mounting EP. Input is given in form of power spectral density (PSD) as shown in fig 6.33 and output response can be observed as shown in fig 6.39.

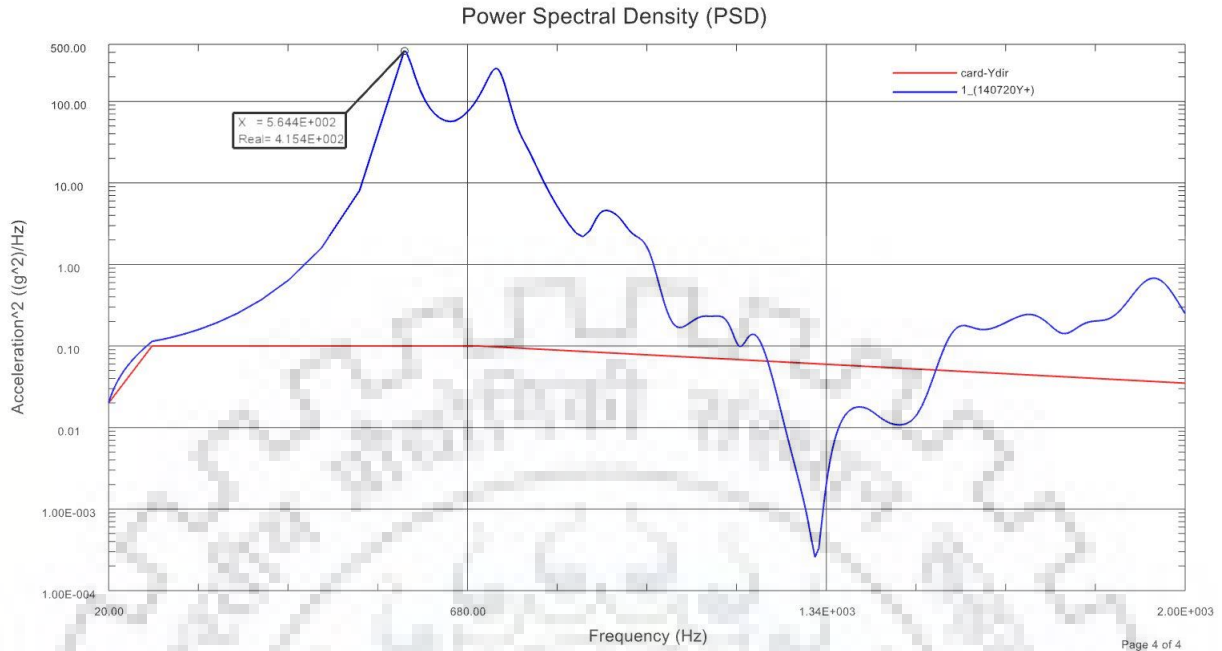


Fig 6-40: PSD curve at node 140720 of vertical mounting EP for AM162 material

Results from the random analysis for vertical mounting EP (AM162 material)

G_{rms} value = 143.34 G

$(\text{Stress})_{\text{rms}}$ value = 45.29 MPa

$(\text{Displacement})_{\text{rms}}$ value = 0.308 mm

G_{rms} value for AM162 material vertical mounting EP is 143.34 G, it means output acceleration level has a magnitude that is 143.34 times greater than the acceleration of gravity. By random analysis, $(\text{Stress})_{\text{rms}}$ value and $(\text{Displacement})_{\text{rms}}$ value for AM162 material is 45.29 MPa and 0.308 mm, while maximum stress and displacement value for this material in quasi-static analysis is 27.74 MPa and 0.0388 mm.

Table 6.9: Comparison for vertical mounting package with different materials

Materials	Fundamental Frequency (Hz)	Transmissibility	G_{rms} value
Al6061	308	61	148.9
AZ31B	307	70.6	193.6
AM162	564	64	143.34

By comparison among different material for vertical mounting EP, it is observed that fundamental frequency is highest for AM162 material and also greater than 150 Hz (minimum required during launch phase). Transmissibility is least for Al6061 material and highest for AZ31B material. G_{rms} value is least for AM162 material. It can be observed that AM162 has least G_{rms} value and also less transmissibility near to Al6061 material. It has high fundamental frequency also.

6.4.4 Random analysis for horizontal mounting electronic package

In random analysis of horizontal mounting package, the entire package is subjected to base excitation from 20 Hz to 2000 Hz frequency range with a damping ratio of 3 % and force is applied in the form of enforced motion in all three direction one by one with gravity load. This analysis has been carried out for Al6061, AZ31B and AM162 material and mass participation has been found at all modes. Then global node is identified for particular material and at this global node, transmissibility and output acceleration curve is obtained. After this, input is given in form of PSD and output response of the horizontal mounting package can be seen in PSD curves for all materials. By these curve, root mean square values of output acceleration level (G_{rms}) can be obtained in form of G for Al6061, AZ31B and AM162 material during launch phase. Similarly root mean square values of stress and displacement can be obtained.

Horizontal mounting package has the maximum mass participation in Z-direction as compare to other direction. Therefore, Z-direction is the critical direction for output parameters such as transmissibility and output acceleration level (G_{rms}) for all materials. It can be observed that

transmissibility and output acceleration level (G_{rms}) value is highest at global node with Z-direction enforced motion.

6.4.4.1 Random analysis of horizontal mounting EP with Al6061 material

For horizontal mounting package, major mass participation modes for Al6061 material is given in the below table.

Table 6.10: Different modes of frequency and mass participation for Al6061 material with Z-direction enforced motion

Mode No.	Frequency (Hz)	X- Direction (%)	Y- Direction (%)	Z- Direction (%)
Mode 1	187	0.00001	0	0.0006
Mode 2	197	0.00036	0.00358	19.17
Mode 3	201	0.00002	0.00014	0.00152
Mode 4	203	0.00017	0.00097	2.13684
Mode 5	213	0.00023	0	0.00064
Mode 6	237	0.00011	0.00049	4.235
Mode 7	269	0.32	0.00791	0.1354
Mode 15	340	0.00061	45.20314	0.12956
Mode 19	371	48.1742	0.00157	0.00227
Mode 30	469	0.00002	0.00016	21.99106

By the table, maximum mass participation is in Z-direction and global mode of this package for Al6061 material is mode 2 with frequency 197 Hz. This is called global mode because it is the first mode where mass participation is maximum. This maximum mass participation obtained at 432328 Node of the horizontal mounting package for Al6061 material.

This node is subjected to maximum enforced loading during launch phase, so transmissibility and output acceleration level (G_{rms}) is to be found out at this node.

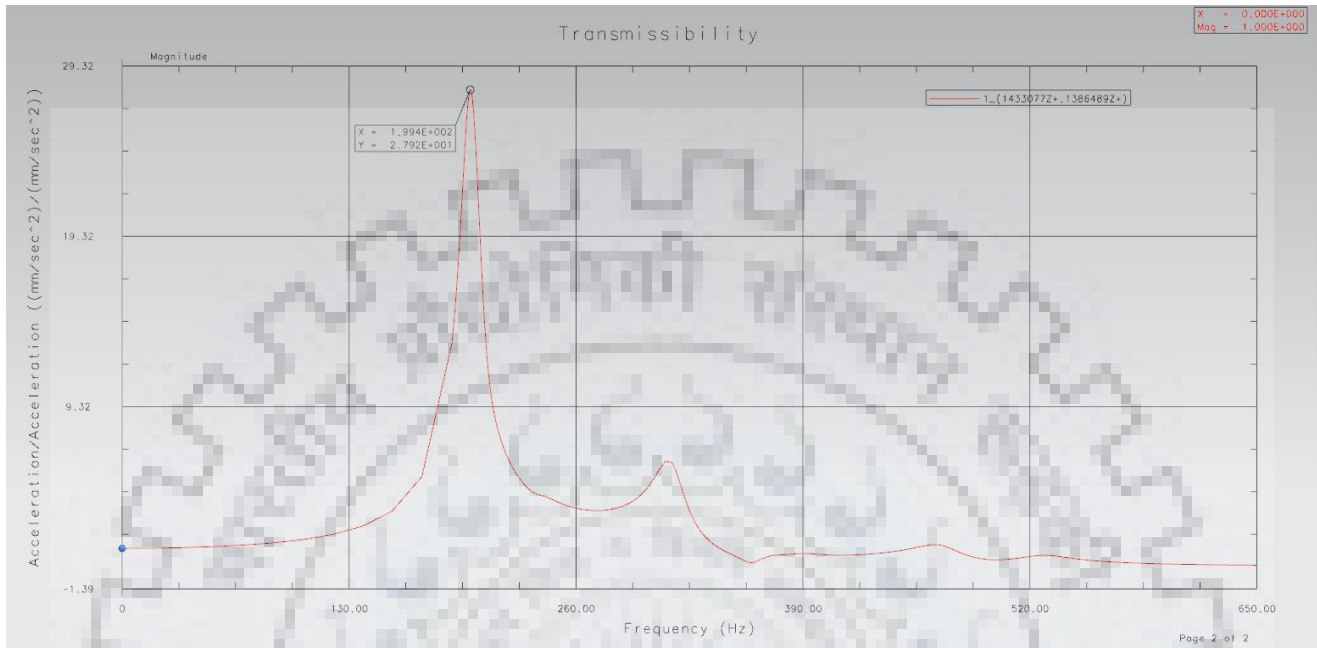


Fig 6-41: Transmissibility of horizontal EP at node 432328 for Al6061 material

Fig 6.40 shows frequency versus transmissibility. In the graph, transmissibility is in the form of output acceleration to input acceleration. From the graph, it is observed that the maximum transmissibility of vertical EP with 3 % damping is 27.9 for Al6061 material. That occurs at 197 Hz. It means, the force or enforced motion that transmits from electronics package to electronic components is 27.9 times of the input/applied force or enforced motion during launch phase. So first tray PCB (critical component because node 432328 lie at this PCB) of horizontal mounting EP of Al6061 material will experience 27.9 times force or enforced motion/acceleration as compared to input force or enforced motion/acceleration.

By random analysis, output acceleration level can be observed at this 432328 node for Al6061 material for horizontal mounting EP. Input is given in form of power spectral density (PSD) as shown in fig 6.33 and output response can be observed as shown in fig 6.41. Random vibration input and response curves are typically plotted on log-log paper, with the power spectral density, expressed in squared acceleration units per Hz (G^2/Hz), plotted along the vertical axis, and the

frequency (Hz) plotted along the horizontal axis. The input RMS acceleration levels can be obtained by integrating under the input random vibration curve, and the output (or response) RMS acceleration levels can be obtained by integrating under the output (or response) random vibration curve. The square root of the area then determines the RMS acceleration level (G_{rms}).

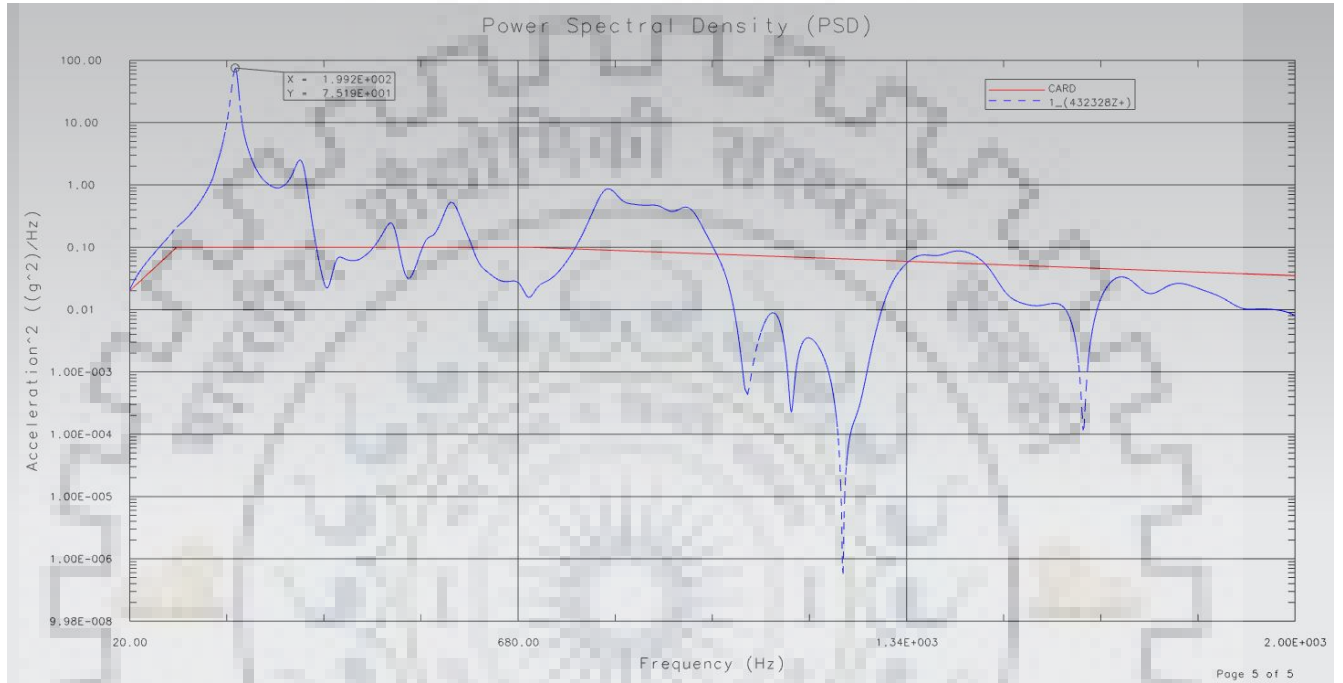


Fig 6-42: PSD curve at node 432328 of horizontal mounting EP for Al6061 material

Results from the random analysis for horizontal mounting EP (Al6061 material)

- G_{rms} value = 38.31 G
- $(Stress)_{rms}$ value = 157.8 MPa
- $(Displacement)_{rms}$ value = 0.551 mm

G_{rms} value for Al6061 material horizontal mounting EP is 38.31 G, it means output acceleration level has a magnitude that is 38.31 times greater than the acceleration of gravity. By random analysis, $(Stress)_{rms}$ value and $(Displacement)_{rms}$ value for Al6061 material is 157.8 MPa and 0.551 mm, while maximum stress and displacement value for this material in quasi-static analysis is 76 MPa and 0.218 mm. Similarly, random analysis has been carried out for

magnesium alloy (AZ31B) horizontal mounting EP and Be-Al alloy (AM162) horizontal mounting EP.

6.4.4.2 Random analysis of horizontal mounting EP with AZ31B material

For horizontal mounting package, major mass participation modes for AZ31B material is given in the below table.

Table 6.11: Different modes of frequency and mass participation of AZ31B material with Z-direction enforced motion

Mode No.	Frequency (Hz)	X- Direction (%)	Y- Direction (%)	Z- Direction (%)
Mode 1	171	0.00038	0.00388	18.4847
Mode 2	177	0.00015	0.00107	1.96474
Mode 6	237	0.00080	0.00249	4.79612
Mode 7	245	0.54271	0.00038	0.04549
Mode 11	289	0.00224	35.09810	0.04957
Mode 12	299	0.04641	1.58232	1.87334
Mode 15	305	0.12934	10.18467	0.15724
Mode 17	322	43.19856	0.02200	3.35503
Mode 23	367	0	0.00204	1.61696
Mode 28	407	0.00106	0.00006	23.9784

By the table, maximum mass participation is in Z-direction and global mode of this package for AZ31B material is mode 1 with frequency 171 Hz. Maximum mass participation is obtained at 398116 Node of the horizontal mounting package for AZ31B material.

This node is be subjected to maximum enforced loading during launch phase, so transmissibility and output acceleration level (G_{rms}) is to be find out at this node.

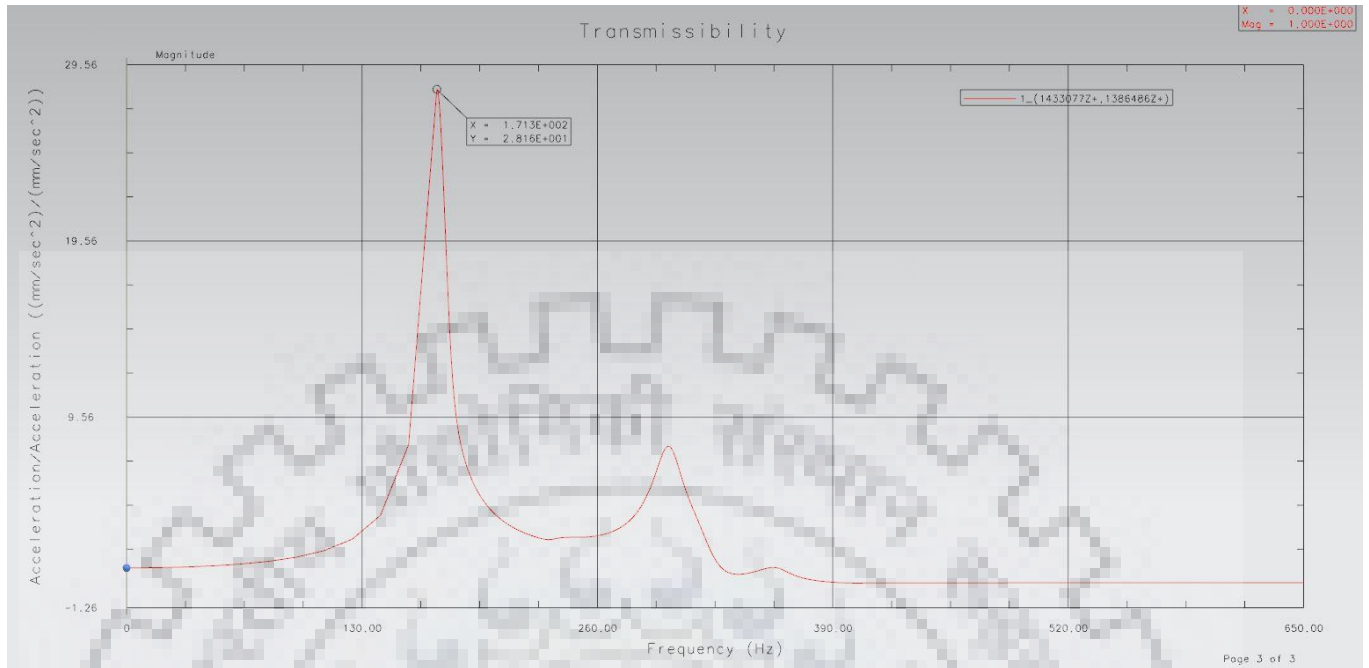


Fig 6-43: Transmissibility of horizontal EP at node 398116 for AZ31B material

Fig 6.42 shows frequency versus transmissibility. In the graph, transmissibility is in the form of output acceleration to input acceleration. From the graph, it is observed that the maximum transmissibility of horizontal EP with 3 % damping is 28.1 for AZ31B material. That occurs at 171 Hz. It means, the force or enforced motion that transmits from electronics package to electronic components is 28.1 times of the input/applied force or enforced motion during launch phase. So first tray PCB (critical component because node 398116 lie at this PCB) of horizontal mounting EP of AZ31B material will experience 28.1 times force or enforced motion/acceleration as compared to input force or enforced motion/acceleration.

By random analysis, output acceleration level is observed at this 398116 node for AZ31B material for horizontal mounting EP. Input is given in form of power spectral density (PSD) as shown in fig 6.33 and output response can be observed as shown in fig 6.43.

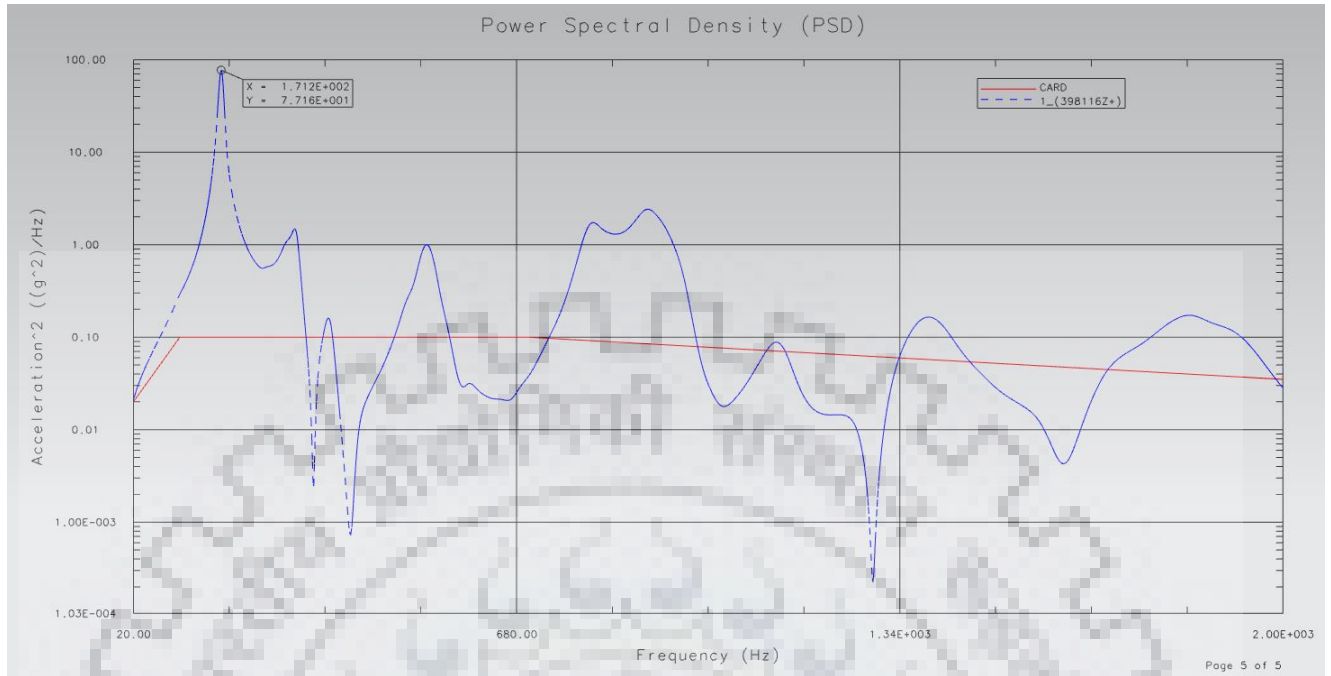


Fig 6-44: PSD curve at node 398116 of horizontal mounting EP for AZ31B material

Results from the random analysis for horizontal mounting EP (AZ31B material)

G_{rms} value = 46 G

$(\text{Stress})_{\text{rms}}$ value = 140.75 MPa

$(\text{Displacement})_{\text{rms}}$ value = 0.608 mm

G_{rms} value for AZ31B material horizontal mounting EP is 46 G, it means output acceleration level has a magnitude that is 46 times greater than the acceleration of gravity. By random analysis, $(\text{Stress})_{\text{rms}}$ value and $(\text{Displacement})_{\text{rms}}$ value for AZ31B material is 140.75 MPa and 0.608 mm, while maximum stress and displacement value for this material in quasi-static analysis is 69.39 MPa and 0.291 mm. Similarly, random analysis has been carried out for Be-Al alloy (AM162) horizontal mounting EP.

6.4.4.3 Random analysis of horizontal mounting EP with AM162 material

For horizontal mounting package, major mass participation modes for AM162 material is given in the below table.

Table 6.12: Different modes of frequency and mass participation of AM162 material with Z-direction enforced motion

Mode No.	Frequency (Hz)	X- Direction (%)	Y- Direction (%)	Z- Direction (%)
Mode 1	280	0.00054	0.00089	20.18904
Mode 2	288	0.00038	0.00200	2.65483
Mode 16	434	0.00002	0.00046	4.19344
Mode 23	580	0.07149	4.52126	0.01836
Mode 25	591	0.00863	23.56221	0.24968
Mode 27	599	0.11930	10.21802	0.35705
Mode 29	602	0.25960	6.03107	0.49165
Mode 30	612	0.05497	1.56411	22.51097
Mode 31	616	2.05152	0.16955	3.88039
Mode 36	642	45.47208	0.00571	0.22549

By the table, maximum mass participation is in Z-direction and global mode of this package for AM162 material is mode 1 with frequency 280 Hz. Maximum mass participation is obtained at 437040 Node of the horizontal mounting package for AM162 material.

This node is be subjected to maximum enforced loading during launch phase, so transmissibility and output acceleration level (G_{rms}) is to be find out at this node.

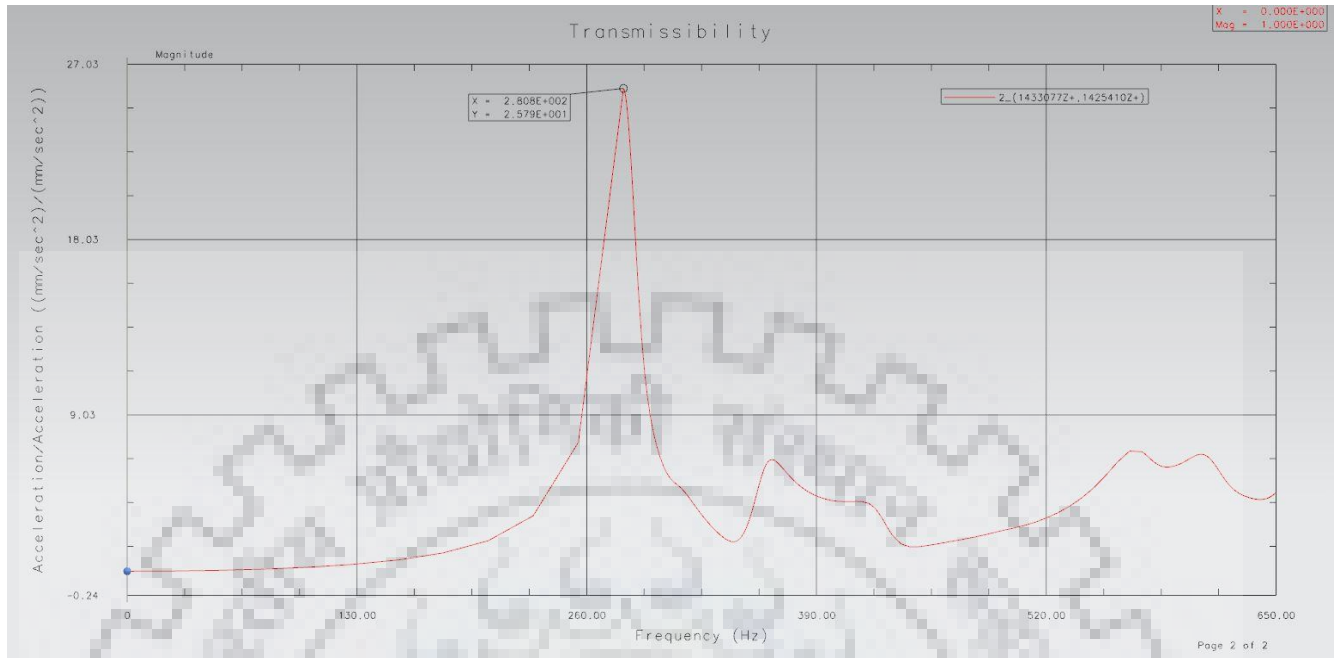


Fig 6-45: Transmissibility of horizontal EP at node 437040 for AM162 material

Fig 6.44 shows frequency versus transmissibility. In the graph, transmissibility is in the form of output acceleration to input acceleration. From the graph, it is observed that the maximum transmissibility of vertical EP with 3 % damping is 25.7 for AM162 material. That occurs at 280 Hz. It means, the force or enforced motion that transmits from electronics package to electronic components is 25.7 times of the input/applied force or enforced motion during launch phase. So first tray PCB (critical component because node 437040 lie at this PCB) of horizontal mounting EP of AM162 material will experience 25.7 times force or enforced motion/acceleration as compared to input force or enforced motion/acceleration.

By random analysis, output acceleration level is observed at this 437040 node for AM162 material for horizontal mounting EP. Input is given in form of power spectral density (PSD) as shown in fig 6.33 and output response can be observed as shown in fig 6.45.

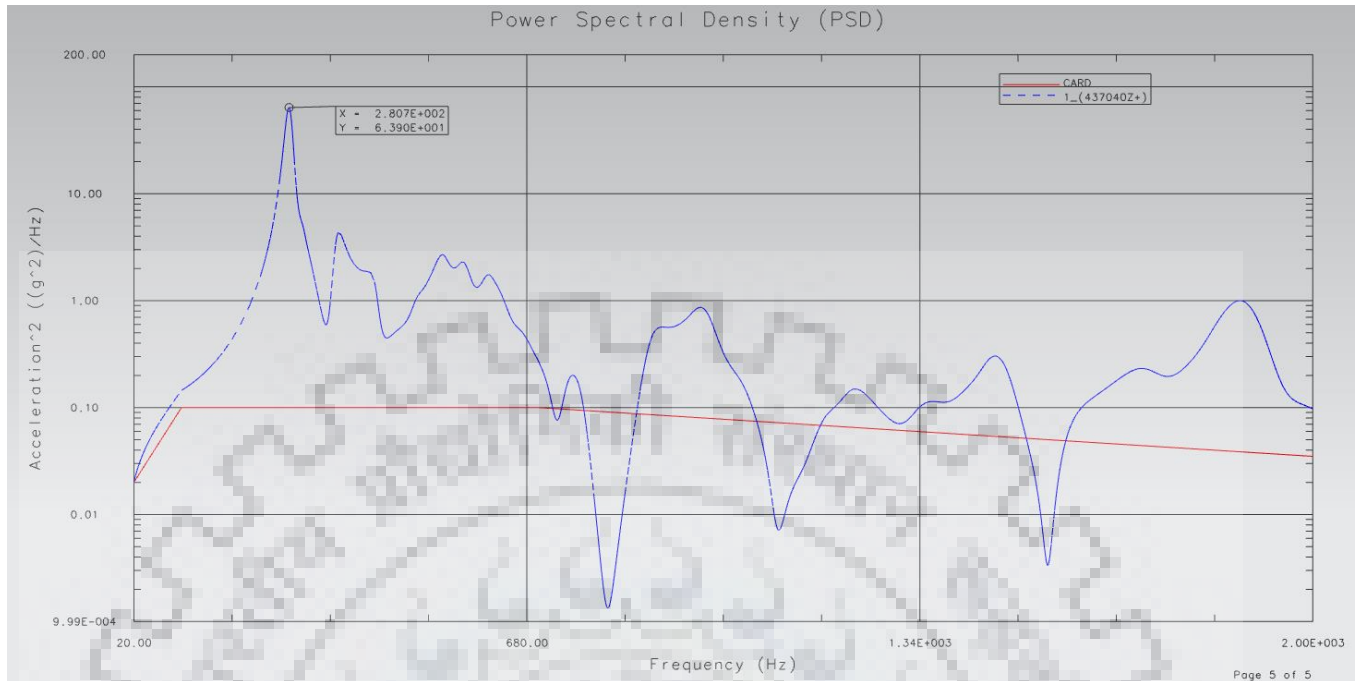


Fig 6-46: PSD curve at node 437040 of horizontal mounting EP for AM162 material

Results from the random analysis for horizontal mounting EP (AM162 material)

G_{rms} value = 37 G

$(Stress)_{rms}$ value = 227.83 MPa

$(Displacement)_{rms}$ value = 0.317 mm

G_{rms} value for AM162 material horizontal mounting EP is 37 G, it means output acceleration level has a magnitude that is 37 times greater than the acceleration of gravity. By random analysis, $(Stress)_{rms}$ value and $(Displacement)_{rms}$ value for AM162 material is 227.83 MPa and 0.317 mm, while maximum stress and displacement value for this material in quasi-static analysis is 75.77 MPa and 0.109 mm.

Table 6.13: Comparison for horizontal mounting package with different materials

Materials	Fundamental Frequency (Hz)	Transmissibility	G_{rms} value
Al6061	187	27.9	38.31
AZ31B	171	28.1	46
AM162	280	25.7	37

By comparison among different for horizontal mounting EP, it is observed that fundamental frequency is highest for AM162 material and also greater than 150 Hz (minimum required during launch phase). Transmissibility is least for AM162 material and highest for AZ31B material. G_{rms} value is least for AM162 material. It can be observed that AM162 has least G_{rms} value and also least transmissibility. It has high fundamental frequency also.

Since, in case of vertical and horizontal mounting EP, fundamental frequency is highest for AM162 for both type of EP and also for AM162 material, both type of EP has least transmissibility and G_{rms} value. Therefore, AM162 is the better material among all three material for making the mechanical housing of EP of the spacecraft.

Table 6.14: Comparison of mass details of both type of EP with different materials

S. No.	Mounting type	Material	Mass (kg)
1.	Vertical mounting	Al6061	5.33
		AZ31B	3.484
		AM162	4.26
2.	Horizontal mounting	Al6061	6.755
		AZ31B	4.39
		AM162	5.336

By comparison in both cases for all three materials, Mass (m) of the package is less for AZ31B material.

$$m_{Al6061} > m_{AM162} > m_{AZ31B}$$

Since specific stiffness is the main concern for fabrication of EP and specific stiffness is highest in case of AM162 material.

Specific stiffness (k)

$$k_{AM162} > k_{AZ31B} > k_{Al6061}$$



Chapter 7

CONCLUSION

Linear static analysis, modal behaviour and random analysis of electronic packages under vibrational loading is studied for strength and natural frequency point of view with AL6061, AZ31B and AM162 as the material for mechanical housing of electronic packages. Both the electronic packages is modelled using FE software UG-NX as pre-processor and MSC NASTRAN is used as solver (post-processor). All geometric features such as ribs, connector cut-outs and holes are considered during modelling to simulate the real condition. Both the packages has been supported (constrained) at eight lug locations. Comparison has been done for different materials for both type of electronic packages.

The following conclusions can be drawn:-

From Linear Static analysis

For the package made up of AM162 material, the maximum displacement observed is 0.1099 mm and maximum Von-Mises stress is 75.77 MPa for horizontal mounting EP and for vertical mounting EP, the maximum displacement observed is 0.0311 mm and maximum Von-Mises stress is 27.13 MPa. The margin of safety by using AM162 material for horizontal and vertical mounting EP is 2.64 and 9.17 respectively as shown in Table 6.1, 6.2 and 6.3. For AZ31B material, the maximum displacement observed is 0.291 mm and maximum Von-Mises stress is 69.39 MPa for horizontal mounting EP and for vertical mounting EP, the maximum displacement observed is 0.1065 mm and maximum Von-Mises stress is 23.51 MPa. The margin of safety by using AZ31B material for horizontal and vertical mounting EP is 1.88 and 7.51 respectively as shown in Table 6.1, 6.2 and 6.3. For Al6061 material, the maximum displacement observed is 0.218 mm and maximum Von-Mises stress is 76.09 MPa for horizontal mounting EP and for vertical mounting EP, the maximum displacement observed is 0.1077 mm and maximum Von-Mises stress is 26.65 MPa. The margin of safety by using Al6061 material for horizontal and vertical mounting EP is 2.63 and 9.35 respectively as shown in Table 6.1, 6.2 and 6.3. Therefore, AM162 shows minimum displacement, reduced mass and enough margin of safety at

the critical regions compared to AL6061 and AZ31B. So, AM-162 qualifies to be a better material from strength point of view for fabrication of electronic packages.

From Normal Modal analysis

The modal analysis shows that package made up of AM162 has its Mode-1(first fundamental frequency) at 280 Hz for horizontal mounting EP and 564 Hz for vertical mounting EP which is well above the desired frequency range. For AZ31B, first mode corresponds to 171 Hz for horizontal mounting EP and 307 Hz for vertical mounting EP. Similarly, for Al6061, first mode corresponds to 187 Hz for horizontal mounting EP and 308 Hz for vertical mounting EP which shows that the package made up of AM162 is stiffer than that of AL6061 and AZ31B for both type of mounting conditions and can sustain higher dynamic loads.

The electronic package made up of AM162 provides a mass saving of about 1 to 1.5 kg for 2 mm module thickness as compared to Al6061.

From Random Analysis

From random analysis, all results are studied and it is observed that the G_{rms} value is least for AM162 material as compare to Al6061 and AZ31B in both mounting conditions and $(Displacement)_{rms}$ value is also least for AM162 material as compare to Al6061 and AZ31B. Transmissibility is least for AM162 in case of horizontal mounting while in case of vertical mounting transmissibility is least for Al6061 material but transmissibility of AM162 material for vertical mounting package is very nearer to Al6061.

Therefore, the electronic package made up of AM162 will experience least amount of random load during launch phase as compared to Al6061 and AZ31B.

7.1 Scope for future work

- Thermal analysis of electronic package can be carried out using FE software and verified experimentally to estimate the thermal effect on package as high heat dissipating electronic components can affect the life of package.
- Going for active vibration test with electronic component mounted on PCB and also carrying out destructive test to find the behaviour of PCB when subjected to excessive loading.
- Mounting of electronic components on PCB and optimization of placement of components which helps in reducing the stress on lead joints and solder joints of electronic components.
- Study on damping characteristics of PCB and package material and obtaining various methods of reducing vibrations.
- Modelling new configurations for mounting of PCB onto the module and optimization of mounting locations and housing wall thickness.

REFERENCES

- [1] D. S. Steinberg, *Vibration Analysis for Electronic Equipment*, John Wiley & Sons, Inc., 2000.
- [2] A.M. Veprik, *Vibration Protection of Critical Components of Electronic Equipment in Harsh Environmental Conditions*, *Journal of Sound and Vibration*, 2003, v.259 (1), p.161-175.
- [3] E. Suhir, *Predicting Fundamental Vibration Frequency of a Heavy Electronic Component Mounted on a Printed Circuit Board*, *Journal of Electronic Packaging*, 2000.
- [4] A. Perkins, S. K. Sitaraman, *Vibration-Induced Solder Joint Failure of a Ceramic Column Grid Array (CCGA) Package*, *Electronic Components and Technology Conference, IEEE-CMPT and EIA*, 2004.
- [5] B Esser, D. Huston, *Active Mass Damping of Electronic Circuit Boards*, *Journal of Sound and Vibration*.
- [6] Jung, Park, Seo, Han, Kim, *Structural Vibration Analysis of Electronic Equipment for Satellite under Launch Environment*, *Key Engineering Materials Vols. 270-273 (2004) pp.1440-1445*.
- [7] A. O. Cifuentes, A. Kalbag, *Dynamic Behavior of Printed Wiring Boards: Increasing Board Stiffness by Optimizing Support Locations*, *IEEE*, 1993.
- [8] A. O. Cifuentes, *Estimating the Dynamic Behavior of Printed Circuit Boards*, *IEEE Transactions on Components, Packaging, and Manufacturing Technology-Part B: Advanced Packaging*, Vol.17, No.1, 1994.
- [9] L. Salvatore, D. Followell, *Vibration Fatigue of Surface Mount Technology (SMT) Solder Joints*, *Proceedings Annual Reliability and Maintainability Symposium*, 1995.
- [10] A. Schaller, *Finite Element Analysis of Microelectronic Systems – State of the art*, *IEEE*, 1988.
- [11] E. G: Veilleux, *Vibration Control of Printed-Circuit Boards in a Dynamic Environment*, *IEEE Transactions on Parts, Materials, and Packaging*, Vol. PMP-6, No. 3, 1970.
- [12] J. M. Pitarresi, *Modeling of Printed Circuit Cards Subject to Vibration*, *IEEE Proceedings of the Circuits and Systems Conference*, New Orleans, LA, May 3-5, 1990, pp. 2104-2107.
- [13] J. H. Lau, C. A. Keely, *Dynamic Characterization of Surface-Mount Component Leads for Solder Joint Inspection*, *IEEE Transaction on Components, Hybrids, and Manufacturing Technology*, Vol. 12, No.4, 1989.

[14] S. J. Ham, S. B. Lee, Experimental Study for Reliability of Electronic Packaging under Vibration, Journal of Experimental Mechanics, Vol. 36, No. 4, 1996.

[15] G. S. Aglietti, C. Schwingshackl, Analysis of Enclosures and Anti Vibration Devices for Electronic Equipment for Space Applications, Proceedings of the 6th International Conference on Dynamics and Control of Systems and Structures in Space 2004.

[16] McKeown, Mechanical Analysis of Electronic Packaging Systems, Marcel Dekker, Inc., 1999.

[17] Jiwan Kumar Pandit, D. Roy Mahapatra, R. Pandiyan* Modal Analysis of Power Electronics Module of Spacecraft and its Health Monitoring - An Approach Elsevier, International Journal, Procedia Engineering 144 (2016) 283 – 288.

